ADSORPTION OF ELECTRON ACCEPTORS ON RARE EARTH OXIDES

THESIS SUBMITTED TO
THE COCHIN UNIVERSITY OF SCIENCE AND TECHNOLOGY
IN PARTIAL FULFILMENT OF THE REQUIREMENTS
FOR THE DEGREE OF DOCTOR OF PHILOSOPHY IN CHEMISTRY
IN THE FACULTY OF SCIENCE

By

DEVIKA RANI G.

DEPARTMENT OF APPLIED CHEMISTRY
COCHIN UNIVERSITY OF SCIENCE AND TECHNOLOGY
KOCHI – 682 022, INDIA

AUGUST 1992

CERTIFICATE

This is to certify that the thesis bound herewith is the authentic record of research work carried out by the author under my supervision in partial fulfilment of the requirements for the degree of Doctor of Philosophy and no part thereof has been presented before for any other degree.

Dr. S. SUGUNAN
(Supervising Teacher)
Reader, Department of
Applied Chemistry
Cochin University of
Science and Technology

Kochi 682022

31 August 1992

DECLARATION

I hereby declare that the work presented in this thesis is based on the original work done by me under the guidance of Dr.S. Sugunan, Reader, Department of Applied Chemistry, Cochin University of Science and Technology, Kochi 682022, and no part of this thesis has been included in any other thesis submitted previously for the award of any degree.

Kochi 682022

31 August 1992

DEVIKA RANI, G.

CONTENTS

CHAPTER I

INTRODUCTION

INTRODUCTION

Although the fundamental catalytic and surface properties of alkali, alkaline earth and other basic oxides have been extensively studied [1], equivalent information about the series of basic rare earth oxides is much less. The gradual decrease in tervalent ionic radius and consequent increase in ionic charge density in going from La^{3+} to Lu^{3+} results in a corresponding decrease in basicity of sesquioxides across the series [2]. Systematic correlations between surface basicity and catalytic properties among rare earth oxides have been explored to only a limited extent.

Empirical studies have demonstrated that, following appropriate pretreatment, rare earth oxides are active catalysts for a number of reactions. Taylor and Diamond have shown that paramagnetic oxides Gd_2O_3 and Nd_2O_3 are more active in catalysing ortho-para hydrogen conversion than the non-paramagnetic lanthanum oxide [3]. The H_2 - D_2 exchange reaction showed a temperature dependence similar to ortho-para hydrogen conversion reaction [4]. Selwood studied the non-dissociative mechanism in a magnetic field and observed an increase in activity towards para hydrogen

conversion in a strong field but no change in activity in a weak field was observed [5]. The magnetic properties of lanthanide oxides depend on the electron structure of the 4f subshell and hence differs from each other. On the other hand, the chemical properties are similar to each other, since the 4f orbital does not contribute significantly to the chemical bond of lanthanide compounds [2,6]. The catalytic activity differs from each other in such a reaction as para-hydrogen conversion which proceeds by paramagnetic mechanism [4]. Hopkins and Taebel have summarized the catalytic activity of rare earths for oxidation, hydrogenation, decomposition and synthesis of organic compounds [7]. McGough and Houghton evaluated the effects of paramagnetism, crystal structure and crystal field on catalytic activity of lanthanides for the dehydrogenation of cyclohexane [8]. They could not detect any effect of support, crystal structure, or paramagnetism, indicating that catalytic activity of lanthanide oxides is associated with outer electronic states. Sozonov and co-workers measured the activation energies of the isotopic exchange of O_2 and of the desorption of CO_2 in the oxidation of CO and found that the dependence of activation energies on atomic number was similar to that of magnetic moment [9]. Minnachev compared the catalytic activity in oxidation

of hydrogen and propylene with that in the isotopic exchange of oxygen and suggested that the catalytic activity depends on the binding energy of oxygen with the surface and on the valence of lanthanide ions [10]. Bakumenko and Chashenikova found in the oxidation of hydrogen that the activity of Neodymium and Erbium oxides were lower than Cerium, Praseodymium and Terbium oxides, which was explained on the basis of the heat of formation of oxide [11]. It has been suggested from the results that the catalytic activity of lanthanide oxides depend on the electronic configuration of inner 4f subshell [9,10]. E.R.S.Winter examined the catalytic activity of rare earth oxides for the decomposition of Nitric Oxide and found that the reaction showed similarity to N_2O decomposition and was first order with respect to pressure [12]. Several studies have been made of the Nitrous oxide decomposition on lanthanide oxides [13,14]. Winter analysed the results for decomposition of N_2O over lanthanide oxides pretreated with oxygen [15]. Read extended the work of Winter to provide a detailed analysis of the effect of pressure on kinetics of decomposition of N_2O on Neodymium oxide, Dysporsium oxide and Erbium oxide [16]. Read suggested that the surface of lanthanide oxides contain a large number of anion vacancies and these centres form the active sites

for decomposition of Nitrous oxide.

The activity of Dysporsium oxide towards n-butane cracking and double bond migration in 1-butene have been described [17,18]. It was shown from results that amount of adsorption depends on temperature, with a maximum adsorption at about 600 K. J.F. Read and E.W. Perkins studied the Hydrogen-Oxygen reaction over Dysporsium oxide catalyst [19]. T.Hattori, I.Inoko and Y.Murakami studied the catalytic oxidation of butane over a series of lanthanide oxides in order to investigate the effect of electronic configuration and catalytic activity [20]. A good correlation has been obtained between the catalytic activity of lanthanide oxides and the fourth ionization potential of lanthanide elements.

M.P. Rosynek and D.T. Magnuson studied the surface parameters and thermal dehydration-rehydration behaviour of $La(OH)_3$ and La_2O_3 [21]. They observed that the surface carbonate layer on the resulting oxide is not removed completely by subsequent thermal treatment at 700-800°C. Thermogravimetric studies demonstrated that the dehydration of $La(OH)_3$ is complete at 300°C. Infrared and gravimetric techniques have been applied to investigate the surface interactions of La_2O_3 and $La(OH)_3$ with CO_2 [22]. Infrared measurements

confirmed the absence of both surface and bulk hydroxyls in La_2O_3 evacuated above 300°C. M.P.Rosynek and J.S.Fox examined the behaviour of La_2O_3 as a catalyst for double bond migration and cis/trans rotation in n-butenes [23]. A considerable increase in specific activity of oxide was obtained in the calcination temperature range of 300-650°C. Active sites for 1-butene isomerization have been suggested to involve surface O^{2-} ions in conjunction with adjacent defect structures such as anion vacancies.

Minachev et al studied the variation in catalytic activity of rare earth oxides in ethylene hydrogenation as a function of the pretreatment temperature [24]. The oxides showed catalytic activity after pretreatment at 600°C. A decrease in hydrogenating activity in the series of oxides from lanthanum to Lutetium is correlated with a decrease in their basicity.

Rare earth oxides are hardly reducible and this character is suited for catalyst support which is applied under reducing atmosphere [25]. It has been known that the incorporation of a small amount of La_2O_3 or CeO_2 to supported Ni, Ni-Rh and Ni-Ru catalysts brought about considerable increase in activity in methanation of carbon

oxides [26]. It was reported that Rh carbonyl clusters dispersed on La_2O_3, Nd_2O_3 and CeO_2 were effective catalysts for ethanol and C_2 oxygenated products formation [27]. The addition of Dy_2O_3, Nd_2O_3, Yb_2O_3, La_2O_3 or Gd_2O_3 to Rh-Al_2O_3 catalyst enhanced the activity of hydrogenation of CO to methane [28]. A linear relationship between carbon skeleton propagation of hydrocarbons formed and the basicity of rare earth oxides was observed.

Osaka et al have demonstrated that certain lanthanide oxides are capable of promoting the oxidation of methane [29]. Lin and co-workers studied the oxidative dimerization of methane over La_2O_3 and observed that La_2O_3 selectively catalyses the conversion of methane to ethane and ethylene [30].

Y. Tong, M.P. Rosynek and J.H. Lunsford studied the reactions between methyl radicals and certain members of lanthanide oxide series [31]. They observed that methyl radicals react extensively with lanthanide oxides which have multiple cationic oxidation states. Choudhary et al found that Lanthanum oxide-promoted MgO catalysts show very high activity and C_2-selectivity in oxidative coupling of methane to C_2-hydrocarbons [32]. Carbon monoxide

hydrogenation over mixed oxides of 3A and 4A groups (Y_2O_3, La_2O_3, CeO_2 and ZrO_2) with 3B group (Al_2O_3, In_2O_3 and Ga_2O_3) was carried out [33]. The addition of Ga_2O_3 or In_2O_3 to Y_2O_3, La_2O_3 and CeO_2 enhanced the formation of light alkenes.

The use of rare earths as promoters or supports in catalytic reactions has grown extensively due to interesting properties encountered in pollution control by catalysis or syngas conversion [34]. In pollution control the reducibility of some rare earth oxides has been put forward to explain the increase in performance of rare earth modified catalysts [35]. In syngas conversion both reducibility and basicity of rare earth oxides have been invoked [36]. On rare earth oxide supports, the high selectivity of Pd or Rh towards methanol synthesis is explained by the easy decomposition of carbon monoxide on basic sites of support [37]. Normand et al tested the influence of the support on the reactivity of Pd/rare earth oxide catalysts [38]. According to the results, they classified oxides into three classes (a) Oxides of the type Re_2O_3 which are unreducible, (b) CeO_2 where anion vacancies can be created extrinsically by reduction process, (c) Pr_6O_{11} and Tb_4O_7 where anion vacancies exist due to

nonstoichiometric nature of these oxides. In syngas conversion production of high alcohols is found to be favoured by the presence of intrinsic anion vacancies on Pr_6O_{11} and Tb_4O_7 supports.

Campbell et al studied the catalytic production of gas-phase methyl radicals from methane over lanthanide oxides and found that catalytic activity can be related to the basicity of oxides. Also pretreatment of oxides had a marked effect on activity [39,40].

Rare earth oxides exhibit activity as oxidation catalysts and have low work functions. Taking advantage of this property of rare earth oxides, negative oxide ions can be produced by negative surface ionisation. J.E.Delmore observed the in situ formation of ReO_4^- and ReO_3^- gas phase ions from rare earth oxide catalysed reaction of water with metallic Rhenium using a surface ionisation mass spectrometer [41].

Nakashima et al investigated the isomerisation of butenes over Samarium oxide and found that rate of reaction was proportional to the pressure of reactants [42].

Osuka et al observed that among rare earth oxides, Sm_2O_3 shows highest activity and selectivity for C_2-hydrocarbons in oxidative coupling of methane [43,44]. Whereas, Campbell et al found that La_2O_3 shows much higher activity than Sm_2O_3 in catalytic production of gas phase methyl radicals from methane [40]. It was pointed out that the relative activities of rare earth metal oxides parallel their basicities [40]. V.R.Choudhary and V.H.Rane compared the surface acidity and basicity of rare earth oxides with the catalytic activity towards oxidative coupling of methane [45]. Among the rare earth oxides, La_2O_3 showed highest activity and selectivity whereas lowest activity was shown by CeO_2. Comparison of acidity with catalytic activity indicated that apart from surface basicity, surface acidity also seemed to play a very significant role, particularly in deciding the C_2 selectivity.

These investigations, however, have been largely aimed at obtaining comparative kinetic data for the various oxides and relatively few details have been reported about the identities, modes of generation, active sites on rare earth oxides, or surface concentrations of catalytically active sites on rare earth oxides, or about the natures of their interactions with adsorbed or reacting molecules. The primary modes of surface interactions on the rare earth oxides remain largely undefined.

REFERENCES

1. K.Tanabe, "Solid Acids and Bases", Academic Press, New York, 1970.

2. T.Moeller, "The Chemistry of the Lanthanides", Pergamon, New York, 1973.

3. H.S.Taylor and H. Diamond, J. Am. Chem. Soc., **57**, 1251 (1935).

4. D.R. Ashmead, D.D. Eley and R. Rudham, J. Catal., **3**, 280 (1964).

5. P.L. Selwood, J. Catal., **22**, 123 (1971).

6. N.E. Topp, "The Chemistry of Rare Earth Elements", Elsevier, Amsterdam, 1965.

7. B.S. Hopkins and W.A. Taebel, Trans. Electrochem. Soc., **71**, 397 (1934).

8. C.B. McGough and G. Houghton, J. Phys. Chem., 65, 1887 (1961).

9. L.A. Sozanov, E.V. Artamonov and G.N. Mitrofanova, Kinet. Katal., **12**, 378 (1971).

10. K.M. Minachev, Proc. Int. Congr. Catal., 5th, 1972, 219 (1973).

11. T.T. Bakumenko and I.T. Chashenikova, Kinet. Katal., **10**, 796 (1969).

12. E.R.S. Winter, J. Catal., **22**, 158 (1971).

13. E. Cremer and E. Marschall, Monatsh. Chem., **82**, 840 (1951).

14. Y. Saito, Y. Yoneda and S. Makishima, Actes. Congr. Int. Catal., 2nd, 1960, 1937 (1961).

15. E.R.S. Winter, J. Catal., **15**, 144 (1969).

16. J.F. Read, J. Catal., **28**, 428 (1973).

17. J.F. Read and A.L. Grandlemix, J. Catal., **38**, 54 (1975).

18. J.F. Read, Canad. J. Chem., **50**, 490 (1972).

19. J.F. Read and E.W. Perkins, J. Catal., **42**, 443 (1976).

20. T. Hattori, J. Inoko and Y. Murakami, J. Catal., **42**, 60 (1976).

21. M.P. Rosynek and D.T. Magnuson, J. Catal., **46**, 402 (1971).

22. M.P. Rosynek and D.T. Magnuson, J. Catal., **48**, 417 (1977).

23. M.P. Rosynek and J.S. Fox, J. Catal., **49**, 285 (1977).

24. Kh.M. Minachev, Yu.S. Khodakov and V.S.Nakhshunov, J. Catal., **49**, 207 (1977).

25. J.A. Arias and P.W. Selwood, J. Catal., **33**, 284 (1974).

26. T. Inui and M. Funabiki, Chem. Lett., 251 (1978).

27. M. Ichikawa, J. Catal., **59**, 67 (1979).

28. Y. Takita, T. Yoko-O, N. Egashira and F.Hori, Bull. Chem. Soc. Jpn., **55**, 2653 (1982).

29. K. Otsuka, K. Jinno and A. Morikawa, Chem. Lett., 499 (1985).

30. C.H. Lin, K.D. Campbell, J. Wang and J.H. Lunsford, J. Phys. Chem., **90**, 534 (1986).

31. Y. Tong, M.P. Rosynek and J.H. Lunsford, J. Phys. Chem., **93**, 2896 (1989).

32. V.R. Choudhary, S.T. Choudhary, A.M. Rajput and V.H. Rane, J. Chem. Soc., Chem. Commun., 555 (1989).

33. T. Arai, K. Maruya, K. Domen and T. Onishi, Bull. Chem. Soc. Jpn., **62**, 349 (1989).

34. K.C. Tayor, "Catalysis-Science and Technology", Springer Verlag, Berlin, Vol.5, 1984, p.119.

35. J.C. Summers and A.J. Ausen, J. Catal., **58**, 131 (1979).

36. C. Diagne, M. Idriss, I. Pepin, J.P. Hindermann and A.Kiennemann, Appl. Catal., **50**, 43 (1989).

37. M.A. Vannice, G. Sudhakar and M. Freeman, J. Catal., **108**, 97 (1987).

38. F. Le Normand, J. Barrault, R. Breault, L. Hilaire and A.Kiennemann, J. Phys. Chem., **95**, 257 (1991).

39. C.H. Lin, K.D. Compbell, J.X.Wang and J.H.Lunsford, J. Phys. Chem., **90**, 534 (1986).

40. K.D. Campbell, H. Zang and J.H. Lunsford, J. Phys. Chem., **92**, 750 (1988).

41. J.E. Delmore, J. Phys. Chem., **91**, 2883 (1987).

42. Y. Nakashima, Y. Sakata, H. Immamura and S.Tsuchiya, Bull. Chem. Soc. Jpn., **63**, 3313 (1990).

43. K. Otsuka, K. Jonno and A. Morikawa, J. Catal., **100**, 353 (1986).

44. K. Otsuka, T. Komatsu, Chem. Lett., 483 (1987).

45. V.R. Choudhary and V.H. Rane, J. Catal., **130**, 411 (1991).

CHAPTER II

SURFACE ELECTRON PROPERTIES OF METAL OXIDES

2.1 ELECTRON DONOR-ACCEPTOR PROPERTIES

It is known that when strong electron acceptors or donors are adsorbed on metal oxides, the corresponding radicals are formed as a result of electron transfer between the adsorbate and the metal oxide surface [1].

The formation of negative radicals on surfaces of various oxides have been demonstrated [2-7]. Flockhart et al., obtained experimental evidence for the presence of electron donor sites on the surfaces of aluminas by electron spin resonance technique [8]. When tetracyanoethylene and 2,3,5,6-tetrachloro-1,4-benzoquinone were adsorbed on activated samples of gibbsite, γ-Al_2O_3 and η-Al_2O_3, corresponding anion radicals were formed. The adsorption of tetracyanoethylene on silica-alumina surfaces was also studied. In this respect, they associated the electron donor sites with the unsolvated hydroxyl ions and the defect centres involving oxide ions (4). B.D.Flockhart, K.Y.Liew and R.C.Pink found that the reduction of iodine to iodide ion occurs readily on the surface of partially dehydrated catalytic aluminas and silica aluminas [9]. An increase in alumina content results in an increase in reducing activity. The findings concur with those obtained on study of reduction of tetra-

cyanoethylene on alumina surface. B.D.Flockhart, I.M.Sesay and R.C.Pink observed that the preadsorption of Lewis acids or bases on the surface of an activated alumina leads to deactivation of reducing or oxidising function of the catalyst [10].

The presence of electron deficient centres on strongly dehydrated alumina surfaces sufficiently powerful to promote the formation of positive radical ions from aromatic hydrocarbons has also been demonstrated [11-16]. The formation of cationic species adsorbed on surfaces has been established by studies of the adsorption of hydrocarbons on silica-alumina catalysts [17-21]. K.Hirota, K.Kuwata and Y.Akagi reported the formation of anion species when tetracyanoethylene and benzophenone were adsorbed on zinc oxide or alumina in vacuo [22]. Chemisorption of O_2 on MgO was observed under conditions which involve different types of electron transfer processes; either from electron donor centres formed by irradiation or by addition of extrinsic impurity ions [23-26]. Carbondioxide is adsorbed as CO_2^- ions by electron transfer from S centres in irradiated Magnesium oxide [27]. A.J.Tench and R.L.Nelson studied the adsorption of nitro compounds on the surface of Magnesium oxide powder by esr

and reflectance spectroscopy [28]. They found that negative radicals are formed on clean magnesium oxide surfaces in vacuo whereas this no longer occurs if surface is contaminated with water and carbondioxide.

Edlund et al., observed the esr spectra of singly charged monomeric and dimeric cation radicals at 77 K in a γ-irradiated C_6H_6-silicagel system [29,30]. The formation of cation radical of triphenyl amine on surface of synthetic zeolites and anion radicals of naphthalene and biphenyl on silica gel have also been reported [31,32]. Kinell et al., detected the cation radicals of naphthalene, anthracene, phenanthrene and biphenyl adsorbed on silica gel by esr spectra [33].

It has been shown that specific adsorption occurs on the surface silanol groups and the adsorption on silica has been measured spectroscopically and heats of adsorption have been obtained [34,35]. M.L.Hair and W.Hertl measured the adsorption isotherms by volumetric, gravimetric and spectroscopic techniques on silica surfaces which have been modified in a variety of ways. For most of the adsorbates, freely vibrating hydroxyl group on silica surface is the strongest surface adsorption site [36].

Flockhart et al., described an investigation of the reduction of aromatic nitrocompounds on the surface of alumina and silica-alumina catalysts [37]. They observed that an increase in alumina content of latter results in an increase in reducing power and maximum reducing activity occurs with samples dehydrated at 600-700°C.

Several investigations have been reported on the esr spectra of methyl radicals stabilized on solid surfaces [38-41]. S.Kubota, M.Iwaizumi and T.Isobe investigated by esr the methyl radicals produced on silica gel surfaces, by photolysis of methyl iodide [42]. They estimated the adsorption sites for these radicals to be siloxane groups.

The effect of dehydroxylation of silica surface on the adsorption of various molecules have been studied using IR spectroscopy [43,44]. Yu A.Eltekov, V.V.Khopina and A.V.Kieselev investigated the adsorption of a series of aromatic hydrocarbons from solution in saturated hydrocarbons on hydroxylated and dehydroxylated silica surfaces [45]. They found that dehydroxylation of surface sharply diminishes the adsorption of aromatic hydrocarbons.

Richardson generated several polyacene cations in copper-modified faujasites and concluded that cations are

formed by electron transfer at the surface [46]. L.Petrakis and K.S.Seshadri generated the radical ion of thianthrene and studied on a variety of oxide surfaces including SiO_2-Al_2O_3 and Molybdena-alumina [47]. The spectral features of thianthrene radical on surfaces are identical with spectral feature of thianthrene monopositive radical ion in frozen sulfuric and boric acids.

In comparing the model of Lewis acidity or basicity of a surface with surface state model, Morrison suggested that basic centres can, in many cases, be coincident with sites providing surfaces states [48]. D.Cordischi and V.Indovina investigated the electron donor properties of CaO, MgO, ZnO, Al_2O_3 and SiO_2-Al_2O_3 activated in vacuo at temperatures upto 1200 K using esr of adsorbed nitro radicals as a probe [49]. The results indicated the existence of a correlation between electron donor activity of oxides and their Lewis base strength.

The active sites on surface of silica-alumina cracking catalyst are assumed to be either Bronsted or Lewis acid which may be interconverted by addition or removal of traces of H_2O [50-55]. J.B.Peri proposed a semiquantiative model for surface of silica-alumina

catalyst in which acid sites of various types are assumed to be created by attachment and subsequent bridging reactions of Al-OH groups on a silica surface [56].

Fowkes et al., have studied the adsorption of acidic and basic molecules from neutral solvents on iron oxide, silica and titania [57]. They found that the calorimetric heats of adsorption are actually the heats of acid-base interaction governed by the Drago equation [58]. Furthermore, Fowkes has extended this acid-base interaction theory to polymer-powder interfaces [59].

The formation of radicals of acetylene on the surface of alumina-CuO catalysts demonstrated the dual-nature of alumina-CuO surface [60]. I.Bodrikov, K.C.Khulbe and R.S.Mann studied the electron donor and acceptor properties of γ-alumina, silica and γ-alumina and silica supported palladium oxide [61]. It was observed that while γ-alumina had both electron donor and acceptor characteristics, γ-alumina supported palladium oxide showed better acceptor properties than donor properties. Silica supported palladium oxide showed only electron acceptor properties.

M.A.Enriquiz and J.P.Fraissard carried out a comparative study of variation of surface properties and catalytic activity of TiO_2 samples with their *in vacuo* pretreatment temperature [62]. The results showed that active sites are electron donor centres, number of which has been determined by adsorption of tetracyanoethylene and trinitrobenzene. These centres are Ti^{3+} ions and O-Ti-OH groups for high and low pretreatment temperatures respectively.

Terephthalic acid adsorbed on to alumina from alcohol solution was studied by using inelastic electron tunneling spectroscopy [63]. A comparison with tunneling spectrum of p-acetyl benzoic acid showed that terephthalic acid is adsorbed predominantly as a monocarboxylate ion onto alumina surface.

Meguro *et al.*, studied the adsorption of electron acceptors on metal oxides to estimate the electron donor properties of a number of metal oxides and their surface characterisation [64-66]. H.Hosaka, T.Fujiwara and K.Meguro investigated the electron donor properties of MgO, SiO_2, TiO_2, ZnO and NiO by adsorption of 7,7,8,8-tetracyanoquinodimethane (TCNQ) [66]. When TCNQ was adsorbed on

surfaces on metal oxides, their surfaces acquired colouration characteristic of each oxide. The order of radical forming activity was obtained from esr spectra as follows: $MgO \rangle ZnO \rangle Al_2O_3 \rangle TiO_2 \rangle SiO_2$.

M.Che, C.Naccache and B.Imelik carried out a systematic study of the adsorption of tetracyanoethylene and trinitrobenzene on the surface of titania and magnesia [67]. They associated the electron donor centres with OH^- groups present on surfaces of solids activated at low temperature and co-ordinated O^{2-} ions at higher temperature.

K.Esumi and K.Meguro investigated the strength and distribution of electron donor sites on Al_2O_3, TiO_2 and ZrO_2-TiO_2 by adsorption of TCNQ, 2,5-dichloro-p-benzoquinone (DCQ), p-dinitrobenzene (PDNB) and m-dinitrobenzene (MDNB) [64,65]. The limiting amounts adsorbed and the radical concentrations formed were found to decrease with decreasing electron affinity of electron acceptor. The limit of electron transfer from Al_2O_3 surface to the electron acceptor ranged between 1.77 and 1.26 eV in the affinity of electron acceptor. The results indicated that the electron donor strengths of Al_2O_3 and TiO_2 are similar

and stronger than ZrO_2-TiO_2. The distribution of electron donor sites having different strengths on Al_2O_3 was larger than that on TiO_2 and ZrO_2-TiO_2. The electron donor property of zirconia was investigated by adsorption of TCNQ [68]. The radical concentration decreased with an increase in calcining temperature, reached a minimum value at 700°C, and then increased. Also, four electron acceptors with varying electron affinity were adsorbed from acetonitrile solution on to a titania sample [69]. It was observed that limit of electron transfer from titania surface to acceptor ranged between 1.77 and 1.26 eV which is the same as that of Al_2O_3.

The electronic state of adsorbed species was studied by UV-Vis Spectroscopy in addition to esr spectroscopy [64-66]. The bands near 600 nm were related to the dimeric TCNQ anion radical which absorbs light at 643 nm [70]. This tentative attribution was supported by the characteristic features that neutral TCNQ absorbs only at 395 nm, that TCNQ has a high electron affinity and TCNQ anion radicals are stable even at room temperature [71-74]. ESR and electronic spectra provided evidence that TCNQ anion radicals are formed as a result of electron transfer from metal oxide surface to adsorbed TCNQ.

The electron donor properties of two component metal oxide systems, SiO_2-Al_2O_3, SiO_2-TiO_2, Al_2O_3-TiO_2 and ZrO_2-TiO_2 were studied by means of TCNQ adsorption [75,76]. Two component metal oxides showed lower radical forming activity than parent oxides and change in activity with composition was characteristic of each metal oxide system. These systems exhibited electron donor properties which would not be qualitatively predicted from consideration of the independent properties of the parent oxides [77,78].

Esumi et al., studied the solvent effect on the acid-base interaction of electron acceptors with metal oxides, Al_2O_3 and TiO_2 [79,80]. The saturated amount of TCNQ adsorbed decreased considerably with increasing basicity of solvent or acidity of solvent for both metal oxides. The results were interpreted in terms of acid-base theory by Drago equation [58]. TCNQ radical concentrations for both metal oxides decreased with increasing basicity of solvent. TCNQ adsorption on metal oxides was found to be strongly influenced by interaction between basic solvents and TCNQ or between acidic solvents and donor sites of metal oxides. Similarly, acid-base interaction at solid-liquid interface has also been confirmed to be important for the adsorption of tetrachloro-p-benzoquinone from

various solvents [81]. Solvent effect of several aromatic solvents on charge transfer adsorption of TCNQ onto metal oxides was also studied and found that TCNQ radical concentration depends on ionisation potential of solvent [82].

The adsorption of TCNQ anion radical salts on alumina from acetonitrile solution was studied by measuring the adsorption isotherm, esr and electronic spectra of adsorbed TCNQ anion radical salts [83]. The order of adsorbed amount at the same equilibrium concentration was $Li^+ TCNQ^- > Na^+ TCNQ^- > K^+ TCNQ^-$. Applying the relationship between solubility and chemical potential expressed by Miller [84], it was found that adsorption of TCNQ anion radical salts on alumina is not affected by solubility, but depends on nature of cation.

K.Esumi and K.Meguro determined the basicity of Al_2O_3, TiO_2 and ZrO_2-TiO_2 by titration and electron acceptor adsorption [85]. The distribution of sites having different basicity were similar for alumina and titania with respect to Lewis and Bronsted sites. In zirconia-titania binary system, only Lewis sites existed. K.Esumi, K.Magura and K.Meguro measured the zeta potentials of Al_2O_3

and TiO_2 by adsorption of TCNQ from organic solvents [86]. They found that the zeta potential of oxide decreased with increasing concentration of TCNQ in acetonitrile and ethyl acetate indicating that TCNQ anion radicals formed on oxide contribute to the decrement in zeta potential.

It has been suggested that two types of donor sites exist on oxide surfaces responsible for electron transfer process [69]. The first type consists of a defect centre involving oxide ions and second is a hydroxyl ion on the oxide surface. Fomin et al., have shown that electron transfer from hydroxyl ion can and does occur in certain solvent systems provided a suitable acceptor is present [87]. Lee and Weller confirmed the existence of surface hydroxyl groups on Al_2O_3 which had been dehydrated at 500°C [88]. The existence of surface hydroxyl groups on MgO has also been observed [89]. Surface silanol groups are found to be more stable than Al-OH groups [90]. Differences in acidity between the hydroxyl groups on several oxide surfaces have been reported [91]. It has been suggested that hydroxyl ions of metal oxide surfaces have different electron donor properties.

The electron donicity of metal oxides were found to be enhanced by a low temperature plasma treatment. The

electron donicity was found to increase by ammonia and nitrogen plasma treatments [92-95].

2.2 ACIDIC AND BASIC PROPERTIES

Solid acids and bases have found uses as catalysts for many important reactions involving cracking of hydrocarbons, isomerization, polymerization and hydration of olefins, alkylation of aromatics and dehydration of alcohols. Systematic study of correlation between catalytic activity and the acidic and basic properties of catalyst surface has enabled the identification of optimum catalyst in terms of acidic and basic properties.

Titration Method

Walling described acid strength of a solid as the ability of the surface to convert an adsorbed neutral base into its conjugate acid and can be expressed by Hammett acidity function [96,97]. The amine titration method was first reported by Tamele [98]. O.Johnson developed a method for determination of acidity of solid surfaces, which consists of titration of solid suspended in benzene with n-butyl amine using p-dimethylaminoazobenzene as the indicator [99]. The use of various indicators with different pKa values enabled a determination of the amount

of acid at various acid strengths by amine titration. Benesi tried to modify the titration technique so that indicators could be added to portions of catalyst in suspension after the catalyst sample had reached equilibrium with n-butyl amine, the end point being determined by a series of approximations (100, 101). Benesi determined the acid strengths of alumina, silica, magnesia mounted acids and cracking catalysts using this method. Hirschler proposed the use of acidity function H_R for determination of protonic surface acidity and used a series of arylmethanols and diphenylmethane as indicators [102]. The transformation of an indicator into its conjugate acid form can be detected spectrometrically and spectroscopic method was introduced by Leftin, Hobson and Terenin [103,104]. Drussel and Sommers presented the use of a series of fluorescent indicator for use in spectrofluorometric titration [105]. UV spectrophotometry has been applied for measurement of acid strength of silica-alumina catalysts using 4-benzeneazodiphenylamine, 4-nitroaniline and 2,4-dinitroquinoline [106]. Titrations of dark coloured solids can be carried out by adding a small known amount of a white solid acid and using this method acid strength and acid amount have been measured for chromic oxide employing alumina as standard material [107].

J.Take, H.Kawai and Y.Yoneda proposed a new method which involves the titration of a solid acid with indicator itself in a nonpolar solvent [108]. The titration of silica-alumina with 4-anilinoazobenzene yielded an acid content smaller than the n-butyl amine titration method with the same indicator. Yoneda and coworkers made a critical analysis of the conditions required for the establishment of adsorption equilibrium in n-butyl amine titration of acid surfaces [109]. Balikova found that butyl amine titer is dependant upon the physical conditions of experiment [110]. T.Yamanaka and K.Tanabe proposed a method of determining basicity at various basic strengths by titrating solid suspended in benzene with trichloro acetic acid using a series of Hammett indicators [111]. The strongest Ho value was termed Ho_{max} and a correlation was found between Ho_{max} and the effective negative charges on combined oxygens [112]. Several reviews dealing with surface acidity and basicity of solid catalysts have been published [113-116]. Malinowski et al., measured the acid base strength of MgO by using bromocresol purple, methyl red and bromophenol blue indicators [117,118]. A series of UV spectroscopic studies have been made for indicators adsorbed on alkaline earth metal oxides and absorption maxima of spectra was correlated with the basic strength of

solid [119,120]. Pure silicagel showed neither acidic nor basic properties while silica treated with ammonium fluoride possessed a large population of strong Bronsted acid sites [121]. Commercial zinc oxide had acid sites corresponding to an Ho value of +4.8 and heat treatment increased the acidity [122]. Acidic properties of chromium oxide was studied and found that acidity in oxidised state is twice that in reduced state [107]. V_2O_5, As_2O_3 and heat treated CeO_2 produced characteristic colour changes in dimethyl yellow and methyl red [123]. Silica-alumina was found to contain very strong acid sites with strength Ho of at least -8.2 [53]. The acidic properties of alumina-boria have been measured by Izumi and Shiba and maximum acidity was obtained when concentration of B_2O_3 is 15 wt. % [124].

J.Take, N.Kikuchi and Y.Yoneda developed a method for the determination of basic strength of solid surfaces which consist of titration of solids suspended in cyclohexane with benzoic acid using a series of H^- indicators [125]. They found that base strength of alkaline earth oxides increased remarkably upon heat treatment in vacuum and basicity decreased in the order $SrO \simeq CaO > MgO$. T.Iizuka, K.Ogasawara and K.Tanabe examined the acid strength of $Nb_2O_5.nH_2O$ by indicator

adsorption method [126]. The surface of $Nb_2O_5.nH_2O$ showed strong acidic character which disappeared on heat treatment at higher temperatures. P.A.Burke and E.I.Ko also observed that acidity of Niobia diminishes with increase in calcination temperature [127]. Basicity of Alumina-Magnesia catalysts have been studied and in the series of Al_2O_3, MgO and Al_2O_3-MgO catalysts, those containing about 75% Al_2O_3 and 25% MgO showed highest basicity [128]. G.W.Wang, H.Hattori and K.Tanabe measured the acid-base properties of ZrO_2-SnO_2 with different compositions by indicator method and ZrO_2-SnO_2 catalyst with atomic ratio 9:1 was found to have highest acid strength [129]. Furuyama et al., investigated the variations in acid amount of hydroxylated and hydrothermally activated silica-alumina catalysts with pretreatment temperature. T.Yamanaka and K.Tanabe determined the basicity of a series of oxides and found that basicity at basic strength ($Ho \geq 1.5$) has the order $ZnO > TiO_2 > \gamma\text{-}Al_2O_3 > BaO >$ activated $Al_2O_3 > B_2O_3 > ZrO_2 > MgSO_4 > MoO_3$ [111]. Tanabe et al., measured the acidity of TiO_2-ZnO by butylamine titration and observed that TiO_2-ZnO containing about 7 to 57% ZnO showed very large acid amount of 0.5-0.9 m mol/g and high acid strength of $Ho \leq -3$ [130]. Fedorynska et al.

studied the acidic and basic properties of alumina-silica catalysts [131]. They found that basicity of alumino-silicates is closely associated with the amount of alumina in the mixed oxide and decreased with decrease in amount of alumina. Also, the samples containing small quantity of SiO_2 in Al_2O_3 and small amount of Al_2O_3 in silica exhibited strongest acid properties. J.L.Zotin and A.C.Faro Jr., prepared alumina from different aluminium hydroxides and characterised with respect to their acidic and basic properties [132].

The acidic properties of single oxides TiO_2, SiO_2, Al_2O_3 and binary systems TiO_2-Al_2O_3, TiO_2-ZnO, SiO_2-ZnO, SiO_2TiO_2, ZnO-Bi_2O_3 and Al_2O_3-MgO have been studied [133-137]. Many combinations of transition metal oxides like TiO_2-MoO_3, TiO_2-V_2O_5, ZnO-FeO_3 and WO_3-TiO_2 have also been found to show remarkable acid properties [138-143]. C.G.R.Nair and co-workers carried out the acidity evaluations of TiO_2-SiO_2-Al_2O_3 catalysts using butylamine titration [144]. A comparative study of acid properties of TiO_2, SiO_2, Al_2O_3, SiO_2-Al_2O_3, SiO_2-TiO_2, Al_2O_3-TiO_2 and TiO_2-SiO_2-Al_2O_3 have also been carried out [145]. Single oxides were found to have low acid strength and TiO_2-SiO_2-Al_2O_3 of 10% by weight of TiO_2 showed highest acid amount.

The acidity of MoO_3-SiO_2-Al_2O_3 have been evaluated using butylamine titration technique and found that incorporation of MoO_3 reduced the acid strength of silica-alumina [146].

The acid-base nature and catalytic activity of rare earth oxides have been reviewed [116]. The rare earth oxides have been classified as base catalysts on the basis of the O_{1S} binding energy study of oxides [147]. Nakashima et al., measured the basicity of samarium oxide by benzoic acid titration method [148]. V.H.Rane and V.R.Choudhary compared the acid and base strength distribution of rare earth oxides by stepwise thermal desorption of CO_2 and temperature programmed desorption of carbondioxide [149]. Lanthanum oxide showed highest surface basicity and strong basic sites whereas cerium oxide and samarium oxide catalysts showed lowest surface basicity. Lanthanum oxide catalyst also showed highest surface acidity but all of its acid sites are of intermediate strength. Both weak and strong acid sites were present on Ytterbium oxide, Europium oxide, Samarium oxide and Cerium oxide catalyst. The strongest acid sites were observed on cerium oxide catalyst.

REFERENCES

1. J.J. Rooney and R.C. Pink, Trans. Faraday Soc., 58, 1632 (1962).

2. B.D. Flockhart, I.R. Leith and R.C. Pink, Chem. Commun., 885 (1966).

3. B.D. Flockhart, I.R. Leith and R.C. Pink, J. Catal., 9, 45 (1967).

4. B.D. Flockhart, I.R. Leith and R.C. Pink, Trans. Faraday Soc., 65, 542 (1969).

5. D.Cordischi, V. Indovina and A. Cimino, J. Chem. Soc. Faraday Trans., 70, 2189 (1974).

6. V.V. Subba Rao, R.D. Iyengar and A.C. Zettlemoyer, J. Catal., 12, 278 (1968).

7. C. Naccache, Y. Kodratoff, R.C. Pink and B. Imelik, J. Chem. Phys., 63, 341 (1966).

8. B.D. Flockhart, C. Naccache, J.A.N. Scott and R.C. Pink, Chem. Commun., 238 (1965).

9. B.D. Flockhart, K.Y. Liew and R.C. Pink, J. Catal., 32, 20 (1974).

10. B.D. Flockhart, I.M. Sesay and R.C. Pink, J. Chem. Soc. Faraday Trans. I, 79, 1009 (1983).

11. A.J. deRossert, C.G.Finstrom and C.J. Adams, J. Catal., 1, 235 (1962).

12. E.P. Parry, J. Catal., 2, 371 (1963).

13. W.K. Hall, H.P. Leftin, F.J. Cheseleke and D.E. O'Reilly, J. Catal., 2, 506 (1963).

14. J.A.N. Scott, B.D. Flockhart and R.C. Pink, Proc. Chem. Soc., 139 (1964).

15. B.D.Flockhart, J.A.N. Scott and R.C. Pink, Trans. Faraday Soc. 62, 730 (1966).

16. A. Terenin, Adv. Catal., 15, 256 (1964).

17. D.M. Brouwer, Chem. Ind., 177 (1961).

18. J.J. Rooney and R.C. Pink, Proc. Chem. Soc., 70 (1961).

19. W.K. Hall, J. Catal., 1, 53 (1962).

20. H.P. Leftin and M.C. Hobson Jr., Advan. Catal., 14, 372 (1963).

21. R.P. Porter and W.K. Hall, J. Catal., 5, 366 (1966).

22. K. Hirota, K. Kuwata and Y. Akagi, Bull. Chem. Soc. Jpn., 38(12) 2209 (1965).

23. R.L. Nelson, A.J. Tench, J. Chem. Phys., 40, 2763 (1964).

24. A.J. Tench and R.L. Nelson, J. Chem. Phys., 44, 1714 (1966).

25. R.L. Nelson, A.J. Tench and B.J. Harmsworth, Trans. Faraday Soc., 63, 1427 (1967).

26. J.H. Lunsford and J.P. Jayne, J. Chem. Phys., 44, 1487 (1966).

27. J.H. Lunsford and J.P. Jayne, J. Phys. Chem., 69, 2182 (1965).

28. A.J. Tench and R.L. Nelson, Trans. Faraday Soc., 63, 2254 (1967).

29. O. Edlund, P.O. Kinell, A. Lund and A. Shimizu, J. Chem. Phys., 46, 3678 (1967).

30. O. Edlund, P.O. Kinell, A. Lund and A. Shimizu, "Advances in chemistry series", No.82, American Chemical Society, Washington DC, 1968, p.311.

31. D.N. Stamires and J. Turkevich, J. Am. Chem. Soc., 86, 749 (1964).

32. P.K. Wong and J.E. Willard, J. Phys. Chem., 72, 2623 (1968).

33. P.O. Kinell, A. Lund and A. Shimizu, J. Phys. Chem., 73, 4175 (1969).

34. M.R. Basila, J. Chem. Phys., 35, 1151 (1961).

35. W. Herth and M.L. Hair, J. Phys. Chem., 72, 4676 (1968).

36. M.L. Hair and W. Hertl, J. Phys. Chem., 73, 4269 (1969).

37. B.D. Flockhart, I.R. Leith and R.C. Pink, Trans. Faraday Soc., 66, 469 (1970).

38. J. Turkevich and Y. Fujita, Science, 152, 1619 (1966).

39. M. Fujimoto, H.D. Gesser, G.B. Garbutt and M. Shimizu, Science, 156, 1105 (1967).

40. G.B. Garbutt, H.D. Gesser, and M. Fujimoto, J. Chem. Phys., 48, 4605 (1968).

41. N. Shimamoto, Y. Fujita and T. Kwan, Bull. Chem. Soc. Jpn., 43, 580 (1970).

42. S. Kubota, M. Iwaizumi and T. Isobe, Bull. Chem. Soc. Jpn., 44, 2684 (1971).

43. A.V. Kieselev, Disc. Faraday Soc., 40, 205 (1965).

44. C. Curthoys and B.A. Elkingston, J. Phys. Chem., 72, 3475 (1968).

45. Yu A. Eltekov, V.V. Khopina and A.V. Kieselev, J. Chem. Soc. Faraday Trans., 68, 889 (1972).

46. J.T. Richardson, J. Catal., 9, 172 (1967).

47. L. Petrakis and K.S. Seshadri, J. Phys. Chem., 76, 1443 (1972).

48. S.R. Morrison, Surface Sci., 50, 329 (1975).

49. D. Cordischi and V. Indovina, J. Chem. Soc. Faraday Trans., 72(10), 2341 (1976).

50. A.E. Hirschler and J.O. Hudson, J. Catal., 3, 239 (1964).

51. A.E. Hirschler, J. Catal., 5, 390 (1966).

52. A.E. Hirschler, J. Catal., 6, 1 (1966).

53. M.R. Basila, T.R. Kantner and K.H. Rhee, J. Phys. Chem., 68, 3197 (1964).

54. K.G. Miesserov, J. Catal., 13, 169 (1969).

55. H.R. Gerberich and W.K. Hall, J. Catal., 5, 99 (1966).

56. J.B. Peri, J. Catal., 41, 227 (1976).

57. F.M. Fowkes, Y.C. Huang, B.A. Shah, M.J. Kulp and T.B. Lloyd, Colloids Surf., 29, 243 (1988).

58. R.S. Drago, L.B. Parr and C.S. Chamerlain, J. Am. Chem. Soc., 99, 3203 (1977).

59. F.M. Fowkes in "Physicochemical aspects of polymer surfaces", K.L. Mittal (Ed.) Vol.2, Pleneum Press, New York (1983), p.583.

60. R.S. Mann and K.C. Khulbe, J. Catal., 42, 115 (1976).

61. I. Bodrikov, K.C. Khulbe and R.S. Mann, J. Catal., 43, 339 (1976).

62. M.A. Enriquez and J. P. Fraissard, J. Catal., 74, 77 (1982).

63. S. Kamata and M. Higo, Chem. Lett., 2017 (1984).

64. K. Meguro and K. Esumi, J. Colloid Interface Sci., 59, 93 (1977).

65. K. Esumi and K. Meguro, J. Colloid Interface Sci., 66, 192 (1978).

66. H. Hosaka, T. Fujiwara and K. Meguro, Bull. Chem. Soc. Jpn., **44**, 2616 (1972).

67. M. Che, C. Naccache and B. Imelik, J. Catal., **24**, 328 (1972).

68. K. Esumi and K. Meguro, Bull. Chem. Soc. Jpn., 55, 315 (1982).

69. K. Esumi and K. Meguro, Bull. Chem. Soc. Jpn., 55, 1647 (1982).

70. R.H. Boyd and W.D. Phillips, J. Chem. Phys., 43, 2927 (1965).

71. D.S. Acker, R.J. Harder, W.R. Hertler, W. Mahler, L.R. Melby, R.E. Benson and W.E. Mochel, J. Am. Chem. Soc., 82, 6408 (1960).

72. R.G. Kepler, P.E. Bierstedt and R.E. Merrifield, Phys. Rev. Lett., 5, 503 (1960).

73. D.B. Chesnut, H. Fosker and W.D. Phillips, J. Chem. Phys., 34, 684 (1961).

74. L.R. Melby, R.J. Harder, W.R. Hertler, W. Mahler, R.E. Benson and W.E. Mochel, J. Am. Chem. Soc., 84, 3374 (1962).

75. H. Hosaka, N. Kawashima and K. Meguro, Bull, Chem. Soc. Jpn., 45, 3371 (1972).

76. K. Esumi, H. Shimiada and K. Meguro, Bull. Chem. Soc. Jpn., 50, 2795 (1977).

77. H. Murayama, K. Kobayashi, M. Koishi and K. Meguro, J. Colloid Interface Sci., 32, 470 (1970).

78. H. Murayama and K. Meguro, Bull. Chem. Soc. Jpn., 43, 2386 (1970).

79. K. Esumi, K. Miyata and K. Meguro, Bull. Chem. Soc. Jpn., 58, 3524 (1985).

80. K. Esumi, K. Miyata, F. Waki and K. Meguro, Colloids Surf., 20, 8 (1986).

81. K. Esumi, K. Miyata, F. Waki and K. Meguro, Bull Chem. Soc. Jpn., 59, 3363 (1986).

82. H. Hosaka and K. Meguro, Colloid Polymn. Sci., 252, 322 (1974).

83. K. Esumi and K. Meguro, J. Colloid and Interface Sci., 61, 191 (1977).

84. L. Miller, J. Phys. Chem. 1, 653 (1897).

85. K. Esumi and K. Meguro, J. Jpn. Soc. Color. Mat., 58, 9 (1985).

86. K. Esumi, K. Magara and K. Meguro, J. Colloid and Interface Sci., 141(2), 578 (1991).

87. G.V. Fomin, C.A. Blyumenfield and V.I. Sukhorukov, Proc. Acad. Sci., 157, 819 (1964).

88. J.K. Lee and S.W. Weller, Anal. Chem., 30, 1057 (1958).

89. P.J. Anderson, R.F. Horlock and P.J. Oliver, Trans. Faraday Soc., 61, 2754 (1965).

90. H.P. Boehm, Adv. Catal., 16, 179 (1966)

91. M.L. Hair and L. Hertl J. Phys. Chem. 74, 91 (1970).

92. M. Sagiura, K. Esumi, K. Meguro and H. Honda, Bull. Chem. Soc. Jpn., 58, 2638 (1985).

93. K. Esumi, M. Sagiura, T. Mori, K. Meguro and H. Honda, Colloids Surf., 19, 331 (1986).

94. K. Esumi, N. Nashiuchi and K. Meguro, J. Surf. Sci. Technol., 4, 207 (1988).

95. K. Meguro and K. Esumi, J. Adhesion Sci. Technol., 4(5), 393 (1990).

96. C. Walling, J. Am. Chem. Soc., 72, 1164 (1950).

97. Hammett and Deyrup, J. Am. Chem. Soc., 54, 2721 (1932).

98. M.W. Tamele, Disc. Faraday Soc., 8, 270 (1950).

99. O. Johnson, J. Phys. Chem., 59, 827 (1955).

100. H.A. Bensi, J. Am. Chem. Soc., 78, 5490 (1956).

101. H.A. Bensi, J. Phys. Chem., 61, 970 (1957).

102. A.E. Hirschler, J. Catal., 2, 428 (1963).

103. H.P. Leftin and M.C. Hobson, Advan. Catal., 14, 115 (1963).

104. A.N. Terenin, Adv. Catal., 15, 227 (1964).

105. H.V. Drussel and A.L. Sommers, J. Anal. Chem., 38, 1723 (1966).

106. J. Take, T. Tsuruya, T. Sato and Y. Yoneda, Bull. Chem. Soc. Jpn., 45, 3409 (1972).

107. S.E. Voltz, A.E. Hirschler and A. Smith, J. Phys. Chem., 64, 1594 (1960).

108. J. Take, H. Kawai and Y. Yoneda, Bull. Chem. Soc. Jpn., 50, 2428 (1977).

109. J. Take, Y. Nomizo and Y. Yoneda, Bull. Chem. Soc. Jpn., **46**, 3568 (1973).

110. M. Balikowa, React. Kinet. Catal. Lett., 2, 323 (1975).

111. T. Yamanaka and K. Tanabe, J. Phys. Chem., 79, 2409 (1975).

112. T. Yamanaka and K. Tanabe, J. Phys. Chem., 80, 1723 (1976).

113. J. Kijenski and A. Baiker, Catal. Today, 5 (1989).

114. F. Forni, Catal. Rev., 8, 69 (1977).

115. K. Tanabe, "Solid acids and Bases--Their catalytic properties", Kodansha, Tokyo (1970).

116. K. Tanabe, M. Misono, Y. Ono and H. Hattori, "New solid acids and bases", Kodansha, Elsevier, New York (1989).

117. S. Malinowski and S. Sczepanska, J. Catal., 2, 310 (1963).

118. S. Malinowski, S. Sczepanska, A. Bielanski and J. Sloczynski, J. Catal., 4, 324 (1965).

119. H. Zeitlin, R. Frei and M. Mccarter, J. Catal., 4, 77 (1965).

120. H.E. Zaugg and A.D. Schaffer, J. Am. Chem. Soc., 87, 1857 (1965).

121. I.D. Chapman and M.L. Hair, J. Catal., 2, 145 (1963).

122. E. Marihari and G. Parravano, J. Am. Chem. Soc., 75, 5233 (1953).

123. K. Tanabe and K. Katayama, J. Res. Inst. Catalysis, Hokkaido Univ., 7, 106 (1959).

124. Y. Izumi and T. Shiba, Bull. Chem. Soc. Jpn., 37, 1797 (1964).

125. J. Take, N. Nikuchi and Y. Yoneda, J. Catal., 21, 164 (1971).

126. T. Iizuka, K. Ogasawara and K. Tanabe, Bull. Chem. Soc. Jpn., 56, 2927 (1983).

127. P.A. Burke and E.I. Ko, J. Catal., 129, 38 (1991).

128. L. Nondek and J. Malek, React. Kinet. Catal. Lett., 14(3), 381 (1980).

129. G.W. Wang, H. Hattori and K. Tanabe, Bull. Chem. Soc. Jpn., 56, 2407 (1983).

130. K. Tanabe, C. Ishiya, I. Matsuzaki, I. Ichikawa and H. Hattori, Bull. Chem. Soc. Jpn., 45, 47 (1972).

131. E. Fedorynska, T. Wozniewski, S. Malinowski, E. Ahmed and A. Madura, J. Colloid and Interface Soc., 69, 469 (1979).

132. J. L. Zotin and A.C. Faro Jr., Appl. Catal., 75, 57 (1991).

133. R. Rodenas, T. Yamaguchi, H. Hattori and K. Tanabe, J. Catal., 69, 434 (1981).

134. K. Tanabe, C. Ishiya, I. Matsuzaki, I. Ichikawa and H. Hattori, Bull. Chem. Soc. Jpn., 45, 47 (1972).

135. K. Tanabe, T. Sumiyoshi and H. Hattori, Chem. Lett., 723 (1972).

136. K. Tanabe, M. Ito and M. Sato, Chem. Commun., 676 (1973).

137. K. Shibata, T. Kiyoura, K. Kitagawa, T. Sumiyoshi and K. Tanabe, Bull. Chem. Soc. Jpn., 46, 2985 (1973).

138. T. Morimoto, J. Imai and M. Nagao, J. Phys. Chem., 78, 704 (1974).

139. H.A. benesi and B.H.C. Winguest, Adv. Catal., 27, 123 (1978).

140. M. Ai, Bull. Chem. Soc. Jpn., 49, 1328 (1976).

141. H. Miyata, K. Fuji, T. Ono, J. Chem. Soc. Faraday Trans., 1, 84, 3121 (1988).

142. T. Kotanigawa, Bull. Chem. Soc. Jpn., 47, 950 (1974).

143. A. Andreini and J.C. Mol, J. Chem. Soc., Faraday Trans., 1, 81, 1705 (1985).

144. K.R. Sabu, K.V.C. Rao and C.G.R. Nair, Bull. Chem. Soc. Jpn., 63, 3632 (1990).

145. K.R. Sabu, K.V.C. Rao and C.G.R. Nair, Bull., Chem. Soc. Jpn., 64, 1920 (1991).

146. K.R. Sabu, K.V.C. Rao and C.G.R. Nair, Bull. Chem. Soc. Jpn., 64, 1926 (1991).

147. H. Vinek, H. Noller, M. Ebel and K. Schwarz, J. Chem. Soc. Faraday Trans., 1, 73, 734 (1977).

148. Y. Nakashima, Y. Sakata, H. Immamura and S. Tsuchiya, Bull. Chem. Soc. Jpn., 63, 3313 (1990).

149. V.R. Choudhary and V.H. Rane, J. Catal. 130, 411 (1991).

CHAPTER III

RESULTS AND DISCUSSION

A perusal of the earlier work in the field of electron donating properties of metal oxides revealed that no effort has been made to study the surface electron properties of rare earth oxides though they are widely used as catalysts and supports in many reactions.

We have attempted to study the surface electron properties of three rare earth oxides Y_2O_3, Pr_6O_{11} and Nd_2O_3. The surface electron properties of metal oxide depend on the activation temperature. Hence the effect of activation temperature on electron transfer is reported. In the case of paramagnetic metal oxide, the extent of electron transfer from metal oxide during chemisorption can be measured as the change in the magnetic moment of the metal oxide. Hence the magnetic properties of the metal oxides as a function of equilibrium concentration of the electron acceptor is studied, in the case of paramagnetic oxides Pr_6O_{11} and Nd_2O_3. Another property that is directly related to the electron transfer between adsorbent and the electron acceptor is the surface acidity and basicity of the metal oxides. Hence the distribution and surface basic strength and acidic strength of the oxides are studied using a series of Hammett indicators. The electron donor properties obviously depend on the basicity of the solvent.

These properties are studied as a function of the basicity of the solvent using three solvents--acetonitrile, ethyl acetate and 1,4-dioxan in the order of increasing basicity. On the surfaces of metal oxides, the electron donor sites are distributed from low electron affinity to a high electron affinity. To study the distribution of electron donor sites, electron acceptors of various electron affinity are used (Table 1).

Table 1 Electron acceptors used

Electron acceptor	Electron affinity (eV)
7,7,8,8-tetracyanoquino-dimethane (TCNQ)	2.84
2,3,5,6-tetrachloro-p-benzo-quinone (chloranil)	2.40
p-dinitrobenzene (PDNB)	1.77
m-dinitrobenzene (MDNB)	1.26

The surface properties of metal oxides depend on method of preparation. The rare earth oxides were prepared by two routes--hydroxide and oxalate method and their

properties are compared. Mixed oxides are also quite often used in industries. The electron transfer and acid-base properties of rare earth oxide-alumina system are studied from 0 to 100% rare earth oxide. The anion of the medium from which hydroxide of the rare earth metal is precipitated plays an important role in surface properties. Hence mixed oxides were prepared by co-hydrolysis from their nitrate and sulfate solutions and their surface electron transfer properties are studied.

The systems under study (in brief) can be listed as follows:

a) Y_2O_3 at activation temperature 300, 400, 500, 600 and 800°C.

b) Y_2O_3-Al_2O_3: 5%, 10%, 15% and 20% by weight of Y_2O_3 at activation temperature 500°C.

c) Y_2O_3-γ-Al_2O_3: 5%, 10%, 15% and 20% by weight of Y_2O_3 at activation temperature 500°C.

d) Pr_6O_{11} at activation temperatures 300, 500 and 800°C

e) Pr_6O_{11}-Al_2O_3 (co-hydrolysis from nitrate solution) 5%, 10%, 20% and 60% by weight of Pr_6O_{11} at activation temperature 500°C.

f) Pr_6O_{11}-Al_2O_3 (co-hydrolysis from sulphate solution) 5%, 10%, 15% and 20% by weight of Pr_6O_{11} at activation temperature 500°C.

g) Nd_2O_3 at activation temperatures 300, 500 and 800°C.

h) Nd_2O_3-Al_2O_3: 5%, 10%, 15% and 20% by weight of Nd_2O_3 at activation temperature 500°C.

Y_2O_3

The surface areas of Y_2O_3 prepared by two routes and activated at different temperatures were determined by BET method and are given in Table 2.

The adsorption of four electron acceptors (Table 1) from acetonitrile and 1,4-dioxan on Y_2O_3 activated at 300, 400, 500, 600 and 800°C are reported. In the case of m-dinitrobenzene (MDNB) adsorption was negligible at all activation temperatures studied. For p-dinitrobenzene (PDNB) adsorption could be measured only

Table 2 Surface area of Y_2O_3

Method of preparation	Activation temperature (°C)	Surface area (m^2/g)
Hydroxide	300	46.3
Hydroxide	400	41.3
Hydroxide	500	81.5
Hydroxide	600	44.4
Hydroxide	800	38.0
Oxalate	800	14.9

on Y_2O_3 activated at 800°C. The data are given in Tables 3-23 and Fig.1. The adsorption obtained are of Langmuir type. It is verified by the plot of C_{eq}/C_{ad} against C_{eq}, where C_{eq} is the equilibrium concentration in mol dm^{-3} and C_{ad} is the amount adsorbed in mol m^{-2}. the plot was found to be linear (Fig.2). The limiting amount of electron acceptor adsorbed is determined from the Langmuir plot. When electron acceptors were adsorbed, surface of Y_2O_3 acquired characteristic colouration owing to interaction between electron acceptor adsorbed and the oxide surface [1]. Chloranil gave light pink colour to the

Table 3 Adsorption of chloranil on Y_2O_3

Activation temperature: 300°C Solvent: Acetonitrile

Initial concentration 10^{-3} mol dm^{-3}	Equilibrium concentration 10^{-3} mol dm^{-3}	Amount adsorbed 10^{-5} mol m^{-2}
0.08	0.07	0.03
0.42	0.37	0.24
0.85	0.78	0.31
1.71	1.46	1.10
3.22	2.51	1.76
4.29	3.89	1.78

Table 4 Adsorption of TCNQ on Y_2O_3

Activation temperature: 300°C Solvent: Acetonitrile

Initial concentration 10^{-3} mol dm^{-3}	Equilibrium concentration 10^{-3} mol dm^{-3}	Amount adsorbed 10^{-5} mol m^{-2}
0.77	0.70	0.31
1.44	1.33	2.49
2.52	1.86	3.02
3.09	2.15	4.14
4.21	2.93	5.61
5.80	4.53	5.72

Table 5 Adsorption of chloranil on Y_2O_3

Activation temperature: 300°C Solvent: Dioxan

Initial concentration 10^{-3} mol dm^{-3}	Equilibrium concentration 10^{-3} mol dm^{-3}	Amount adsorbed 10^{-5} mol m^{-2}
0.07	0.05	0.09
0.38	0.30	0.40
0.77	0.65	0.54
1.54	1.31	1.04
2.89	2.63	1.16
3.85	3.60	1.16

Table 6 Adsorption of TCNQ on Y_2O_3

Activation temperature: 300°C Solvent: Dioxan

Initial concentration 10^{-3} mol dm^{-3}	Equilibrium concentration 10^{-3} mol dm^{-3}	Amount adsorbed 10^{-5} mol m^{-2}
0.14	0.13	0.03
0.72	0.67	0.22
1.45	1.39	0.28
2.17	1.81	1.05
2.90	2.46	1.91
4.35	3.92	1.91

Table 7 Adsorption of chloranil on Y_2O_3

Activation temperature: 400°C Solvent: Acetonitrile

Initial concentration 10^{-3} mol dm^{-3}	Equilibrium concentration 10^{-3} mol dm^{-3}	Amount adsorbed 10^{-5} mol m^{-2}
0.07	0.06	0.08
0.39	0.33	0.32
0.79	0.70	0.48
1.59	1.39	1.01
2.99	2.59	1.79
3.99	3.61	1.79

Table 8 Adsorption of TCNQ on Y_2O_3

Activation temperature: 400°C Solvent: Acetonitrile

Initial concentration 10^{-3} mol dm^{-3}	Equilibrium concentration 10^{-3} mol dm^{-3}	Amount adsorbed 10^{-5} mol m^{-2}
0.15	0.14	0.07
0.79	0.74	0.36
1.58	1.44	0.53
2.37	2.06	1.63
3.17	2.02	5.96
5.94	4.78	6.08

Table 9 Adsorption of chloranil on Y_2O_3

Activation temperature: 400°C Solvent: Dioxan

Initial concentration 10^{-3} mol dm^{-3}	Equilibrium concentration 10^{-3} mol dm^{-3}	Amount adsorbed 10^{-5} mol m^{-2}
0.08	0.07	0.02
0.40	0.32	0.39
0.81	0.67	0.68
1.62	1.43	0.96
3.04	2.83	1.03
4.06	3.85	1.05

Table 10 Adsorption of TCNQ on Y_2O_3

Activation temperature: 400°C Solvent: Dioxan

Initial concentration 10^{-3} mol dm^{-3}	Equilibrium concentration 10^{-3} mol dm^{-3}	Amount adsorbed 10^{-5} mol m^{-2}
0.83	0.69	0.73
1.38	1.16	1.09
1.92	1.65	1.22
2.24	1.91	1.63
2 98	2.60	1.90
3.73	3.34	1.92

Table 11 Adsorption of chloranil on Y_2O_3

Activation temperature: 500°C Solvent: Acetonitrile

Initial concentration 10^{-3} mol dm^{-3}	Equilibrium concentration 10^{-3} mol dm^{-3}	Amount adsorbed 10^{-5}mol m^{-2}	Radical concentration 10^{16} spins m^{-2}
1.20	0.55	0.79	0.44
1.60	0.74	1.05	0.59
2.46	1.45	1.24	0.69
3.68	1.70	2.43	1.36
4.18	2.17	2.46	1.38

Table 12 Adsorption of TCNQ on Y_2O_3

Activation temperature: 500°C Solvent: Acetonitrile

Initial concentration 10^{-3} mol dm^{-3}	Equilibrium concentration 10^{-3} mol dm^{-3}	Amount adsorbed 10^{-5}mol m^{-2}	Radical concentration 10^{18} spins m^{-2}
0.29	0.16	0.30	0.16
0.97	0.52	1.08	0.58
1.94	0.95	2.41	1.31
3.64	1.13	5.49	2.99
4.85	2.32	7.01	3.82
7.27	4.65	7.21	3.93

Table 13 Adsorption of chloranil on Y_2O_3

Activation temperature: 500°C Solvent: Dioxan

Initial concentration 10^{-3} mol dm^{-3}	Equilibrium concentration 10^{-3} mol dm^{-3}	Amount adsorbed 10^{-5} mol m^{-2}
0.09	0.08	0.03
0.91	0.53	0.82
1.83	1.71	1.08
3.44	3.11	1.23
4.59	4.25	1.26

Table 14 Adsorption of TCNQ on Y_2O_3

Activation temperature: 500°C Solvent: Dioxan

Initial concentration 10^{-3} mol dm^{-3}	Equilibrium concentration 10^{-3} mol dm^{-3}	Amount adsorbed 10^{-5} mol m^{-2}
0.47	0.38	0.21
0.94	0.80	0.73
3.84	2.90	2.36
4.40	3.41	2.41
4.73	3.73	2.42

Table 15 Adsorption of chloranil on Y_2O_3

Activation temperature: 600°C Solvent: Acetonitrile

Initial concentration 10^{-3} mol dm^{-3}	Equilibrium concentration 10^{-3} mol dm^{-3}	Amount adsorbed 10^{-5} mol m^{-2}
0.44	0.25	0.99
0.89	0.54	1.67
1.34	0.92	2.16
1.78	1.22	2.73
3.35	2.66	3.33
4.47	3.76	3.38

Table 16 Adsorption of TCNQ on Y_2O_3

Activation temperature: 600°C Solvent: Acetonitrile

Initial concentration 10^{-3} mol dm^{-3}	Equilibrium concentration 10^{-3} mol dm^{-3}	Amount adsorbed 10^{-5} mol m^{-2}
1.52	1.41	0.55
3.05	2.66	6.59
4.85	4.13	7.70
6.87	5.28	7.81
7.63	6.02	7.91

Table 17 Adsorption of chloranil on Y_2O_3

Activation temperature: 600°C Solvent: Dioxan

Initial concentration 10^{-3} mol dm^{-3}	Equilibrium concentration 10^{-3} mol dm^{-3}	Amount adsorbed 10^{-5} mol m^{-2}
0.85	0.82	0.14
1.28	1.23	0.22
1.70	1.65	0.77
2.56	2.41	1.05
3.41	3.15	1.24
4.27	4.01	1.25

Table 18 Adsorption of TCNQ on Y_2O_3

Activation temperature: 600°C Solvent: Dioxan

Initial concentration 10^{-3} mol dm^{-3}	Equilibrium concentration 10^{-3} mol dm^{-3}	Amount adsorbed 10^{-5} mol m^{-2}
0.74	0.61	0.61
1.48	1.18	1.47
2.97	2.38	2.86
4.46	3.71	3.66
5.95	5.18	3.71

Table 19 Adsorption of chloranil on Y_2O_3

Activation temperature: 800°C Solvent: Acetonitrile

Initial concentration 10^{-3} mol dm^{-3}	Equilibrium concentration 10^{-3} mol dm^{-3}	Amount adsorbed 10^{-5} mol m^{-2}
0.93	0.81	0.06
1.87	1.72	0.17
2.81	2.40	2.71
3.75	3.24	2.84
4.22	3.40	4.05
4.69	3.91	4.10

Table 20 Adsorption of TCNQ on Y_2O_3

Activation temperature: 800°C Solvent: Acetonitrile

Initial concentration 10^{-3} mol dm^{-3}	Equilibrium concentration 10^{-3} mol dm^{-3}	Amount adsorbed 10^{-5} mol m^{-2}
0.77	0.70	0.39
1.55	1.45	3.65
3.11	2.79	5.83
6.22	4.54	8.00
7.00	5.79	9.05
7.78	6.04	9.15

Table 21 Adsorption of chloranil on Y_2O_3

Activation temperature: 800°C Solvent: Dioxan

Initial concentration 10^{-3} mol dm^{-3}	Equilibrium concentration 10^{-3} mol dm^{-3}	Amount adsorbed 10^{-5} mol m^{-2}
0.89	0.85	0.50
1.78	1.71	0.71
2.68	2.31	0.98
3.57	2.49	1.31
4.02	2.92	1.36

Table 22 Adsorption of TCNQ on Y_2O_3

Activation temperature: 800°C Solvent: Dioxan

Initial concentration 10^{-3} mol dm^{-3}	Equilibrium concentration 10^{-3} mol dm^{-3}	Amount adsorbed 10^{-5} mol m^{-2}
0.61	0.31	1.61
1.22	0.74	2.58
2.44	1.84	3.18
3.67	2.73	4.78
4.89	3.88	5.71
6.12	5.05	5.82

Table 23 Adsorption of PDNB on Y_2O_3

Activation temperature: 800°C Solvent: Acetonitrile

Initial concentration 10^{-4} mol dm^{-3}	Equilibrium concentration 10^{-4} mol dm^{-3}	Amount adsorbed 10^{-7} mol m^{-2}
0.85	0.83	0.79
1.70	1.66	1.75
3.41	3.36	2.16
5.12	5.06	4.98
6.83	6.69	8.65
8.54	8.40	8.86

Table 24 Adsorption of chloranil on Y_2O_3
(Regenerated by oxalate method)

Activation temperature: 800°C Solvent: Acetonitrile

Initial concentration 10^{-4} mol dm^{-3}	Equilibrium concentration 10^{-4} mol dm^{-3}	Amount adsorbed 10^{-5} mol m^{-2}
0.18	0.09	0.11
0.62	0.31	0.40
1.46	0.62	0.81
2.76	1.90	1.21
5.38	3.20	2.99
12.0	9.80	3.01

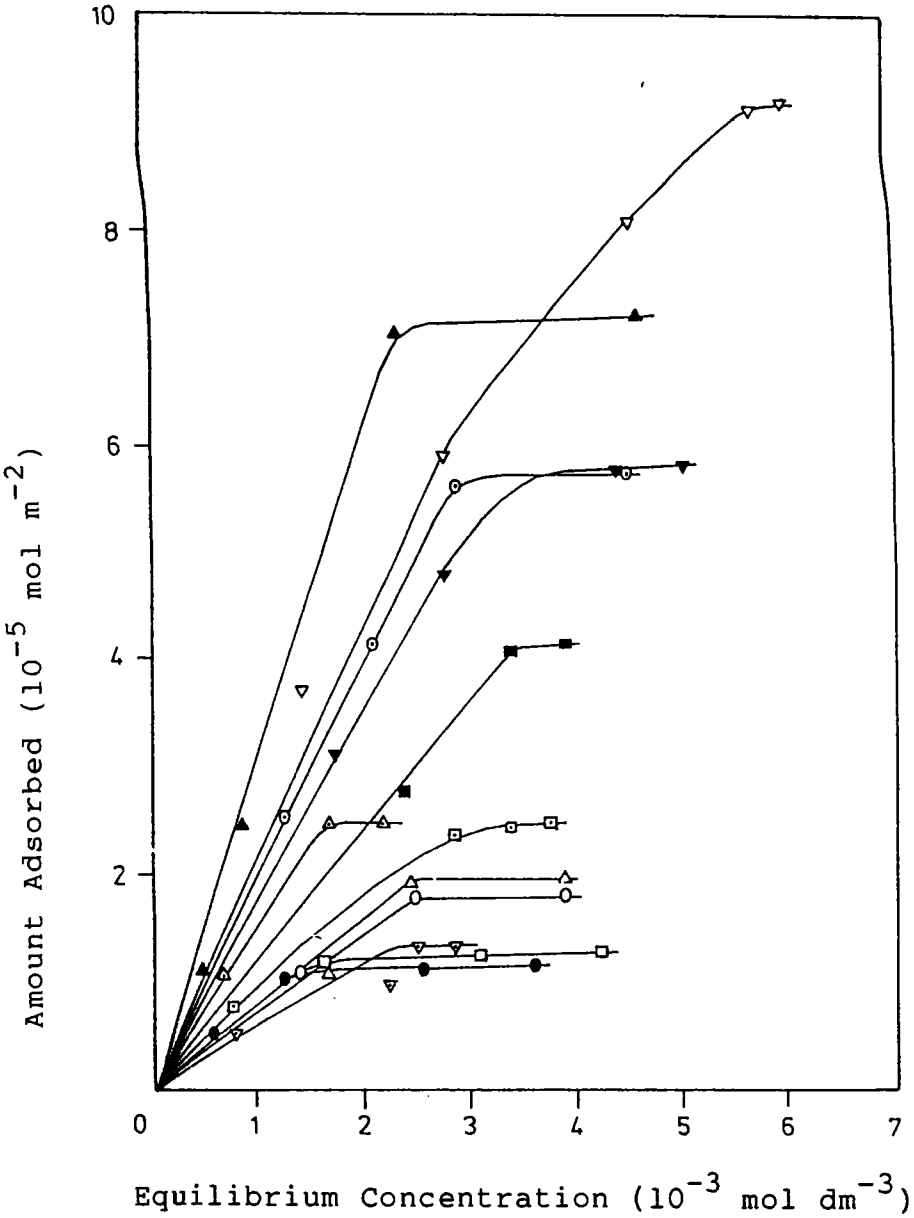

Electron acceptor/Solvent/Activation temperature (°C)

(CA - Chloranil; AN - Acetonitrile; TC - TCNQ; D - Dioxan)

○ CA/AN/300 ⊙ TC/AN/300 ● CA/D/300 △ TC/D/300 △ CA/AN/500
▲ TC/AN/500 □ CA/D/500 ⊡ TC/D/500 ■ CA/AN/800 ▽ TC/AN/800
▽ CA/D/800 ▼ TC/D/800

Fig.1 Adsorption isotherms on Y_2O_3

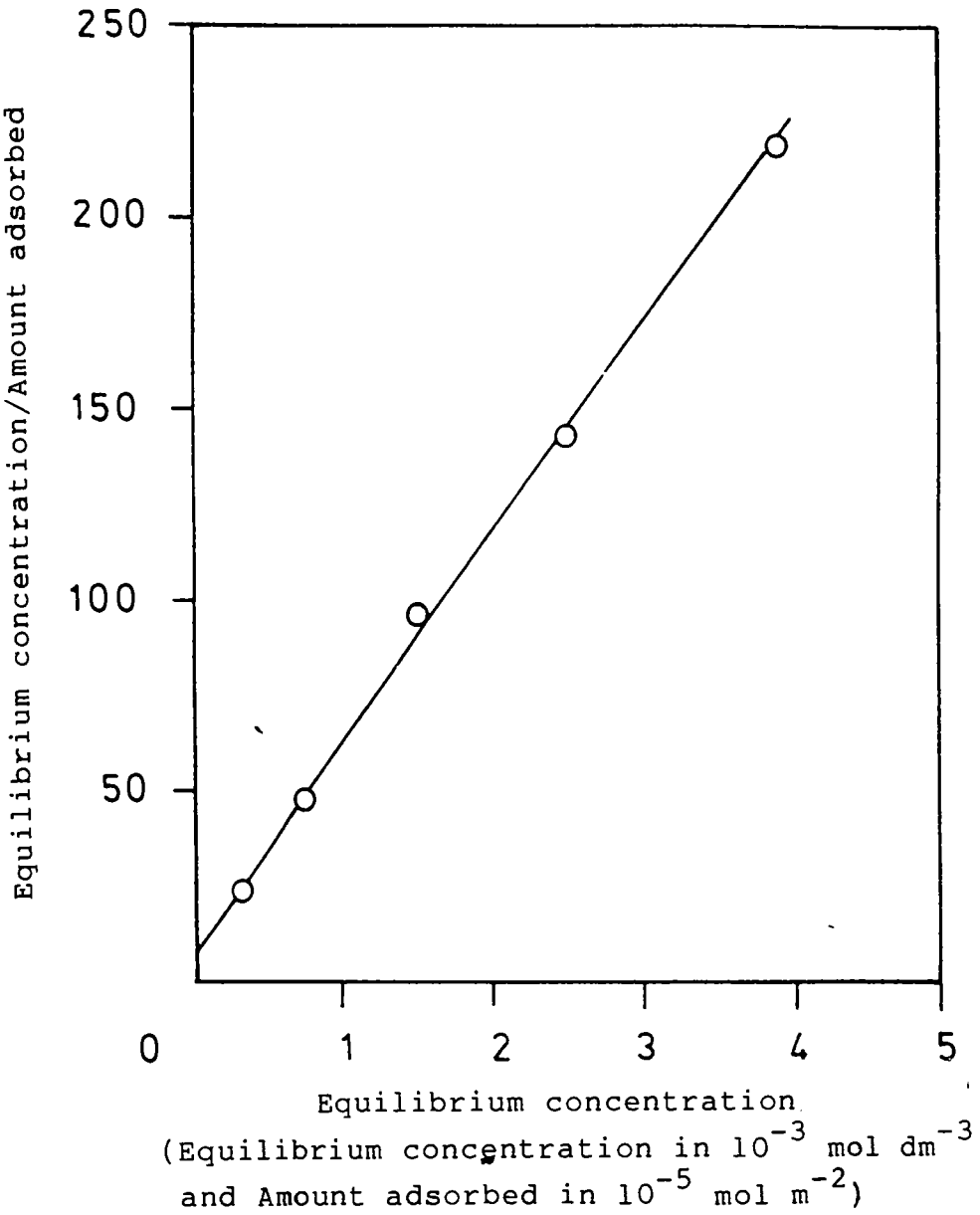

Fig.2 Linear form of Langnuir isotherm obtained for adsorption of chloranil on Y_2O_3 (300°C)

oxide while for TCNQ, Y_2O_3 acquired green colour. To study the nature of interaction, reflectance spectra of coloured samples were measured. The bands appearing below 400 nm correspond to physically adsorbed state of neutral TCNQ which has an absorption band at 395 nm [2]. The bands near 600 nm is attributed to the dimeric TCNQ radical which absorbs at 643 nm [3]. The broad band extending upto 700 nm corresponds to chloranil anion radical [4] and the band at 420 nm is attributed to the PDNB anion radical. In the case of oxides studied this assignment does not hold completely because these oxides have characteristic band in the same region. The electronic state of adsorbed species was studied by ESR spectroscopy in addition to electronic spectroscopy. The radical concentrations of chloranil and TCNQ adsorbed on Y_2O_3 activated at 500°C were determined from the ESR spectra. The ESR spectra indicated the presence of radical species. The samples coloured by TCNQ adsorption gave unresolved ESR spectra with a g value of 2.003. These spectra have been identified as being those of TCNQ anion radicals [5]. The coloured samples obtained by the adsorption of chloranil gave an unresolved ESR spectra having a g value of 2.011 [6]. The radical concentrations of TCNQ and chloranil adsorbed are given in Table 11-12. Fig.3 shows the radical concentration of TCNQ

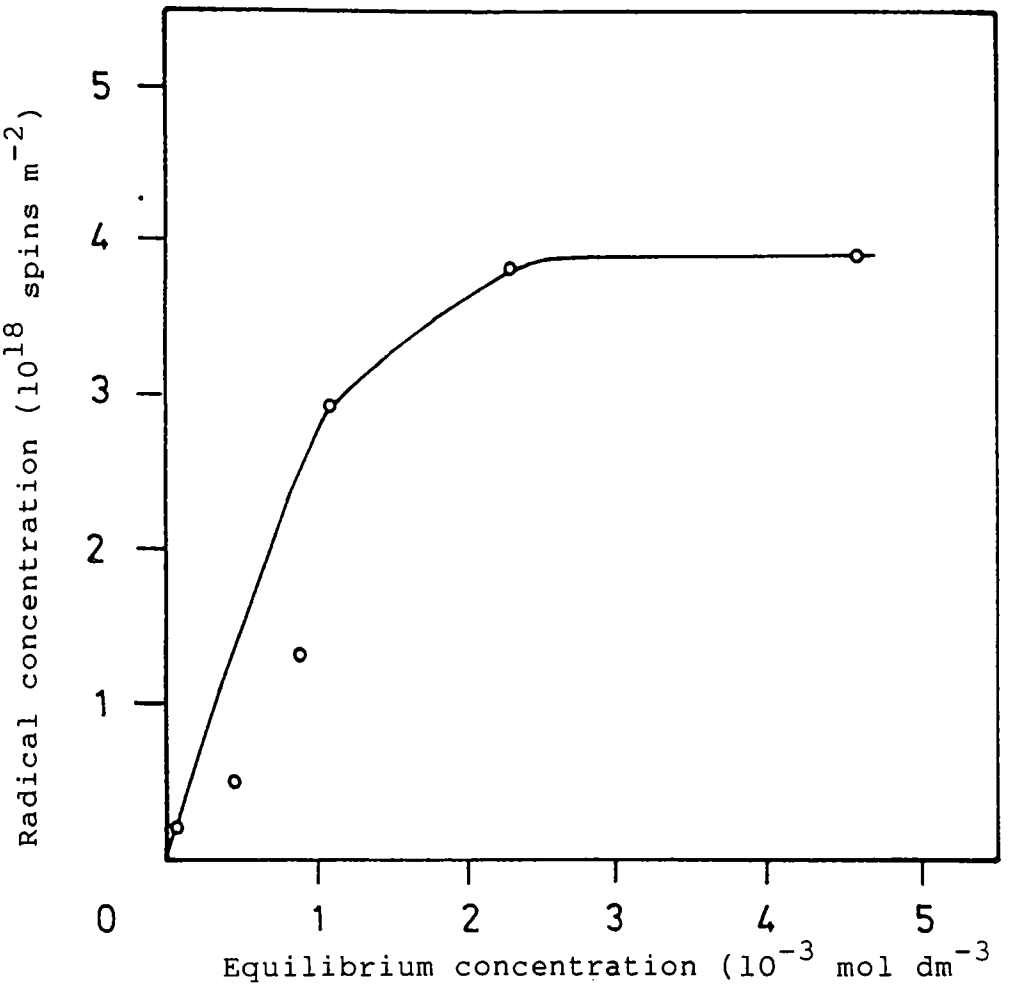

Fig.3 Radical concentration of TCNQ on Y_2O_3 vs. equilibrium concentration of TCNQ

adsorbed against the equilibrium concentration of TCNQ in solution. The isotherm obtained is of Langmuir type and is of the same shape as the plot of amount of electron acceptor adsorbed. Limiting radical concentrations are also calculated from the Langmuir plot.

The limiting amount of radical concentration of TCNQ on the surface is a measure of the total number of electron donor sites on the oxide surface. The electron donicity of Y_2O_3 is found to depend on the electron affinity of electron acceptors adsorbed. The amount adsorbed increased with increase in electron affinity of electron acceptor. The electron donor strength can be expressed as the conversion ratio of an electron acceptor adsorbed on the surface into its anion radical. Strong electron acceptors like TCNQ are capable of forming anions even from weak donor sites whereas weak acceptors like MDNB are capable of forming anions only at strong donor sites. Hence the limiting radical concentration of the weak acceptor is a measure of the number of strong donor sites on the surface and that for a strong acceptor is the total of all weak and strong donor sites on the surface. It is found that the limiting radical concentration and also limiting amount of the electron acceptor adsorbed decreases

with decrease in electron affinity of the electron acceptor. The electron donor strength on a metal oxide can be expressed as the limiting electron affinity value at which free anion radical formation is not observed at metal oxide surface. The limiting amount decreased steeply between p-dinitrobenzene and m-dinitrobenzene in the case of Y_2O_3 activated at 800°C. This suggests that adsorption sites on Y_2O_3 activated at 800°C act as electron donors to the adsorbed molecule with electron affinity greater than 1.77 but not smaller than 1.26 eV in acetonitrile. Accordingly the limit of electron transfer from electron donor site of Y_2O_3 to the electron acceptor molecule is located between 1.26 and 1.77 eV. In all other cases the limit is between 2.40 and 1.77 eV.

The limiting amount of electron acceptors adsorbed is found to decrease with increase in basicity of the solvent. The decrease in adsorption of electron acceptors with increasing basicity of solvents shows the competition between basic solvents and basic sites (electron donor sites) of metal oxides for electron acceptors. Thus, adsorption onto metal oxides is strongly influenced by interaction between basic solvents and electron acceptors.

Two possible electron sources exist on oxide surface responsible for electron transfer. One of these has electrons trapped in intrinsic defects and other has hydroxyl ions [7]. At lower activation temperature surface sites may be associated with the presence of unsolvated hydroxyl ions and at higher activation temperature an electron defect centre is produced. It is reported that free electron defect site on metal oxide surface is created at an activation temperature of above 500°C [8]. Fomin et al., have shown that electron transfer from OH^- ions can and does occur in certain solvent systems, provided a suitable electron acceptor is present [9]. Surface hydroxyls on metal oxides are shown to differ in chemical properties and difference in acidity between hydroxyl groups on several oxide surfaces have been reported [10]. These suggest that hydroxyl ions of metal oxide surfaces have electron donor sites of varying electron donicity.

IR spectral data of Y_2O_3 activated at 300°C and 500°C confirm the presence of hydroxyl groups (peak near 3400 cm^{-1}). Fig.4 shows the limiting amounts of electron acceptors adsorbed on Y_2O_3 as a function of activation temperature. The limiting amount adsorbed remained almost constant for activation temperatures below 500°C. Above

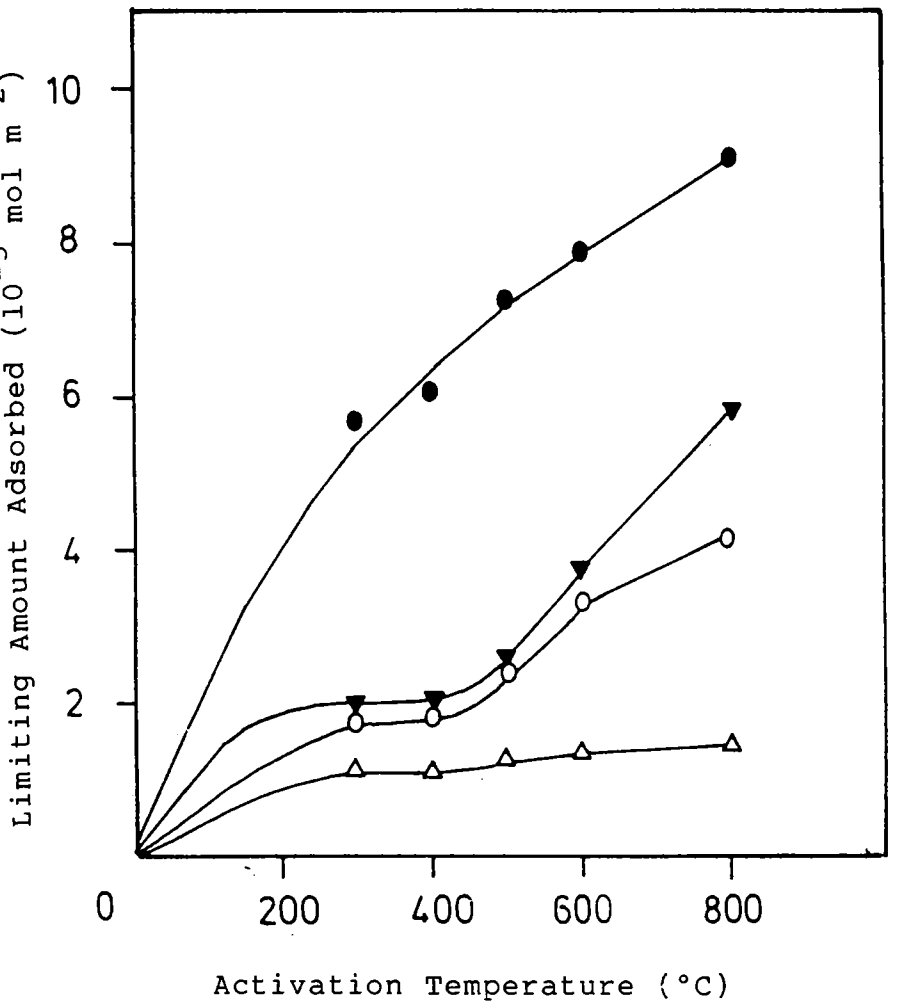

Electron acceptor/Solvent

(CA - Chloranil; AN - Acetonitrile; TC - TCNQ; D - Dioxan)

○ CA/AN ● TC/AN △ CA/D ▲ TC/D

Fig.4 Limiting amount of electron acceptors adsorbed on Y_2O_3 as a function of activation temperature

500°C the amount adsorbed increased considerably with increasing activation temperature. Since the concentration of surface hydroxyl ions decreased with increasing temperature and the concentration of trapped electrons increased with increasing temperature it might be expected that trapped electrons are solely responsible for adsorption of electron acceptors on the surface of Y_2O_3 activated at higher temperatures. It is observed that the concentrations of both weak and strong donor sites increase with increase in temperature. The limiting amount of electron acceptors adsorbed on Y_2O_3 prepared by oxalate method are given in Tables 24-27. The amount adsorbed is greater when Y_2O_3 is prepared by hydroxide method. Since the limiting amount adsorbed on the oxide prepared by two methods differ it is inferred that the amount of electron acceptors adsorbed depends on the method of preparation of oxide. When the oxide is prepared by oxalate method, it is reported that the surface of oxide is not completely free from surface carbonate layer which is formed by decomposition of oxalate during heating [11].

Acidity and basicity of Y_2O_3 was determined by titration using Hammett indicators. Acidity at various acid strengths of the oxide was measured by titrating solid

Table 25 Adsorption of TCNQ on Y_2O_3
(Regenerated by oxalate method)

Activation temperature: 800°C Solvent: Acetonitrile

Initial concentration 10^{-4} mol dm^{-3}	Equilibrium concentration 10^{-4} mol dm^{-3}	Amount adsorbed 10^{-5} mol m^{-2}
1.05	0.31	0.98
2.45	0.98	2.01
5.30	2.22	4.31
7.71	4.01	5.18
9.89	5.92	5.23

Table 26 Adsorption of chloranil on Y_2O_3
(Regenerated by oxalate method)

Activation temperature: 800°C Solvent: Dioxan

Initial concentration 10^{-3} mol dm^{-3}	Equilibrium concentration 10^{-3} mol dm^{-3}	Amount adsorbed 10^{-5} mol m^{-2}
0.11	0.08	0.42
0.19	0.13	0.86
0.27	0.20	0.97
0.42	0.35	1.01
0.59	0.49	1.31
1.34	1.30	1.33

Table 27 Adsorption of TCNQ on Y_2O_3
(Regenerated by oxalate method)

Activation temperature: 800°C Solvent: Dioxan

Initial concentration 10^{-3} mol dm^{-3}	Equilibrium concentration 10^{-3} mol dm^{-3}	Amount adsorbed 10^{-5} mol m^{-2}
0.13	0.09	0.46
0.17	0.12	0.78
0.39	0.26	1.80
0.68	0.48	2.90
1.60	1.39	3.00

suspended in benzene with a 0.1 N solution of n-butyl amine in benzene. Basicity was measured by titrating with trichloroacetic acid using the same indicators as those used for acidity measurement. This enabled us to measure the acid-base strength on a common scale [11]. Visible colour change was obtained only for four indicators which are listed in Table 28.

Table 28 Hammett indicators used

Indicator	pKa	COLOUR	
		Basic	Acidic
p-Dimethylaminoazobenzene	+3.3	Yellow	Red
Methyl red	+4.8	Yellow	Red
Neutral red	+6.8	Yellow	Red
Bromothymol blue	+7.2	Blue	Yellow

Fig.5 shows the acidity and basicity of Y_2O_3 at various acid-base strengths at different activation temperatures. The data are given in Table 29. The acid-base strength distribution curves intersect at a point on the abcissa where acidity = basicity = 0 [12]. Each Ho_{max} value determined from the point of intersection of acid-

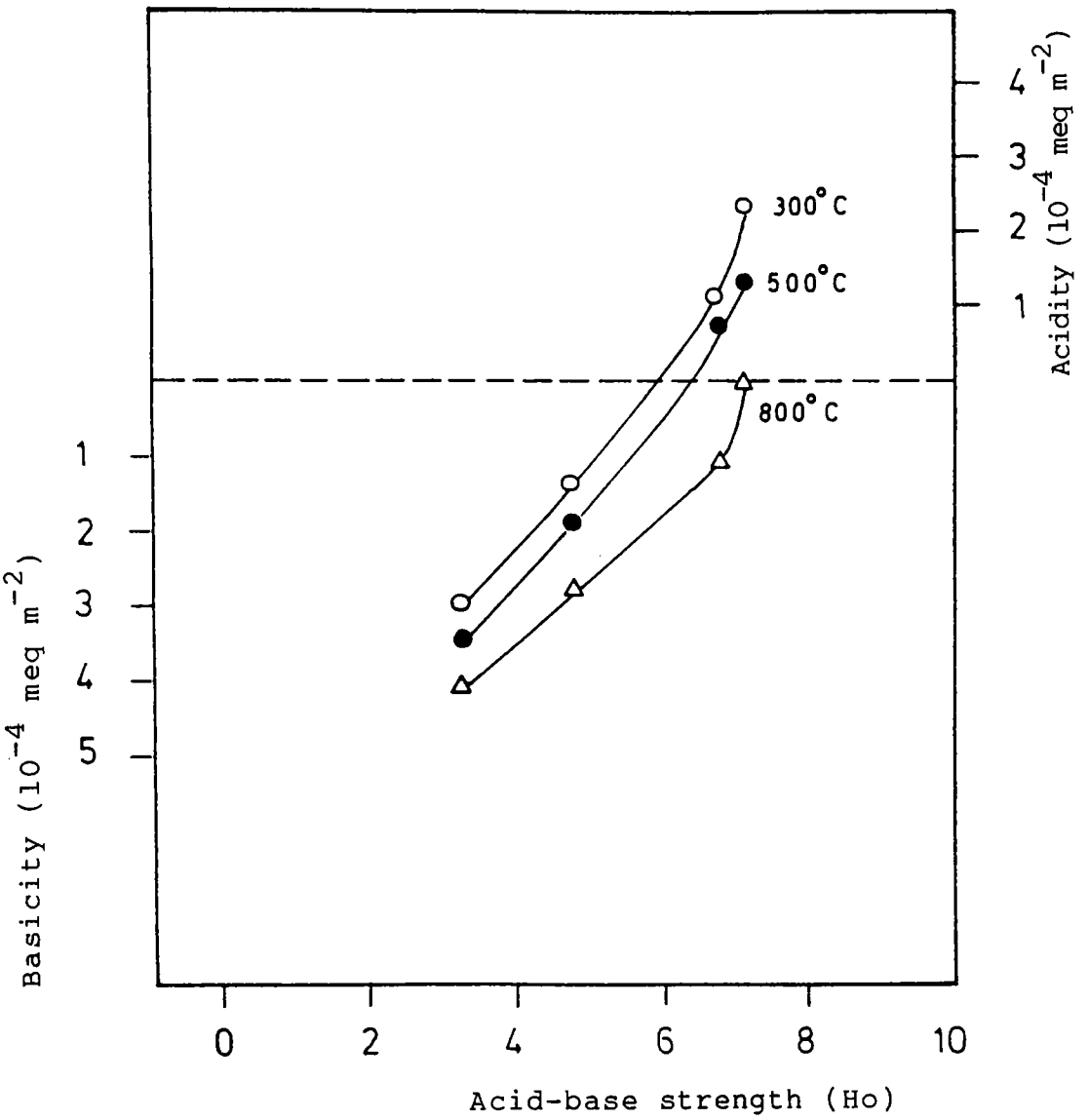

Fig.5 Acid-base strength distribution of Y_2O_3

Table 29 Acidity, Basicity and Ho_{max} of Y_2O_3 at different activation temperatures

Activation temperature (°C)	Basicity (10^{-4} meq m^{-2})				Acidity (10^{-4} meq m^{-2})				Ho_{max}
	Ho ≥ 3.3	Ho ≥ 4.8	Ho ≥ 6.8	Ho ≥ 7.2	Ho ≤ 3.3	Ho ≤ 4.8	Ho ≤ 6.8	Ho ≤ 7.2	
300	3.07	1.42	--	--	--	--	1.17	2.38	5.80
500	3.43	2.04	--	--	--	--	0.71	1.32	6.30
800	4.12	2.85	1.18	0.18	--	--	--	--	7.20

base distribution curve with abcissa is given in Table 29. For Y_2O_3 activated at 800°C only basic sites were present while at activation temperatures of 300°C and 500°C, both acidic and basic sites were present. It is known that a solid with a large positive Ho_{max} value has strong basic sites and that with a large negative Ho_{max} value has weak sites. Data show that for Y_2O_3 as the activation temperature increases Ho_{max} value increases which in turn shows the increase in basic sites on oxide.

Y_2O_3-Al_2O_3

The following compositions of mixed oxides were studied. The surface area of Y_2O_3-Al_2O_3 of different compositions activated at 500°C is given in Table 30.

Table 30 Surface area of Y_2O_3-Al_2O_3

% by weight of Y_2O_3	Surface area (m^2/g)
5	106.40
10	108.48
15	108.68
20	104.20
Al_2O_3 (from Aluminium sulfate)	41.20

The mixed oxide system Y_2O_3-Al_2O_3, prepared by co-hydrolysis of the mixture of their sulfates, showed much less electron donicity than the parent oxide Y_2O_3. Also as the weight percentage of rare earth oxide in the mixed oxide increases, the limiting amount of electron acceptor adsorbed also increases. Fig.6 shows the adsorption isotherms on Y_2O_3-Al_2O_3 of different compositions and the value are given in Tables 31-46. The limiting amounts of electron acceptors adsorbed as a function of composition of mixed oxide is shown in Fig.7. The order of electron donicity is found to increase with the increase in concentration of Y_2O_3 in the mixed oxides. The amount adsorbed decreases with increase in basicity of solvent as in case of pure Y_2O_3. The limit of electron transfer from electron donor sites of Y_2O_3-Al_2O_3 is located between 2.40 and 1.77 eV as is the case of pure Y_2O_3 activated at 500°C. It must be inferred that surface electron transfer properties of Al_2O_3 (Tables 47-50) is increased by Y_2O_3 in its mixed oxide Y_2O_3-Al_2O_3 for low concentration of Y_2O_3 without changing the limit of electron transfer. It can be seen that the effect of Y_2O_3 on Al_2O_3 is to increase the concentration of both weak and strong donor sites on Al_2O_3 surface to the same extent.

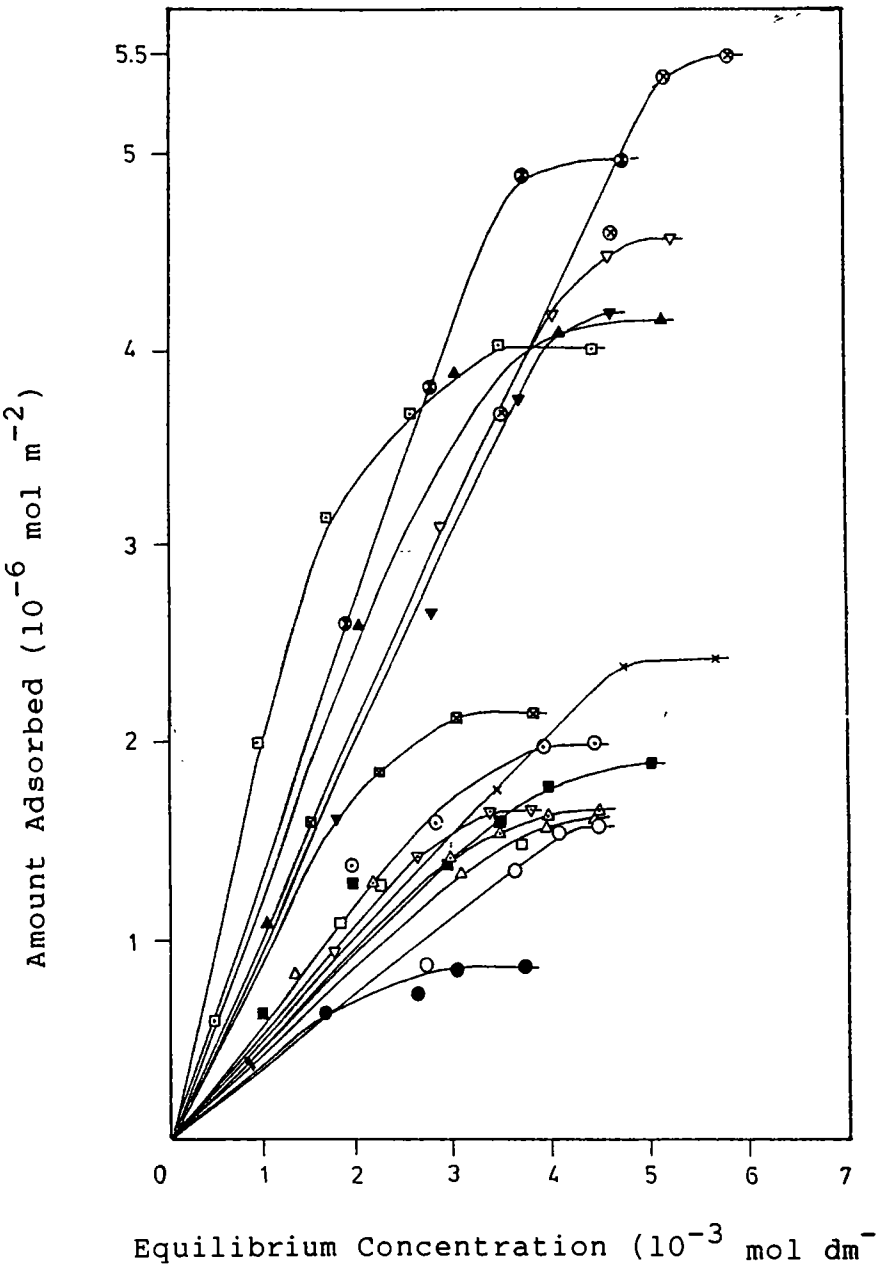

Electron acceptor/Solvent/wt. % of Y_2O_3

(CA - Chloranil; AN - Acetonitrile; TC - TCNQ; D - Dioxan)

○ CA/AN/5 ⊙ TC/AN/5 ● CA/D/5 △ TC/D/5 ◬ CA/AN/10
▲ TC/AN/10 □ CA/D/10 ⊡ TC/D/10 ■ CA/AN/15 ▽ TC/AN/15
▽ CA/D/15 ▼ TC/D/15 × CA/AN/20 ⊗ TC/AN/20 ⊠ CA/D/20
⊗ TC/D/20

Fig.6 Adsorption isotherms on Y_2O_3-Al_2O_3

Table 31 Adsorption of chloranil on Y_2O_3-Al_2O_3 (5%)

Activation temperature: 500°C Solvent: Acetonitrile

Initial concentration 10^{-3} mol dm^{-3}	Equilibrium concentration 10^{-3} mol dm^{-3}	Amount adsorbed 10^{-6} mol m^{-2}
1.82	1.78	0.62
2.74	2.69	0.86
3.65	3.58	1.35
4.11	4.03	1.54
4.56	4.47	1.58

Table 32 Adsorption of TCNQ on Y_2O_3-Al_2O_3 (5%)

Activation temperature: 500°C Solvent: Acetonitrile

Initial concentration 10^{-3} mol dm^{-3}	Equilibrium concentration 10^{-3} mol dm^{-3}	Amount adsorbed 10^{-6} mol m^{-2}
1.00	0.98	0.92
2.00	1.90	0.14
3.01	2.81	1.62
4.01	3.91	1.97
4.52	4.41	1.98

Table 33 Adsorption of chloranil on Y_2O_3-Al_2O_3 (5%)

Activation temperature: 500°C Solvent: Dioxan

Initial concentration 10^{-3} mol dm^{-3}	Equilibrium concentration 10^{-3} mol dm^{-3}	Amount adsorbed 10^{-7} mol m^{-2}
0.37	0.35	3.12
1.02	0.99	4.29
1.70	1.66	6.48
2.61	2.58	7.42
3.06	3.01	8.81
3.74	3.69	8.84

Table 34 Adsorption of TCNQ on Y_2O_3-Al_2O_3 (5%)

Activation temperature: 500°C Solvent: Dioxan

Initial concentration 10^{-3} mol dm^{-3}	Equilibrium concentration 10^{-3} mol dm^{-3}	Amount adsorbed 10^{-6} mol m^{-2}
0.44	0.42	0.41
1.34	1.29	0.86
2.24	2.17	2.28
3.14	3.06	1.36
4.04	3.95	1.58
4.49	4.40	1.61

Table 35 Adsorption of chloranil on Y_2O_3-Al_2O_3 (10%)

Activation temperature: 500°C Solvent: Acetonitrile

Initial concentration 10^{-3} mol dm^{-3}	Equilibrium concentration 10^{-3} mol dm^{-3}	Amount adsorbed 10^{-6} mol m^{-2}
1.00	0.98	0.30
3.02	2.96	1.42
3.53	3.46	1.56
4.03	3.94	1.63
4.54	4.44	1.65

Table 36 Adsorption of TCNQ on Y_2O_3-Al_2O_3 (10%)

Activation temperature: 500°C Solvent: Acetonitrile

Initial concentration 10^{-3} mol dm^{-3}	Equilibrium concentration 10^{-3} mol dm^{-3}	Amount adsorbed 10^{-6} mol m^{-2}
0.53	0.48	0.89
1.06	1.00	1.09
2.13	1.99	2.61
3.20	2.99	3.89
4.27	4.05	4.10
5.34	5.12	4.17

Table 37 Adsorption of chloranil on Y_2O_3-Al_2O_3 (10%)

Activation temperature: 500°C Solvent: Dioxan

Initial concentration 10^{-3} mol dm^{-3}	Equilibrium concentration 10^{-3} mol dm^{-3}	Amount adsorbed 10^{-6} mol m^{-2}
1.50	1.45	0.91
1.87	1.81	1.10
2.25	2.18	1.31
3.00	2.92	1.42
3.75	3.66	1.49

Table 38 Adsorption of TCNQ on Y_2O_3-Al_2O_3 (10%)

Activation temperature: 500°C Solvent: Dioxan

Initial concentration 10^{-3} mol dm^{-3}	Equilibrium concentration 10^{-3} mol dm^{-3}	Amount adsorbed 10^{-6} mol m^{-2}
0.46	0.45	0.61
0.92	0.91	2.01
1.84	1.66	3.14
2.77	2.57	3.71
3.69	3.46	4.08
4.62	4.40	4.02

Table 39 Adsorption of chloranil on Y_2O_3-Al_2O_3 (15%)

Activation temperature: 500°C Solvent: Acetonitrile

Initial concentration 10^{-3} mol dm^{-3}	Equilibrium concentration 10^{-3} mol dm^{-3}	Amount adsorbed 10^{-6} mol m^{-2}
1.01	0.97	0.64
2.02	1.95	1.30
3.54	3.45	1.63
4.05	3.95	1.78
5.07	4.97	1.80

Table 40 Adsorption of TCNQ on Y_2O_3-Al_2O_3 (15%)

Activation temperature: 500°C Solvent: Acetonitrile

Initial concentration 10^{-3} mol dm^{-3}	Equilibrium concentration 10^{-3} mol dm^{-3}	Amount adsorbed 10^{-6} mol m^{-2}
1.80	1.74	0.96
3.01	2.86	3.11
4.22	4.01	4.21
4.82	4.57	4.50
5.42	5.18	4.58

Table 41 Adsorption of chloranil on Y_2O_3-Al_2O_3 (15%)

Activation temperature: 500°C Solvent: Dioxan

Initial concentration 10^{-3} mol dm^{-3}	Equilibrium concentration 10^{-3} mol dm^{-3}	Amount adsorbed 10^{-6} mol m^{-2}
0.38	0.37	0.30
1.14	1.09	0.85
1.90	1.84	1.08
2.66	2.59	1.42
3.42	3.33	1.64
3.81	3.72	1.65

Table 42 Adsorption of TCNQ on Y_2O_3-Al_2O_3 (15%)

Activation temperature: 500°C Solvent: Dioxan

Initial concentration 10^{-3} mol dm^{-3}	Equilibrium concentration 10^{-3} mol dm^{-3}	Amount adsorbed 10^{-6} mol m^{-2}
0.96	0.91	0.92
1.92	1.83	1.61
2.89	2.74	2.64
3.85	3.64	3.78
4.33	4.10	4.08
4.82	4.58	4.19

Table 43 Adsorption of chloranil on Y_2O_3-Al_2O_3 (20%)

Activation temperature: 500°C Solvent: Acetonitrile

Initial concentration 10^{-3} mol dm^{-3}	Equilibrium concentration 10^{-3} mol dm^{-3}	Amount adsorbed 10^{-6} mol m^{-2}
2.03	2.01	1.05
2.54	2.47	1.69
3.55	3.47	1.76
4.57	4.46	1.96
4.82	4.69	2.41
5.78	5.61	2.43

Table 44 Adsorption of TCNQ on Y_2O_3-Al_2O_3 (20%)

Activation temperature: 500°C Solvent: Acetonitrile

Initial concentration 10^{-3} mol dm^{-3}	Equilibrium concentration 10^{-3} mol dm^{-3}	Amount adsorbed 10^{-6} mol m^{-2}
1.21	1.16	0.11
2.43	2.34	1.62
3.64	3.48	3.71
4.86	4.62	4.62
5.46	5.17	5.41
6.07	5.79	5.54

Table 45 Adsorption of chloranil on Y_2O_3-Al_2O_3 (20%)

Activation temperature: 500°C Solvent: Dioxan

Initial concentration 10^{-3} mol dm^{-3}	Equilibrium concentration 10^{-3} mol dm^{-3}	Amount adsorbed 10^{-6} mol m^{-2}
0.39	0.36	0.62
0.78	0.77	1.42
1.56	1.47	1.61
2.35	2.25	1.86
3.13	3.02	2.12
3.92	3.81	2.15

Table 46 Adsorption of TCNQ on Y_2O_3-Al_2O_3 (20%)

Activation temperature: 500°C Solvent: Dioxan

Initial concentration 10^{-3} mol dm^{-3}	Equilibrium concentration 10^{-3} mol dm^{-3}	Amount adsorbed 10^{-6} mol m^{-2}
0.49	0.46	0.60
0.98	0.93	1.08
1.97	1.84	2.61
2.96	2.76	3.82
3.95	3.69	4.90
4.94	4.70	4.97

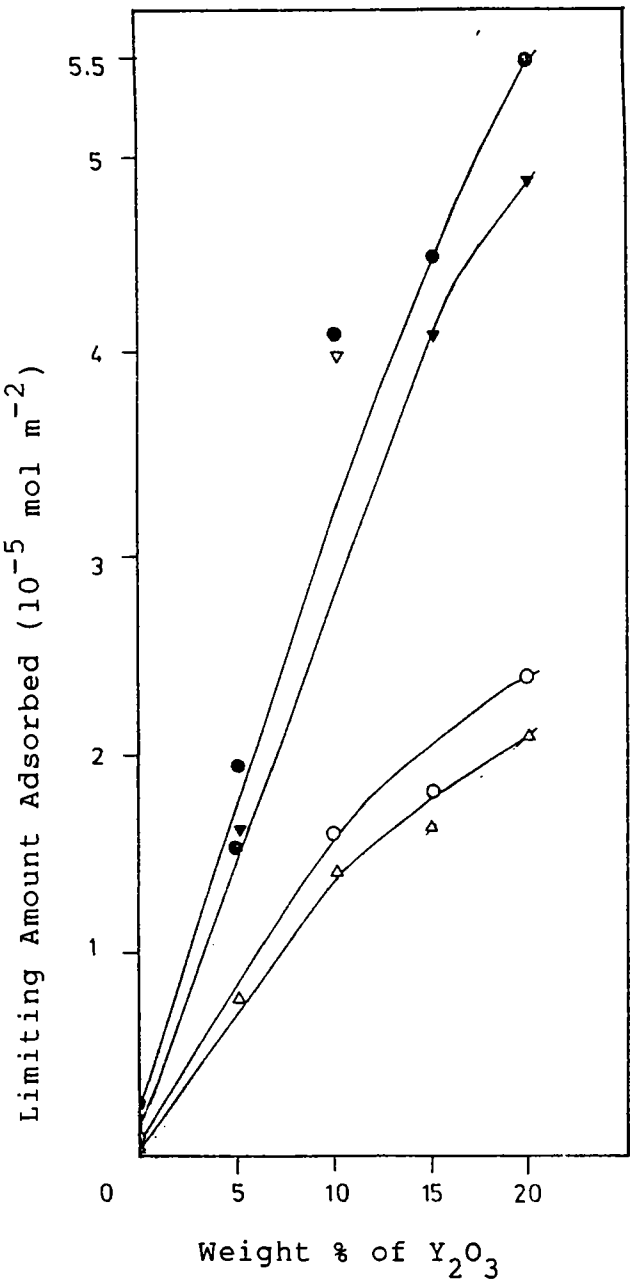

Electron acceptor/Solvent

(CA - Chloranil; AN - Acetonitrile; TC - TCNQ; D - Dioxan)

○ CA/AN ● TC/AN △ CA/D ▲ TC/D

Fig.7 Limiting amount of electron acceptors adsorbed as a function of composition of Y_2O_3-Al_2O_3

Table 47 Adsorption of chloranil on Al_2O_3

Activation temperature: 500°C Solvent: Acetonitrile

Initial concentration 10^{-4} mol dm^{-3}	Equilibrium concentration 10^{-4} mol dm^{-3}	Amount adsorbed 10^{-8} mol m^{-2}
0.75	0.74	0.11
2.09	2.08	3.01
2.74	2.73	5.22
4.32	4.31	8.01
6.83	6.81	9.78
8.54	8.52	9.85

Table 48 Adsorption of TCNQ on Al_2O_3

Activation temperature: 500°C Solvent: Acetonitrile

Initial concentration 10^{-4} mol dm^{-3}	Equilibrium concentration 10^{-4} mol dm^{-3}	Amount adsorbed 10^{-7} mol m^{-2}
1.70	1.68	0.49
2.19	2.17	0.82
3.50	3.47	1.14
5.24	5.21	1.28
7.05	7.01	1.49
8.22	8.18	1.52

Table 49 Adsorption of chloranil on Al_2O_3

Activation temperature: 500°C Solvent: Dioxan

Initial concentration 10^{-4} mol dm^{-3}	Equilibrium concentration 10^{-4} mol dm^{-3}	Amount adsorbed 10^{-8} mol m^{-2}
1.33	1.31	2.13
2.79	2.77	3.88
4.01	3.98	6.17
6.13	6.11	9.11
7.89	7.87	9.20

Table 50 Adsorption of TCNQ on Al_2O_3

Activation temperature: 500°C Solvent: Dioxan

Initial concentration 10^{-4} mol dm^{-3}	Equilibrium concentration 10^{-4} mol dm^{-3}	Amount adsorbed 10^{-7} mol m^{-2}
1.15	1.12	0.29
3.45	3.42	0.88
4.15	4.11	1.16
6.46	6.42	1.25
8.12	8.08	1.27

Titration with Hammett indicators showed that only basic sites were present on mixed oxide Y_2O_3-Al_2O_3 and strength of these sites were lower compared to Y_2O_3. There was not much difference between the strength of basic sites as the composition varied from 5% to 20% Y_2O_3 in the mixed oxide. The data are given in Table 51 and Fig.8. Al_2O_3 prepared from Aluminium sulfate showed much less basicity.

Y_2O_3-γ-Al_2O_3

The following compositions of mixed oxides have been studied at an activation temperature of 500°C. The surface area of mixed oxide system Y_2O_3-γ-Al_2O_3 of various compositions is given in the Table 52.

Table 52 Surface area of Y_2O_3-γ-Al_2O_3

% by weight of Y_2O_3	Surface area (m^2/g)
5	148.20
10	154.50
20	152.25
γ-Al_2O_3	84.80

Table 51 Basicity and Ho_{max} of Y_2O_3-Al_2O_3 of different compositions

% by weight by mixed oxide	Basicity (10^{-4} meq m^{-2})				Ho_{max}
	Ho ≥ 3.3	Ho ≥ 4.8	Ho ≥ 6.8	Ho ≥ 7.2	
5	1.11	0.67	0.21	0.09	7.4
10	1.52	0.78	0.36	0.16	7.5
15	1.72	1.01	0.59	0.20	7.5
20	1.98	1.21	0.61	0.27	7.6
Al_2O_3	0.58	0.82	0.17	--	6.8

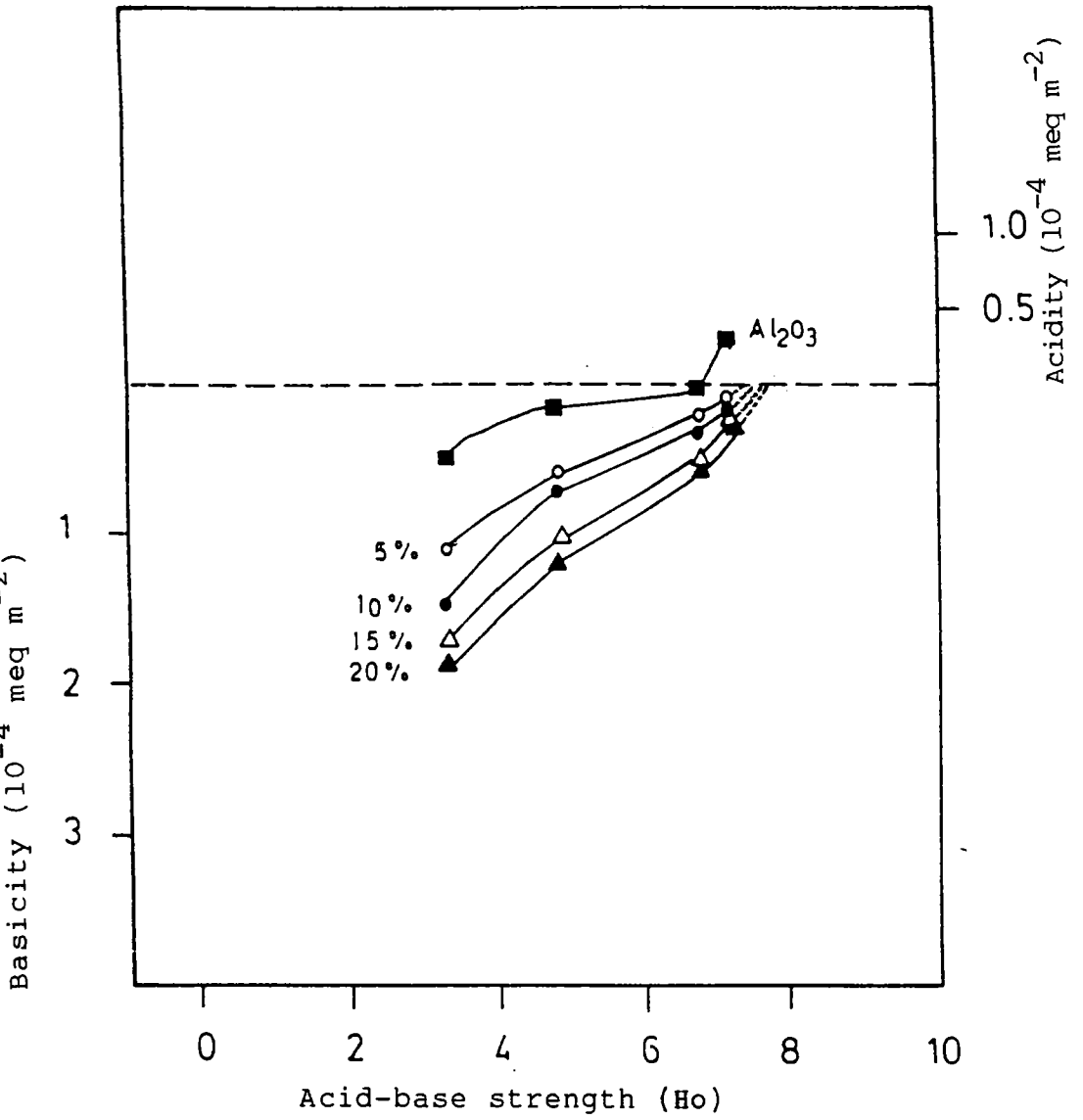

Fig.8 Acid-base strength distribution of Y_2O_3-Al_2O_3

When the mixed oxide Y_2O_3-γ-Al_2O_3 was prepared by impregnating Y_2O_3 on γ-Al_2O_3 the electron donicity is found to be in the reverse order, ie., it decreased with increase in concentration of Y_2O_3 in the binary oxide. Here the mixed oxides showed greater electron donicity than pure Y_2O_3. The data on the adsorption of electron acceptors on Y_2O_3-γ-Al_2O_3 of different compositions and γ-Alumina and given in Tables 53-68 and Fig.9. The limiting amounts of electron acceptors adsorbed as a function of composition of mixed oxide is shown in Fig.10.

Fig.11 shows the basicity of Y_2O_3-γ-Al_2O_3 of different compositions at various basic strengths. The basicity obtained for γ-Al_2O_3 is much greater than that of mixed oxide. Basicity of mixed oxides followed the same order as that of electron donicity.

γ-Al_2O_3 has a very complex structure and consists of many types of active sites [13]. It is reported that γ-Alumina supported PdO_2 decreased noticeably the intensity of ESR signal for both donor and acceptor compounds [14]. The relative greater decrease in donor properties in PdO_2-γ-Al_2O_3 showed that added metal oxide interferes with the basic centre $Al^+ - O^-$ in Alumina. The results with

Table 53 Adsorption of chloranil on Y_2O_3-γ-Al_2O_3 (5%)

Activation temperature: 500°C Solvent: Acetonitrile

Initial concentration 10^{-3} mol dm^{-3}	Equilibrium concentration 10^{-3} mol dm^{-3}	Amount adsorbed 10^{-5} mol m^{-2}
0.51	0.17	0.46
1.41	0.49	1.35
3.15	1.75	2.05
5.29	3.72	2.25
7.25	5.40	2.65
8.18	6.27	2.68

Table 54 Adsorption of TCNQ on Y_2O_3-γ-Al_2O_3 (5%)

Activation temperature: 500°C Solvent: Acetonitrile

Initial concentration 10^{-3} mol dm^{-3}	Equilibrium concentration 10^{-3} mol dm^{-3}	Amount adsorbed 10^{-5} mol m^{-2}
1.93	0.21	2.29
3.86	0.30	3.38
5.79	0.65	7.20
7.72	1.57	8.63
9.65	3.31	8.90

Table 55 Adsorption of chloranil on Y_2O_3-γ-Al_2O_3 (5%)

Activation temperature: 500°C Solvent: Dioxan

Initial concentration 10^{-3} mol dm^{-3}	Equilibrium concentration 10^{-3} mol dm^{-3}	Amount adsorbed 10^{-5} mol m^{-2}
1.01	0.71	0.50
2.03	0.91	1.05
3.05	2.56	1.40
4.06	2.71	1.81
8.13	6.67	1.88

Table 56 Adsorption of TCNQ on Y_2O_3-γ-Al_2O_3 (5%)

Activation temperature: 500°C Solvent: Dioxan

Initial concentration 10^{-3} mol dm^{-3}	Equilibrium concentration 10^{-3} mol dm^{-3}	Amount adsorbed 10^{-5} mol m^{-2}
0.98	0.63	0.48
1.86	1.31	2.30
3.73	2.70	3.40
5.90	3.26	3.71
7.87	5.00	3.79

Table 57 Adsorption of chloranil on Y_2O_3-γ-Al_2O_3 (10%)

Activation temperature: 500°C Solvent: Acetonitrile

Initial concentration 10^{-3} mol dm^{-3}	Equilibrium concentration 10^{-3} mol dm^{-3}	Amount adsorbed 10^{-5} mol m^{-2}
0.81	0.23	0.37
1.62	1.05	0.76
3.48	2.58	1.21
5.07	3.52	2.49
7.01	5.06	2.52

Table 58 Adsorption of TCNQ on Y_2O_3-γ-Al_2O_3 (10%)

Activation temperature: 500°C Solvent: Acetonitrile

Initial concentration 10^{-3} mol dm^{-3}	Equilibrium concentration 10^{-3} mol dm^{-3}	Amount adsorbed 10^{-5} mol m^{-2}
2.71	0.12	0.97
3.82	0.30	6.68
4.63	0.54	7.21
6.34	0.74	7.60
7.24	1.31	7.83

Table 59 Adsorption of chloranil on Y_2O_3-γ-Al_2O_3 (10%)

Activation temperature: 500°C Solvent: Dioxan

Initial concentration 10^{-3} mol dm^{-3}	Equilibrium concentration 10^{-3} mol dm^{-3}	Amount adsorbed 10^{-5} mol m^{-2}
0.83	0.79	0.05
1.67	1.41	0.34
2.57	2.18	0.77
3.35	2.87	0.93
5.02	3.86	1.56
6.70	5.49	1.59

Table 60 Adsorption of TCNQ on Y_2O_3-γ-Al_2O_3 (10%)

Activation temperature: 500°C Solvent: Dioxan

Initial concentration 10^{-3} mol dm^{-3}	Equilibrium concentration 10^{-3} mol dm^{-3}	Amount adsorbed 10^{-5} mol m^{-2}
0.92	0.72	0.26
1.98	1.49	1.71
2.87	2.25	2.56
5.55	3.06	3.29
7.40	4.87	3.33

Table 61 Adsorption of chloranil on Y_2O_3-γ-Al_2O_3 (20%)

Activation temperature: 500°C Solvent: Acetonitrile

Initial concentration 10^{-3} mol dm^{-3}	Equilibrium concentration 10^{-3} mol dm^{-3}	Amount adsorbed 10^{-5} mol m^{-2}
1.02	0.07	0.33
2.04	1.65	0.53
2.50	0.56	1.65
3.28	0.81	2.41
3.68	1.44	2.46

Table 62 Adsorption of TCNQ on Y_2O_3-γ-Al_2O_3 (20%)

Activation temperature: 500°C Solvent: Acetonitrile

Initial concentration 10^{-3} mol dm^{-3}	Equilibrium concentration 10^{-3} mol dm^{-3}	Amount adsorbed 10^{-5} mol m^{-2}
0.88	0.06	1.11
2.64	0.25	3.02
3.52	0.32	3.54
6.28	0.57	7.34
7.05	1.36	7.35

Table 63 Adsorption of chloranil on Y_2O_3-γ-Al_2O_3 (20%)

Activation temperature: 500°C Solvent: Dioxan

Initial concentration 10^{-3} mol dm^{-3}	Equilibrium concentration 10^{-3} mol dm^{-3}	Amount adsorbed 10^{-5} mol m^{-2}
0.75	0.60	0.20
1.51	1.13	0.47
3.02	2.61	0.60
6.05	4.99	1.41
6.80	5.68	1.45

Table 64 Adsorption of TCNQ on Y_2O_3-γ-Al_2O_3 (20%)

Activation temperature: 500°C Solvent: Dioxan

Initial concentration 10^{-3} mol dm^{-3}	Equilibrium concentration 10^{-3} mol dm^{-3}	Amount adsorbed 10^{-5} mol m^{-2}
1.44	0.81	1.90
2.97	2.02	2.69
4.46	3.15	2.88
5.95	3.77	3.01
6.69	4.38	2.98

Table 65 Adsorption of chloranil on γ-Al_2O_3

Activation temperature: 500°C Solvent: Acetonitrile

Initial concentration 10^{-3} mol dm^{-3}	Equilibrium concentration 10^{-3} mol dm^{-3}	Amount adsorbed 10^{-5} mol m^{-2}
0.55	0.51	0.88
1.55	0.95	1.48
2.19	1.38	2.01
3.87	2.78	2.70
5.06	3.95	2.75

Table 66 Adsorption of TCNQ on γ-Al_2O_3

Activation temperature: 500°C Solvent: Acetonitrile

Initial concentration 10^{-3} mol dm^{-3}	Equilibrium concentration 10^{-3} mol dm^{-3}	Amount adsorbed 10^{-5} mol m^{-2}
0.96	0.11	0.92
1.57	0.31	3.11
4.06	1.11	7.12
7.32	3.13	10.30
8.74	4.51	10.41

Table 67 Adsorption of chloranil on γ-Al_2O_3

Activation temperature: 500°C Solvent: Dioxan

Initial concentration 10^{-3} mol dm^{-3}	Equilibrium concentration 10^{-3} mol dm^{-3}	Amount adsorbed 10^{-5} mol m^{-2}
0.80	0.61	0.51
2.63	2.02	1.51
3.69	2.90	1.95
4.69	3.81	2.15
5.37	4.51	2.21

Table 68 Adsorption of TCNQ on γ-Al_2O_3

Activation temperature: 500°C Solvent: Dioxan

Initial concentration 10^{-3} mol dm^{-3}	Equilibrium concentration 10^{-3} mol dm^{-3}	Amount adsorbed 10^{-5} mol m^{-2}
0.42	0.21	0.51
1.64	0.62	2.52
3.11	1.49	3.91
4.98	2.98	5.15
6.60	4.52	5.24

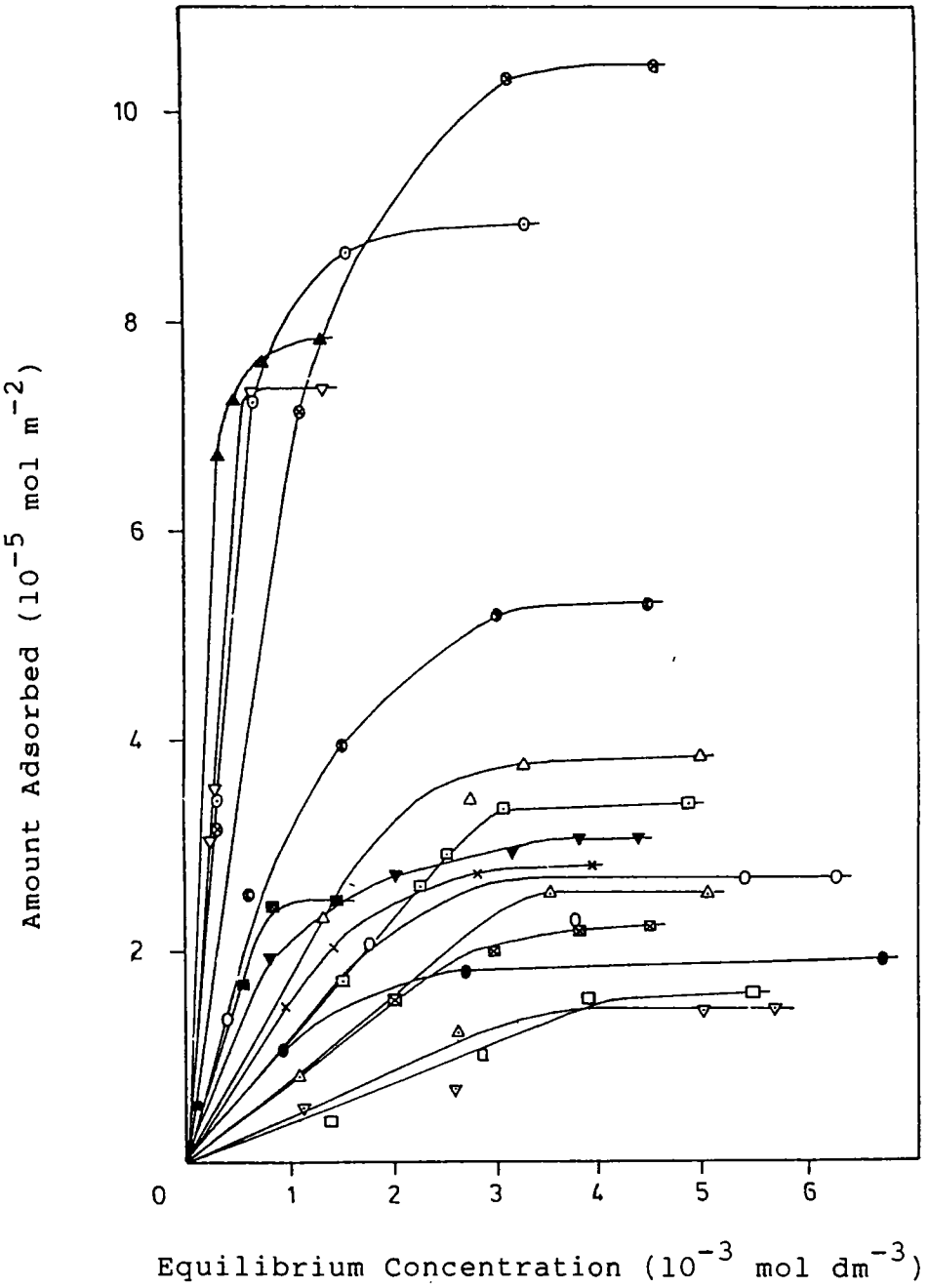

Electron acceptor/Solvent/wt. % of Y_2O_3

(CA - Chloranil ; AN - Acetonitrile ; TC - TCNQ ; D - Dioxan)

○ CA/AN/5 ⊙ TC/AN/5 ● CA/D/5 △ TC/D/5 ◬ CA/AN/10
▲ TC/AN/10 □ CA/D/10 ⊡ TC/D/10 ■ CA/AN/20 ▽ TC/AN/20
▽ CA/D/20 ▼ TC/D/20 × CA/AN/γ-Al_2O_3 ⊗ TC/AN/γ- Al_2O_3
⊠ CA/D/γ- Al_2O_3 ⊗ TC/D/γ-Al_2O_3

Fig.9 Adsorption isotherms on Y_2O_3-γ-Al_2O_3

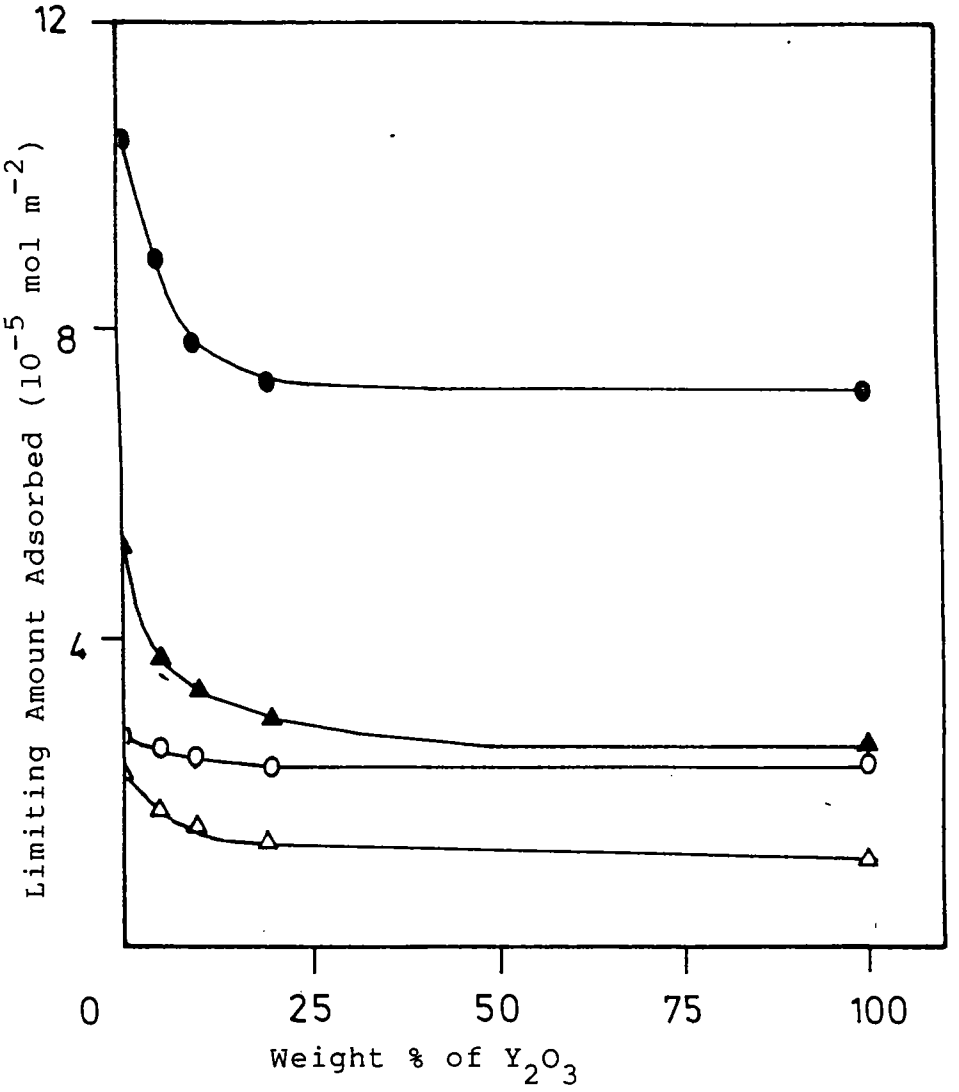

Electron acceptor/Solvent

(CA - Chloranil; AN - Acetonitrile; TC - TCNQ; D - Dioxan)

○CA/AN ●TC/AN △CA/D ▲TC/D

Fig.10 Limiting amount of electron acceptors adsorbed as a function of composition of Y_2O_3-Al_2O_3

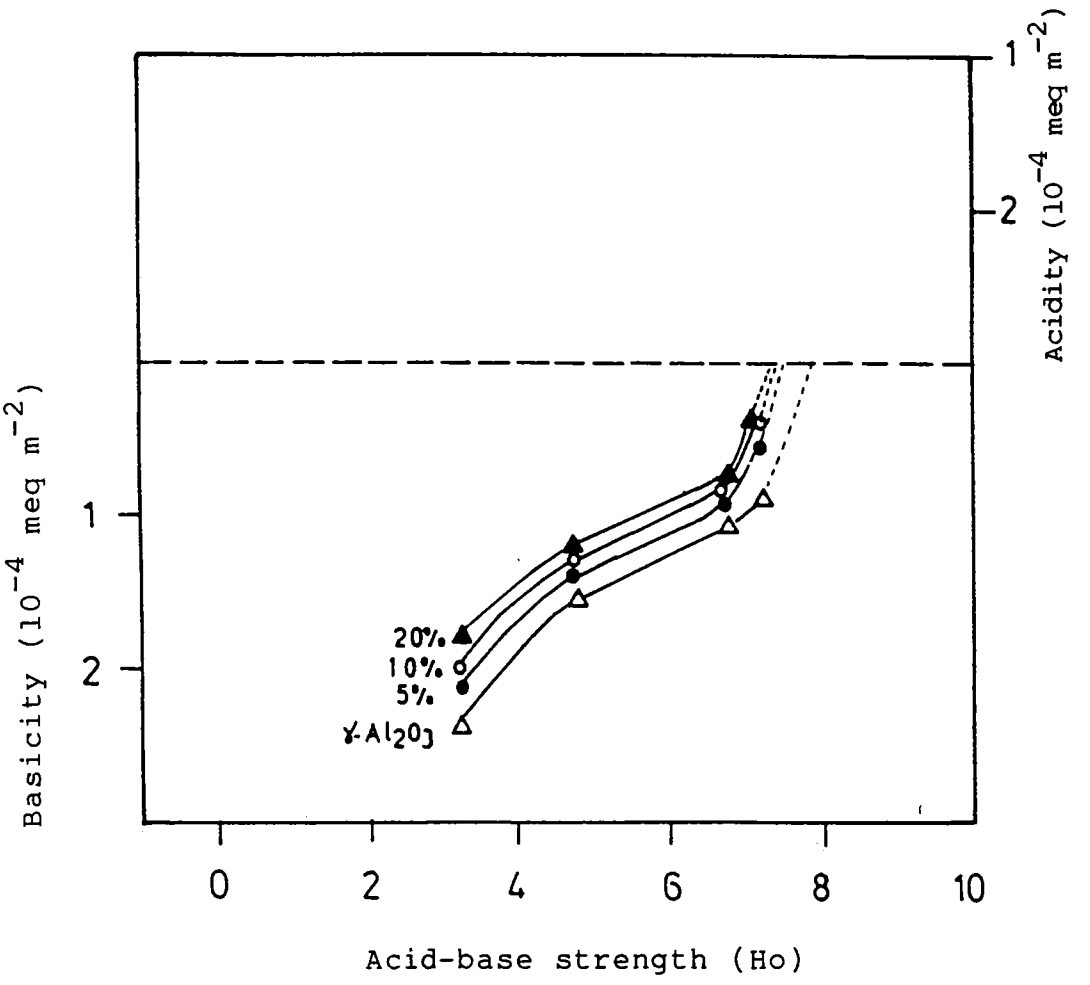

Fig.11 Acid-base strength distribution of Y_2O_3-γ-Al_2O_3

Y_2O_3-γ-Al_2O_3 system can be thus accounted. Added Y_2O_3 lower the surface electron properties by interfering with the basic center $Al^+ - O^-$ (Fig.11).

Pr_6O_{11}

The surface areas of Pr_6O_{11} activated at 300°C, 500°C and 800°C determined by BET method are given in Table 69.

Table 69 Surface area of Pr_6O_{11}

Method of preparation	Activation temperature (°C)	Surface area (m^2/g)
Hydroxide	300	8.6
Hydroxide	500	11.4
Hydroxide	800	9.20
Oxalate	800	10.51

The adsorption isotherms obtained for Pr_6O_{11} at different activation temperatures are shown in Fig.12 and values are given in Tables 70-87. In the case of Pr_6O_{11}, colourations acquired after the adsorption of electron acceptors could not be distinguished from the black colour

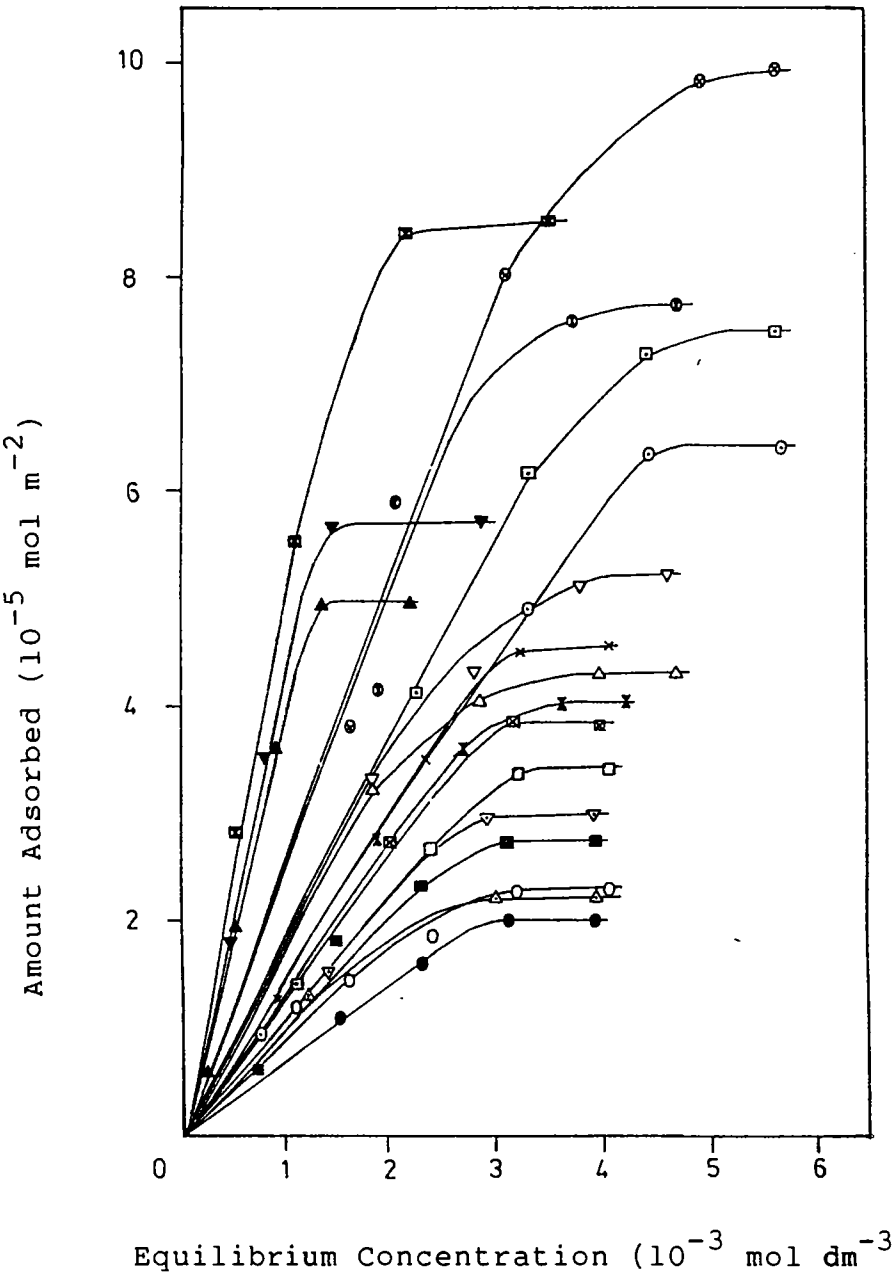

Electron acceptor/Solvent/Activation temperature (°C)

(CA - Chloranil; AN - Acetonitrile; TC - TCNQ; D - Dioxan)
EA - Ethylacetate)

○ CA/AN/300 ⊙ TC/AN/300 ● CA/D/300 △ TC/D/300 ◬ CA/EA/300
▲ TC/EA/300 □ CA/AN/500 ⊡ TC/AN/500 ■ CA/D/500 ▽ TC/D/500
▽ CA/EA/500 ▼ TC/EA/500 × CA/AN/800 ⊗ TC/AN/800 ⊠ CA/D/800
⊗ TC/D/800 ⧗ CA/EA/800 ⧈ TC/EA/800

Fig.12 Adsorption isotherms on Pr_6O_{11}

Table 70 Adsorption of chloranil on Pr_6O_{11}

Activation temperature: 300°C Solvent: Acetonitrile

Initial concentration 10^{-3} mol dm^{-3}	Equilibrium concentration 10^{-3} mol dm^{-3}	Amount adsorbed 10^{-5}mol m^{-2}	Magnetic Moment BM
0.41	0.40	0.31	--
0.83	0.78	0.95	--
1.66	1.59	1.47	1.71
2.49	2.41	1.84	1.55
3.32	3.22	2.23	1.32
4.15	4.05	2.22	1.29

Table 71 Adsorption of TCNQ on Pr_6O_{11}

Activation temperature: 300°C Solvent: Acetonitrile

Initial concentration 10^{-3} mol dm^{-3}	Equilibrium concentration 10^{-3} mol dm^{-3}	Amount adsorbed 10^{-5}mol m^{-2}	Magnetic Moment BM
0.59	0.57	0.76	--
1.18	1.10	1.22	1.72
2.37	2.26	2.53	1.72
3.55	3.34	4.93	0.91
4.74	4.46	6.38	0.74
5.92	5.64	6.44	0.73

Table 72 Adsorption of chloranil on Pr_6O_{11}

Activation temperature: 300°C Solvent: Dioxan

Initial concentration 10^{-3} mol dm^{-3}	Equilibrium concentration 10^{-3} mol dm^{-3}	Amount adsorbed 10^{-5} mol m^{-2}
0.79	0.76	0.08
1.59	1.53	1.18
2.39	2.31	1.58
3.18	3.09	2.00
3.98	3.89	2.00

Table 73 Adsorption of TCNQ on Pr_6O_{11}

Activation temperature: 300°C Solvent: Dioxan

Initial concentration 10^{-3} mol dm^{-3}	Equilibrium concentration 10^{-3} mol dm^{-3}	Amount adsorbed 10^{-5} mol m^{-2}
0.95	0.92	0.92
1.91	1.85	3.21
2.97	2.85	4.05
3.87	3.69	4.31
4.83	4.65	4.33

Table 74 Adsorption of chloranil on Pr_6O_{11}

Activation temperature: 300°C Solvent: Ethylacetate

Initial concentration 10^{-3} mol dm^{-3}	Equilibrium concentration 10^{-3} mol dm^{-3}	Amount adsorbed 10^{-5} mol m^{-2}
0.79	0.73	0.55
1.22	1.18	1.29
2.38	2.32	1.61
3.09	3.01	2.17
3.96	3.88	2.18

Table 75 Adsorption of TCNQ on Pr_6O_{11}

Activation temperature: 300°C Solvent: Ethylacetate

Initial concentration 10^{-3} mol dm^{-3}	Equilibrium concentration 10^{-3} mol dm^{-3}	Amount adsorbed 10^{-5} mol m^{-2}
0.22	0.20	0.61
0.59	0.51	1.93
1.06	0.91	3.61
1.55	1.35	4.92
2.39	2.17	4.96

Table 76 Adsorption of chloranil on Pr_6O_{11}

Activation temperature: 500°C Solvent: Acetonitrile

Initial concentration 10^{-3} mol dm^{-3}	Equilibrium concentration 10^{-3} mol dm^{-3}	Amount adsorbed 10^{-5}mol m^{-2}	Radical concentration 10^{16} spins m^{-2}	Magnetic Moment BM
0.42	0.34	0.23	0.13	--
0.84	0.74	1.20	0.67	2.91
1.69	0.76	2.00	1.12	2.72
2.54	2.39	2.64	1.48	1.84
3.39	3.21	3.35	1.88	1.58
4.24	4.00	3.39	1.90	1.56

Table 77 Adsorption of TCNQ on Pr_6O_{11}

Activation temperature: 500°C Solvent: Acetonitrile

Initial concentration 10^{-3} mol dm^{-3}	Equilibrium concentration 10^{-3} mol dm^{-3}	Amount adsorbed 10^{-5}mol m^{-2}	Radical concentration 10^{18} spins m^{-2}	Magnetic Moment BM
1.19	1.10	1.42	0.79	2.52
2.39	2.25	4.09	2.21	1.41
3.59	3.30	6.15	3.33	1.12
4.78	4.40	7.24	3.92	0.98
5.98	5.57	7.44	4.03	0.96

Table 78 Adsorption of chloranil on Pr_6O_{11}

Activation temperature: 500°C Solvent: Dioxan

Initial concentration 10^{-3} mol dm^{-3}	Equilibrium concentration 10^{-3} mol dm^{-3}	Amount adsorbed 10^{-5} mol m^{-2}
0.79	0.71	0.58
1.69	1.52	1.78
2.79	2.31	2.29
3.19	3.09	2.70
3.99	3.88	2.71

Table 79 Adsorption of TCNQ on Pr_6O_{11}

Activation temperature: 500°C Solvent: Dioxan

Initial concentration 10^{-3} mol dm^{-3}	Equilibrium concentration 10^{-3} mol dm^{-3}	Amount adsorbed 10^{-5} mol m^{-2}
0.96	0.91	0.91
1.93	1.84	3.28
2.90	2.77	4.31
3.97	3.74	5.18
4.94	4.67	5.21

Table 80 Adsorption of chloranil on Pr_6O_{11}

Activation temperature: 500°C Solvent: Ethylacetate

Initial concentration 10^{-3} mol dm^{-3}	Equilibrium concentration 10^{-3} mol dm^{-3}	Amount adsorbed 10^{-5} mol m^{-2}
0.78	0.77	0.21
1.44	1.40	1.52
2.34	2.21	2.46
2.98	2.82	2.94
4.08	3.92	2.98

Table 81 Adsorption of TCNQ on Pr_6O_{11}

Activation temperature: 500°C Solvent: Ethylacetate

Initial concentration 10^{-3} mol dm^{-3}	Equilibrium concentration 10^{-3} mol dm^{-3}	Amount adsorbed 10^{-5} mol m^{-2}
0.14	0.12	0.47
0.54	0.44	1.82
1.01	0.81	3.52
1.70	1.41	5.69
3.17	2.85	5.71

Table 82 Adsorption of chloranil on Pr_6O_{11}

Activation temperature: 800°C Solvent: Acetonitrile

Initial concentration 10^{-3} mol dm^{-3}	Equilibrium concentration 10^{-3} mol dm^{-3}	Amount adsorbed 10^{-5}mol m^{-2}	Magnetic Moment BM
0.85	0.79	0.13	3.18
1.70	1.53	2.49	2.52
2.56	2.37	3.49	2.11
3.41	3.20	4.53	1.82
4.26	4.06	4.54	1.80

Table 83 Adsorption of TCNQ on Pr_6O_{11}

Activation temperature: 800°C Solvent: Acetonitrile

Initial concentration 10^{-3} mol dm^{-3}	Equilibrium concentration 10^{-3} mol dm^{-3}	Amount adsorbed 10^{-5}mol m^{-2}	Magnetic Moment BM
1.20	1.01	2.71	2.78
2.41	1.64	3.76	1.72
3.62	3.07	8.02	1.28
4.83	4.41	9.86	0.86
6.03	5.62	9.96	0.86

Table 84 Adsorption of chloranil on Pr_6O_{11}

Activation temperature: 800°C Solvent: Dioxan

Initial concentration 10^{-3} mol dm^{-3}	Equilibrium concentration 10^{-3} mol dm^{-3}	Amount adsorbed 10^{-5} mol m^{-2}
0.82	0.80	0.57
1.66	1.48	2.57
2.49	2.03	2.71
3.38	3.14	3.86
4.20	3.96	3.81

Table 85 Adsorption of TCNQ on Pr_6O_{11}

Activation temperature: 800°C Solvent: Dioxan

Initial concentration 10^{-3} mol dm^{-3}	Equilibrium concentration 10^{-3} mol dm^{-3}	Amount adsorbed 10^{-5} mol m^{-2}
0.98	0.96	0.93
1.96	1.93	4.16
3.05	2.05	5.91
3.99	3.68	7.56
5.08	4.66	7.71

Table 86 Adsorption of chloranil on Pr_6O_{11}

Activation temperature: 800°C Solvent: Ethylacetate

Initial concentration 10^{-3} mol dm^{-3}	Equilibrium concentration 10^{-3} mol dm^{-3}	Amount adsorbed 10^{-5} mol m^{-2}
0.50	0.46	0.98
2.03	1.92	2.71
2.86	2.71	3.61
3.79	3.62	3.98
4.39	4.21	4.01

Table 87 Adsorption of TCNQ on Pr_6O_{11}

Activation temperature: 800°C Solvent: Ethylacetate

Initial concentration 10^{-3} mol dm^{-3}	Equilibrium concentration 10^{-3} mol dm^{-3}	Amount adsorbed 10^{-5} mol m^{-2}
0.29	0.27	0.28
0.65	0.51	2.80
1.33	1.10	5.52
2.52	2.14	8.42
3.88	3.50	8.48

of pure oxide. For Pr_6O_{11} activated at 300, 500, and 800°C the limit of electron transfer is between 2.40 and 1.77 eV in both acetonitrile and 1,4-dioxan. The radical concentrations of TCNQ and chloranil adsorbed on Pr_6O_{11} activated at 500°C is given Tables 76-77.

To interpret the solvent effect in terms of acid-base theory, adsorption studies of Pr_6O_{11} is carried out in three solvents-acetonitrile, 1,4-dioxan and ethyl acetate. The limiting amount of electron acceptors adsorbed is found to decrease with increasing basicity of solvent. The heats of mixing of substances with acid-base interaction are expressed by Drago equation.

$$-\Delta H^{ab} = C_A C_B + E_A E_B$$

where E and C are Drago constants for acidic compound (A) and basic compound (B) [15]. Drago et al., determined many E and C values for organic compounds from measurements of the heat of acid-base interactions using calorimetric and spectroscopic method [16]. Their studies demonstrated that, Drago equation usually predicted ΔH^{ab} values within 3%. Accordingly, a very useful approach for relating the interfacial interactions quantitatively has been provided

by Drago equation of enthalpy change in acid-base complexation. When Drago equation is applied to present systems, basic compound corresponds to solvents acetonitrile, ethyl acetate and dioxan and acidic compound to TCNQ and chloranil. The basicity of solvents was estimated by the heat of interaction with TCNQ and chloranil and the values are listed in Tables 88-89. As the values of E and C for TCNQ are not available, E and C values of TCNE which is similar to TCNQ are employed. The saturated amounts of TCNQ and chloranil adsorbed onto Pr_6O_{11} at 300, 500 and 800°C are plotted as a function of basicity of solvents in Figs.13 and 14. It shows that the amount of TCNQ saturated on Pr_6O_{11} decreases with an increase in acid-base interactions (ΔH^{ab}) between basic solvents and TCNQ. For these basic solvents, limiting amounts of TCNQ decreased in the following order: acetonitrile ethyl acetate dioxan ie., decreasing with increasing basicity of solvents. In the Fig.13 the decrease in adsorption of TCNQ with increase in basicity of solvent shows the competition with basic solvents and basic sites of oxide for TCNQ. In the Fig.14 the adsorption of chloranil onto Pr_6O_{11} is also shown to decrease with more basic solvents. Thus, TCNQ or chloranil adsorption onto Pr_6O_{11} is strongly influenced by interaction between basic solvents and TCNQ or chloranil and

Table 88 Acid-base parameters

TCNE: $C_A = 1.51$, $E_A = 1.68$

Solvent	C_B	E_B	C_A	E_A	$-\Delta H^{ab}$ with TCNE k J mol^{-1}
Acetonitrile	1.34	0.88	--	--	14.74
Ethylacetate	1.74	0.97	--	--	17.90
Dioxan	2.38	1.09	--	--	21.90

Table 89 Acid-base parameters

Chloranil: $C_A = 2.39$, $E_A = 2.56$

Solvent	C_B	E_B	C_A	E_A	$-\Delta H^{ab}$ with chloranil k J mol^{-1}
Acetonitrile	2.74	1.81	--	--	11.19
Ethylacetate	3.56	1.99	--	--	13.61
Dioxan	4.87	2.23	--	--	17.35

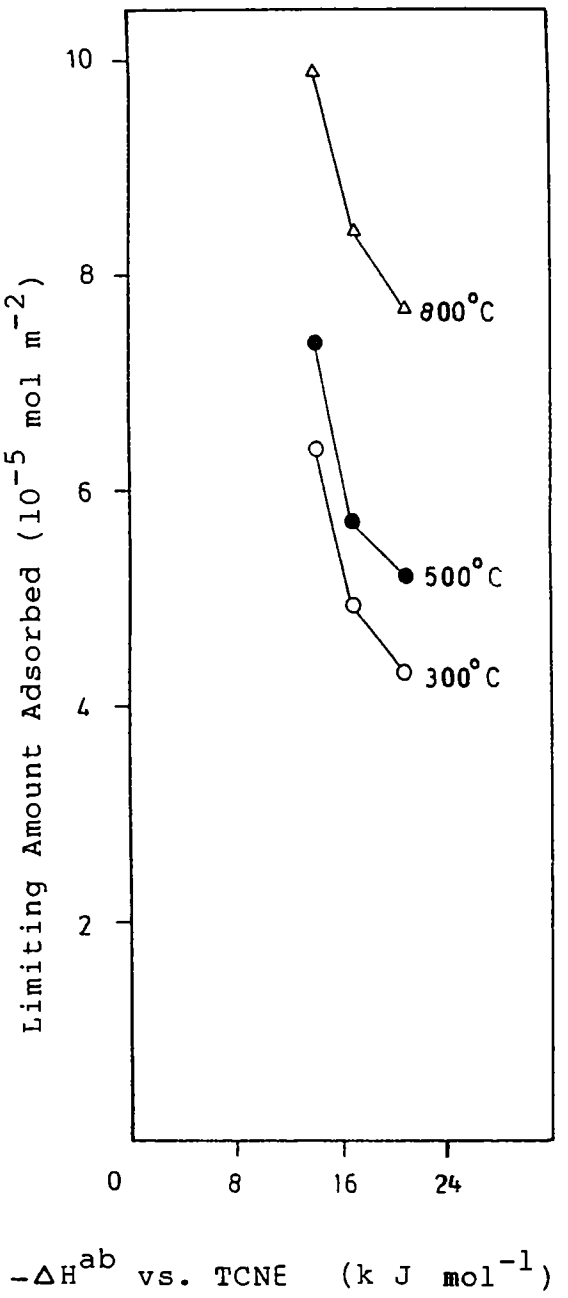

Fig.13 Limiting amount of TCNQ adsorbed on Pr_6O_{11} as a function of acid-base interaction enthalpy

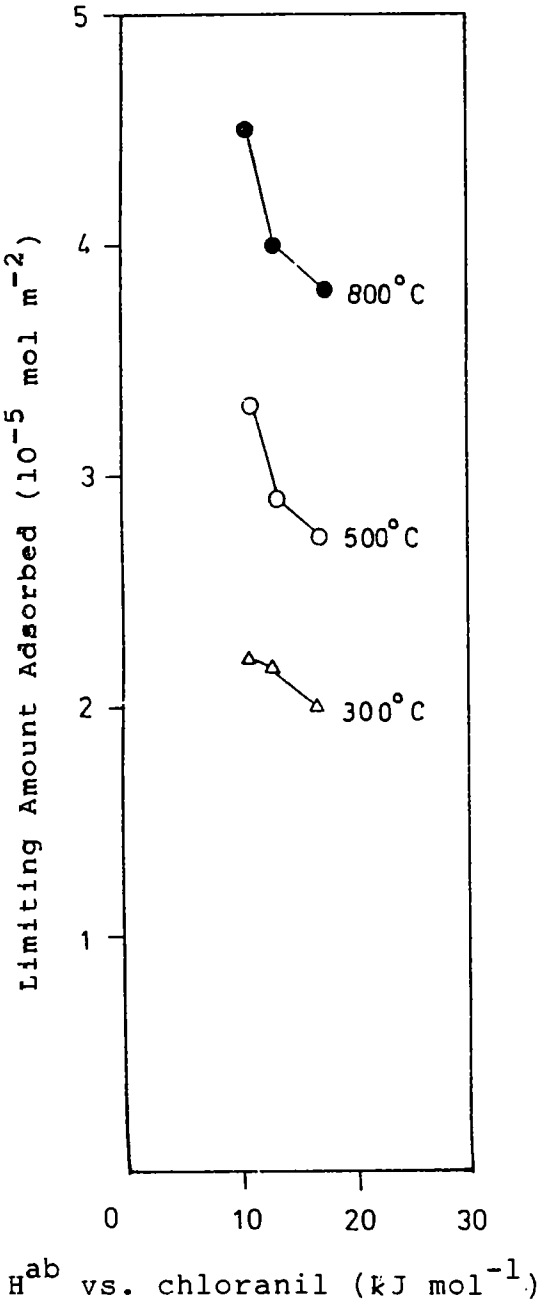

Fig.14 Limiting amount of chloranil adsorbed on Pr_6O_{11} as a function of acid-base interaction enthalpy

these interactions can be estimated from acid-base enthalpy predicted by Drago equation.

The limiting amount of electron acceptors adsorbed on Pr_6O_{11} prepared by hydroxide method is greater than that adsorbed on Pr_6O_{11} prepared by oxalate method (Table 90-93).

Fig.15 shows the basicity of Pr_6O_{11} at 300, 500 and 800°C. The data are given in Table 94. On Pr_6O_{11} at the three activation temperatures studied only basic sites were present. Ho_{max} values determined from acid-base distribution curves are given in Table 94. As the activation temperature of Pr_6O_{11} increases, Ho_{max} value also increases.

The magnetic moment of Pr_6O_{11} before and after adsorption of electron acceptors was determined. It is found that during the adsorption of electron acceptors the magnetic moment of oxide decreases. The values are given in Tables 70,71,76,77,82,83. In Fig.16 magnetic moment of oxide is plotted as a function of equilibrium concentration of electron acceptor. Fig.16 shows that magnetic moment of Pr_6O_{11} decreases and reaches a limiting value at the same

Table 90 Adsorption of chloranil on Pr_6O_{11}
(Regenerated by oxalate method)

Activation temperature: 800°C Solvent: Acetonitrile

Initial concentration 10^{-3} mol dm^{-3}	Equilibrium concentration 10^{-3} mol dm^{-3}	Amount adsorbed 10^{-5} mol m^{-2}
0.24	0.21	0.46
0.98	0.92	0.86
1.44	1.34	1.81
2.31	2.11	3.42
3.34	3.08	4.38
4.18	3.92	4.41

Table 91 Adsorption of TCNQ on Pr_6O_{11}
(Regenerated by oxalate method)

Activation temperature: 800°C Solvent: Acetonitrile

Initial concentration 10^{-3} mol dm^{-3}	Equilibrium concentration 10^{-3} mol dm^{-3}	Amount adsorbed 10^{-5} mol m^{-2}
0.49	0.41	1.51
1.45	1.22	3.81
2.45	2.02	5.56
3.56	2.84	7.81
4.71	4.12	9.79
6.27	5.63	9.82

Table 92 Adsorption of chloranil on Pr_6O_{11}
(Regenerated by oxalate method)

Activation temperature: 800°C Solvent: Dioxan

Initial concentration 10^{-3} mol dm^{-3}	Equilibrium concentration 10^{-3} mol dm^{-3}	Amount adsorbed 10^{-5} mol m^{-2}
0.86	0.81	0.86
1.62	1.55	2.01
2.21	2.07	2.43
3.0	2.82	2.98
3.89	3.72	3.04

Table 93 Adsorption of TCNQ on Pr_6O_{11}
(Regenerated by oxalate method)

Activation temperature: 800°C Solvent: Dioxan

Initial concentration 10^{-3} mol dm^{-3}	Equilibrium concentration 10^{-3} mol dm^{-3}	Amount adsorbed 10^{-5} mol m^{-2}
0.64	0.55	1.56
1.32	1.17	2.51
2.39	1.97	3.59
2.85	2.62	4.52
3.82	3.51	5.42
5.06	4.72	5.47

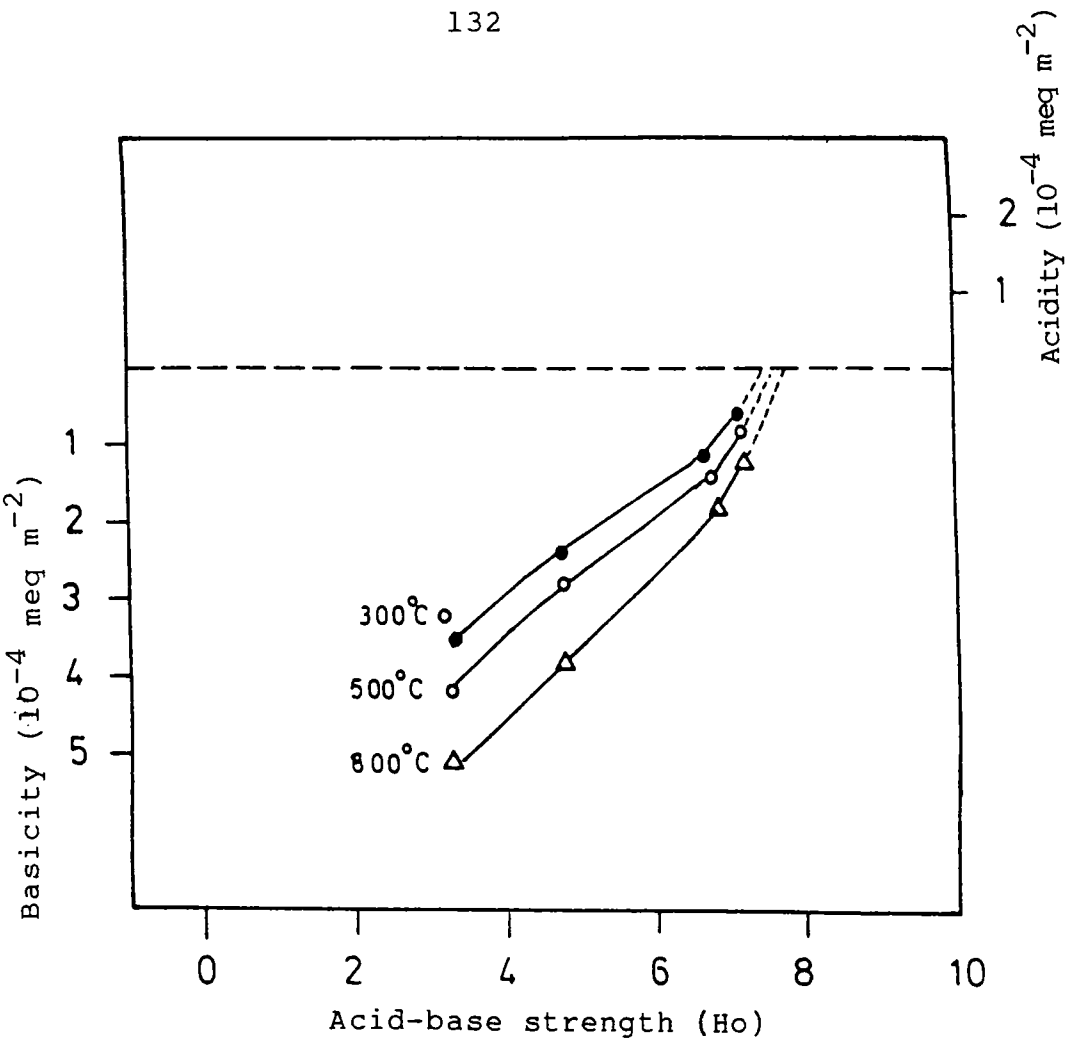

Fig.15 Acid-base strength distribution of Pr_6O_{11}

Table 94 Basicity and Ho_{max} of Pr_6O_{11} at different activation temperatures

Activation Temperature (°C)	Basicity (10^{-3} meq m^{-2})				Ho_{max}
	Ho ≥ 3.3	Ho ≥ 4.8	Ho ≥ 6.8	Ho ≥ 7.2	
300	3.68	2.41	1.14	0.65	7.5
500	4.21	2.88	1.42	0.82	7.6
800	5.12	3.84	1.81	1.21	7.8

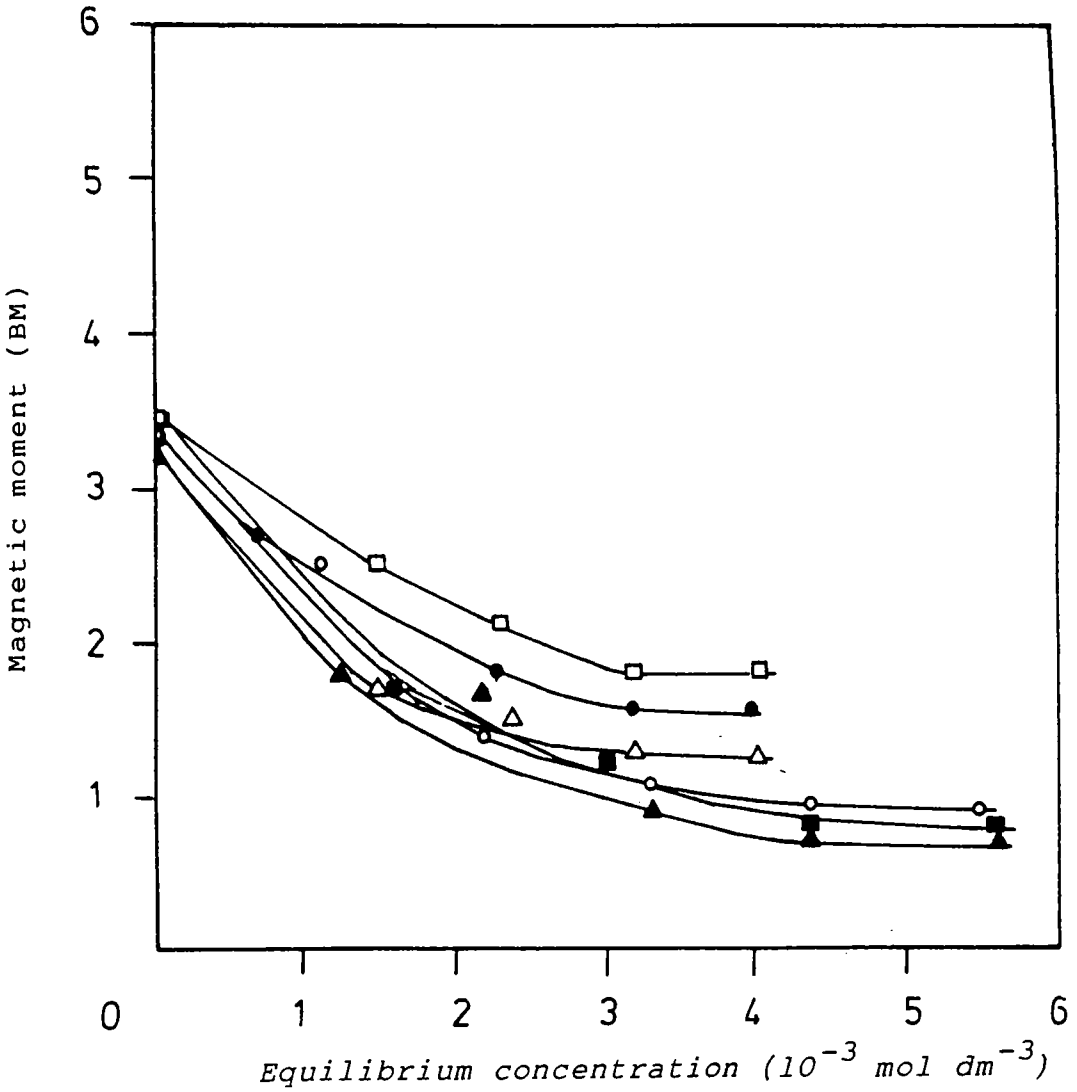

Electron acceptor/Solvent/Activation temperature

(CA - Chloranil; AN - Acetonitrile; TC - TCNQ)

△ CA/AN/300 ▲ TC/AN/300 ● CA/AN/500 ○ TC/AN/500 □ CA/AN/800
■ TC/AN/800

Fig.16 Magnetic moment of Pr_6O_{11} as a function of equilibrium concentration of electron acceptor

concentration at which the limiting amount of electron acceptors was obtained establishing the electron transfer from the oxide surface to the electron acceptor. As expected, an increase in temperature increase the concentration of electron donor sites.

Pr_6O_{11}-Al_2O_3 (Co-hydrolysis from sulphate solution)

The following systems have been studied at an activation temperature of 500°C. The surface areas of Pr_6O_{11}-Al_2O_3 of various compositions are given in Table 95.

Table 95 Surface area of Pr_6O_{11}-Al_2O_3

% by weight of Pr_6O_{11}	Surface area (m^2/g)
5	134.60
10	141.55
15	136.81
20	132.50

Fig.17 shows the adsorption isotherms obtained for different compositions of Pr_6O_{11}-Al_2O_3 and values are given in Tables 96-111. The adsorption of TCNQ on mixed oxide

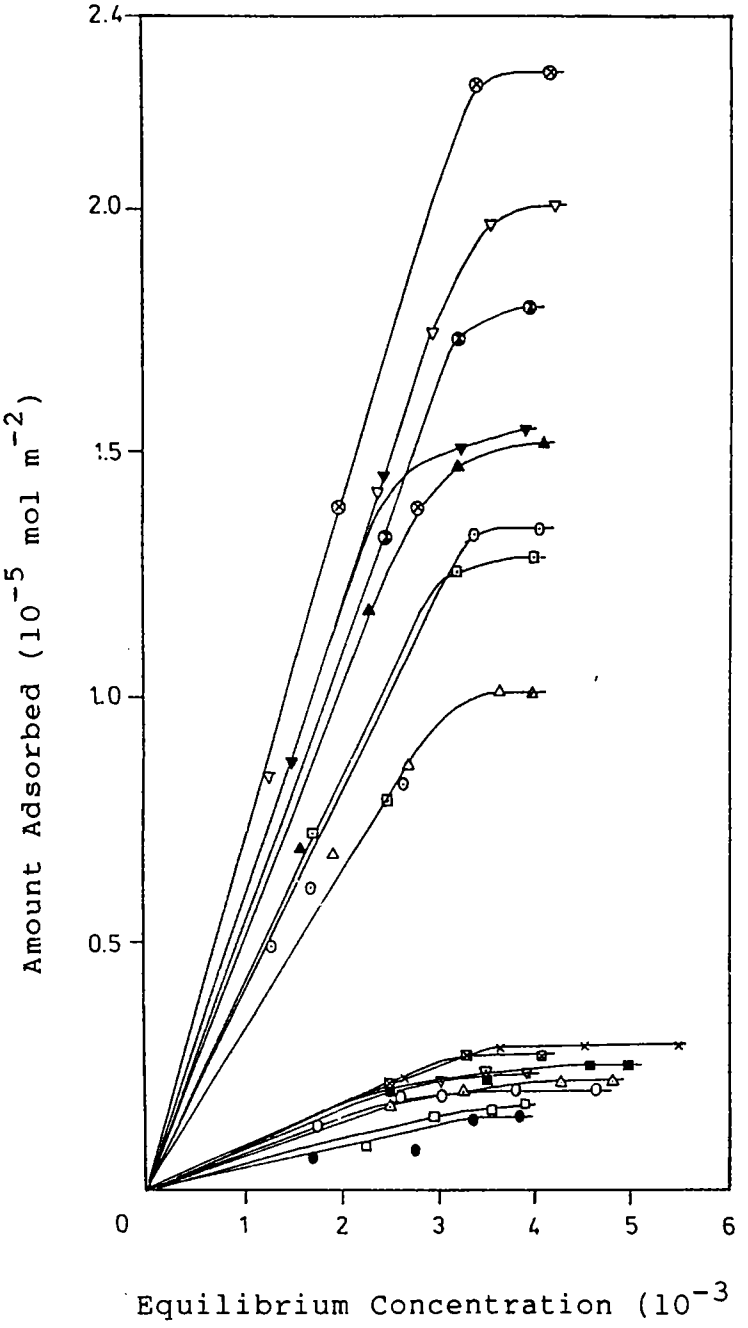

Electron acceptor/Solvent/wt. % of Pr_6O_{11}

(CA - Chloranil; AN - Acetonitrile; TC - TCNQ; D - Dioxan)

○ CA/AN/5 ⊙ TC/AN/5 ● CA/D/5 △ TC/D/5 ◬ CA/AN/10
▲ TC/AN/10 □ CA/D/10 ⊡ TC/D/10 ■ CA/AN/15 ▽ TC/AN/15
▽ CA/D/15 ▽ TC/D/15 × CA/AN/20 ⊗ TC/AN/20 ⊠ CA/D/20
⊗ TC/D/20

Fig.17 Adsorption isotherms on Pr_6O_{11}-Al_2O_3 (Prepared from sulphate)

Table 96 Adsorption of chloranil on Pr_6O_{11}-Al_2O_3 (5%)

Activation temperature: 500°C Solvent: Acetonitrile

Initial concentration 10^{-3} mol dm^{-3}	Equilibrium concentration 10^{-3} mol dm^{-3}	Amount adsorbed 10^{-6} mol m^{-2}
1.24	1.21	0.32
1.81	1.76	1.36
2.67	2.60	1.98
3.15	3.04	1.96
3.92	3.78	2.06
4.78	4.64	2.09

Table 97 Adsorption of TCNQ on Pr_6O_{11}-Al_2O_3 (5%)

Activation temperature: 500°C Solvent: Acetonitrile

Initial concentration 10^{-3} mol dm^{-3}	Equilibrium concentration 10^{-3} mol dm^{-3}	Amount adsorbed 10^{-6} mol m^{-2}
0.89	0.84	0.67
1.59	1.30	4.90
2.09	1.69	6.09
3.18	2.64	8.24
4.28	3.42	13.20
4.97	4.11	13.30

Table 98 Adsorption of chloranil on Pr_6O_{11}-Al_2O_3 (5%)

Activation temperature: 500°C Solvent: Dioxan

Initial concentration 10^{-3} mol dm^{-3}	Equilibrium concentration 10^{-3} mol dm^{-3}	Amount adsorbed 10^{-6} mol m^{-2}
0.70	0.69	0.13
1.26	1.23	3.69
1.73	1.69	6.40
2.83	2.77	8.24
3.46	3.36	14.20
3.94	3.84	14.90

Table 99 Adsorption of TCNQ on Pr_6O_{11}-Al_2O_3 (5%)

Activation temperature: 500°C Solvent: Dioxan

Initial concentration 10^{-3} mol dm^{-3}	Equilibrium concentration 10^{-3} mol dm^{-3}	Amount adsorbed 10^{-5} mol m^{-2}
1.40	1.08	0.32
2.34	1.89	0.68
3.28	2.71	0.86
4.32	3.64	1.08
4.69	3.98	1.10

Table 100 Adsorption of chloranil on Pr_6O_{11}-Al_2O_3 (10%)

Activation temperature: 500°C Solvent: Acetonitrile

Initial concentration 10^{-3} mol dm^{-3}	Equilibrium concentration 10^{-3} mol dm^{-3}	Amount adsorbed 10^{-6} mol m^{-2}
0.39	0.38	0.21
1.49	1.45	1.30
2.58	2.53	1.73
3.47	3.26	1.99
4.47	4.32	2.16
4.96	4.82	2.20

Table 101 Adsorption of TCNQ on Pr_6O_{11}-Al_2O_3 (10%)

Activation temperature: 500°C Solvent: Acetonitrile

Initial concentration 10^{-3} mol dm^{-3}	Equilibrium concentration 10^{-3} mol dm^{-3}	Amount adsorbed 10^{-5} mol m^{-2}
0.52	0.41	0.15
1.04	0.75	0.42
2.08	1.58	0.69
3.12	2.31	1.17
4.16	3.18	1.46
5.21	4.16	1.51

Table 102 Adsorption of chloranil on Pr_6O_{11}-Al_2O_3 (10%)

Activation temperature: 500°C Solvent: Dioxan

Initial concentration 10^{-3} mol dm^{-3}	Equilibrium concentration 10^{-3} mol dm^{-3}	Amount adsorbed 10^{-7} mol m^{-2}
0.64	0.63	0.59
1.44	1.41	4.37
2.32	2.27	7.30
2.96	2.91	14.80
3.69	3.57	16.70
4.01	3.89	17.00

Table 103 Adsorption of $TCNQ^-$ on Pr_6O_{11}-Al_2O_3 (10%)

Activation temperature: 500°C Solvent: Dioxan

Initial concentration 10^{-3} mol dm^{-3}	Equilibrium concentration 10^{-3} mol dm^{-3}	Amount adsorbed 10^{-6} mol m^{-2}
0.48	0.45	0.15
1.07	0.93	2.05
2.14	1.72	7.23
3.01	2.52	7.93
3.99	3.18	12.40
4.89	4.03	12.80

Table 104 Adsorption of chloranil on Pr_6O_{11}-Al_2O_3 (15%)

Activation temperature: 500°C Solvent: Acetonitrile

Initial concentration 10^{-3} mol dm^{-3}	Equilibrium concentration 10^{-3} mol dm^{-3}	Amount adsorbed 10^{-6} mol m^{-2}
0.52	0.51	0.14
1.57	1.52	0.80
2.63	2.57	2.06
3.68	3.57	2.26
4.73	4.57	2.47
5.26	5.09	2.49

Table 105 Adsorption of TCNQ on Pr_6O_{11}-Al_2O_3 (15%)

Activation temperature: 500°C Solvent: Acetonitrile

Initial concentration 10^{-3} mol dm^{-3}	Equilibrium concentration 10^{-3} mol dm^{-3}	Amount adsorbed 10^{-5} mol m^{-2}
0.56	0.53	0.47
1.59	1.25	0.83
2.84	2.38	1.40
3.86	2.98	1.73
5.00	3.63	1.96
5.68	4.32	2.03

Table 106 Adsorption of chloranil on Pr_6O_{11}-Al_2O_3 (15%)

Activation temperature: 500°C Solvent: Dioxan

Initial concentration 10^{-3} moldm^{-3}	Equilibrium concentration 10^{-3} moldm^{-3}	Amount adsorbed 10^{-6} mol m^{-2}
0.91	0.90	0.05
1.56	1.52	0.46
2.22	2.17	1.90
3.12	3.06	2.03
3.74	3.59	2.36
4.11	3.96	2.31

Table 107 Adsorption of TCNQ on Pr_6O_{11}-Al_2O_3 (15%)

Activation temperature: 500°C Solvent: Dioxan

Initial concentration 10^{-3} moldm^{-3}	Equilibrium concentration 10^{-3} moldm^{-3}	Amount adsorbed 10^{-5} mol m^{-2}
0.49	0.45	0.06
1.29	1.15	0.20
2.29	1.53	0.86
3.28	2.40	1.45
4.28	3.30	1.49
4.98	3.96	1.54

Table 108 Adsorption of chloranil on Pr_6O_{11}-Al_2O_3 (20%)

Activation temperature: 500°C Solvent: Acetonitrile

Initial concentration 10^{-3} mol dm^{-3}	Equilibrium concentration 10^{-3} mol dm^{-3}	Amount adsorbed 10^{-6} mol m^{-2}
2.05	2.00	0.74
2.74	2.65	2.32
3.76	3.65	2.92
4.79	4.73	2.98
5.71	5.52	2.91

Table 109 Adsorption of TCNQ on Pr_6O_{11}-Al_2O_3 (20%)

Activation temperature: 500°C Solvent: Acetonitrile

Initial concentration 10^{-3} mol dm^{-3}	Equilibrium concentration 10^{-3} mol dm^{-3}	Amount adsorbed 10^{-5} mol m^{-2}
0.91	0.87	0.57
2.74	1.91	1.38
3.77	2.85	1.58
4.91	3.47	2.25
5.72	4.24	2.27

Table 110 Adsorption of chloranil on Pr_6O_{11}-Al_2O_3 (20%)

Activation temperature: 500°C Solvent: Dioxan

Initial concentration 10^{-3} mol dm^{-3}	Equilibrium concentration 10^{-3} mol dm^{-3}	Amount adsorbed 10^{-6} mol m^{-2}
0.42	0.41	0.23
0.48	0.46	0.67
1.88	1.82	0.82
2.73	2.58	2.24
3.51	3.35	2.74
4.28	4.12	2.71

Table 111 Adsorption of TCNQ on Pr_6O_{11}-Al_2O_3 (20%)

Activation temperature: 500°C Solvent: Dioxan

Initial concentration 10^{-3} mol dm^{-3}	Equilibrium concentration 10^{-3} mol dm^{-3}	Amount adsorbed 10^{-5} mol m^{-2}
1.02	0.96	0.08
1.43	1.27	0.63
2.36	1.93	1.07
3.28	2.47	1.32
4.31	3.23	1.72
5.13	3.98	1.79

produced bluish green colour while chloranil adsorption gave pink colour to Pr_6O_{11}-Al_2O_3. The limiting amount of electron acceptor adsorbed is plotted as a function of composition of the mixed oxide in Fig.18. Mixed oxide Pr_6O_{11}-Al_2O_3 showed much less electron donicity than pure Pr_6O_{11} and electron donicity is found to increase with increase in the concentration of Pr_6O_{11} in the mixed oxide showing the modification of electron donor sites of Al_2O_3 by added Pr_6O_{11}. The limit of electron transfer of the mixed oxide is located between 2.40 and 1.77 eV as in the case of pure Pr_6O_{11}.

The basicity of Pr_6O_{11}-Al_2O_3 determined is given in Table 112 and acid-base distribution curves are shown in Fig.19. The basic strength of mixed oxide Pr_6O_{11}-Al_2O_3 is much lower than the pure oxide Pr_6O_{11} and is higher than Al_2O_3. Electron donicity of Pr_6O_{11}-Al_2O_3 is in the same order as that of electron donicity of mixed oxide Y_2O_3-Al_2O_3. The effect of Pr_6O_{11} on electron donor properties of Al_2O_3 can be understood in the same lines as in the case of Y_2O_3-Al_2O_3 systems.

$\underline{Pr_6O_{11}\text{-}Al_2O_3}$ (Co-hydrolysis from nitrate solution)

The following systems have been studied at an activation temperature of 500°C. The surface area of the mixed oxides are given in Table 113.

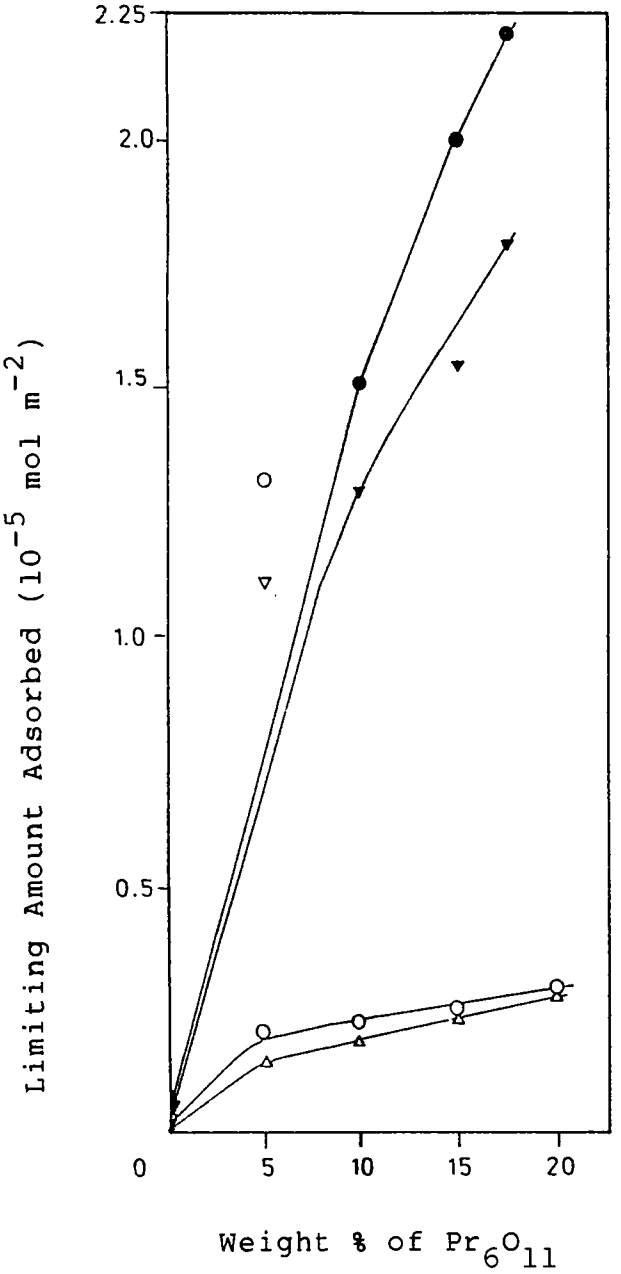

Electron acceptor/Solvent

(CA - Chloranil; AN - Acetonitrile; TC - TCNQ; D - Dioxan)

○ CA/AN ● TC/AN △ CA/D ▲ TC/D

Fig.18 Limiting amount of electron acceptors adsorbed as a function of composition of Pr_6O_{11}-Al_2O_3

Table 112 Basicity and Ho_{max} of Pr_6O_{11}-Al_2O_3 of various compositions

% by weight of mixed oxide	Basicity (10^{-4} meq m^{-2})				Ho_{max}
	$Ho \geq 3.3$	$Ho \geq 4.8$	$Ho \geq 6.8$	$Ho \geq 7.2$	
5	1.48	0.72	0.21	0.11	7.2
10	1.72	0.90	0.38	0.18	7.4
15	1.91	1.17	0.53	0.21	7.5
20	2.18	1.38	0.71	0.35	7.5

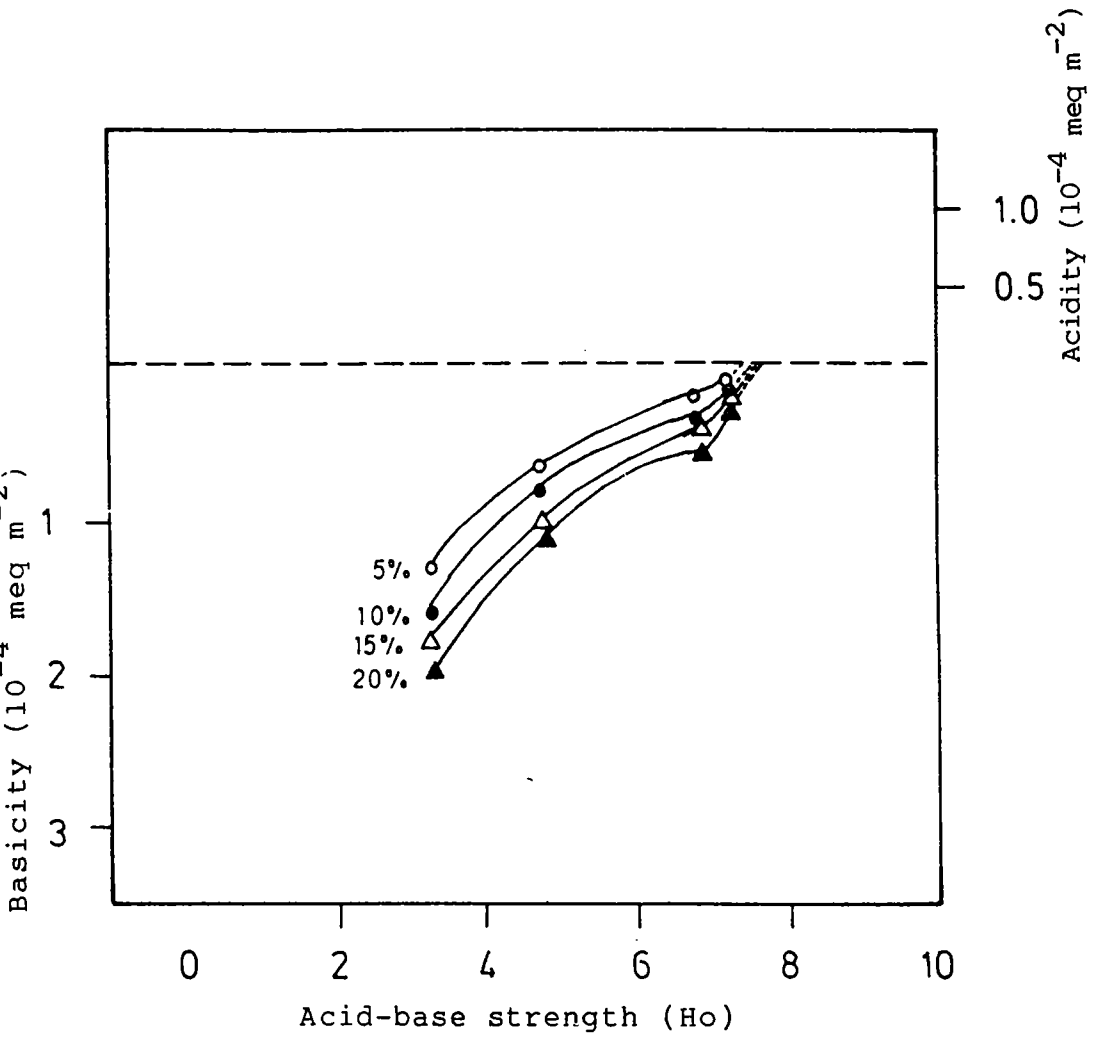

Fig.19 Acid-base strength distribution of Pr_6O_{11}-Al_2O_3 (Prepared from sulfate)

Table 113 Surface area of Pr_6O_{11}-Al_2O_3

% by weight of Pr_6O_{11}	Surface area m^2/g
5	168.20
10	171.50
20	174.81
60	178.22
Al_2O_3	193.90
Pr_6O_{11}	71.40

The adsorption isotherms are shown in Fig.20 and values are given in Tables 114-129. Here the mixed systems Pr_6O_{11}-Al_2O_3 showed greater electron donicity than Pr_6O_{11}.

The amount of electron acceptors adsorbed as a function of composition of mixed system is shown in Fig.21. The electron donicity of Al_2O_3 increased with increase in concentration of added Pr_6O_{11} for low concentrations of Pr_6O_{11} (20% by weight). It goes to a maximum at about 40% of Pr_6O_{11} and then decreased gradually upto 60% Pr_6O_{11} and finally decreased steeply from 60% Pr_6O_{11} to pure Pr_6O_{11}. Here Al_2O_3 prepared from Aluminium nitrate solution had greater electron donicity than Pr_6O_{11}, but much less than that of γ-alumina (Tables 130-133).

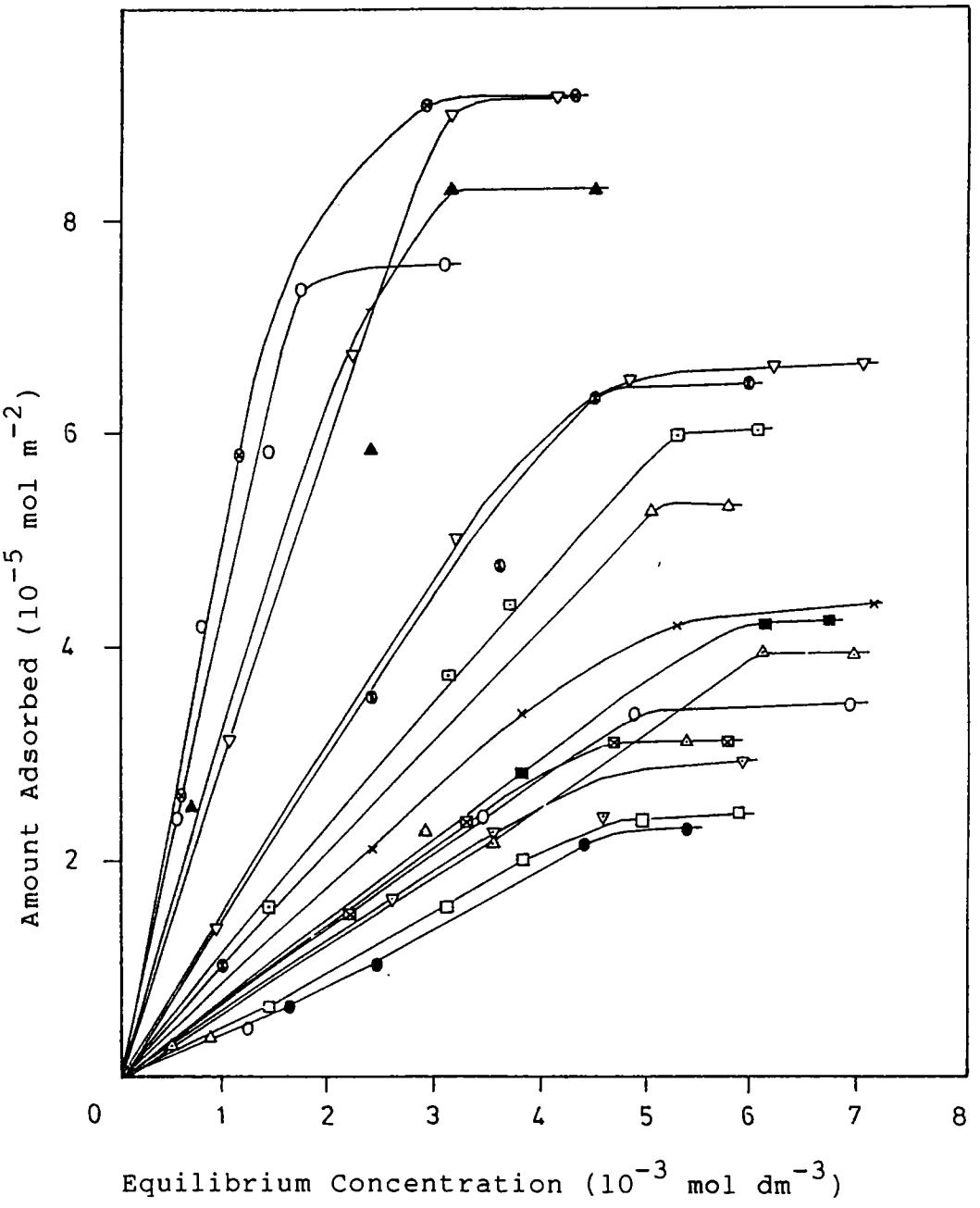

Electron acceptor/Solvent/wt. % of Pr_6O_{11}

(CA - Chloranil; AN - Acetonitrile; TC - TCNQ; D - Dioxan)

○ CA/AN/5 ⊙ TC/AN/5 ● CA/D/5 △ TC/D/5 ◬ CA/AN/10
▲ TC/AN/10 □ CA/D/10 ⊡ TC/D/10 ■ CA/AN/20 ▽ TC/AN/20
▽ CA/D/20 ▼ TC/D/20 × CA/AN/60 ⊗ TC/AN/60 ⊠ CA/D/60
⊗ TC/D/60

Fig.20 Adsorption isotherms on Pr_6O_{11}-Al_2O_3

Table 114 Adsorption of chloranil on Pr_6O_{11}-Al_2O_3 (5%)

Activation temperature: 500°C Solvent: Acetonitrile

Initial concentration 10^{-3}mol dm^{-3}	Equilibrium concentration 10^{-3} mol dm^{-3}	Amount adsorbed 10^{-5} mol m^{-2}
1.08	0.72	0.42
1.73	1.27	0.80
3.24	2.50	0.89
5.41	3.45	2.40
7.57	4.86	3.35
9.74	6.96	3.44

Table 115 Adsorption of TCNQ on Pr_6O_{11}-Al_2O_3 (5%)

Activation temperature: 500°C Solvent: Acetonitrile

Initial concentration 10^{-3} mol dm^{-3}	Equilibrium concentration 10^{-3} mol dm^{-3}	Amount adsorbed 10^{-5} mol m^{-2}
0.92	0.37	0.66
2.05	0.55	2.42
4.17	0.76	4.22
6.17	1.45	5.83
7.81	1.73	7.37
9.25	3.10	7.60

Table 116 Adsorption of chloranil on Pr_6O_{11}-Al_2O_3 (5%)

Activation temperature: 500°C Solvent: Dioxan

Initial concentration 10^{-3} mol dm^{-3}	Equilibrium concentration 10^{-3} mol dm^{-3}	Amount adsorbed 10^{-5} mol m^{-2}
0.81	0.59	0.57
1.62	1.18	0.66
3.24	2.46	1.05
4.87	3.89	1.25
6.17	4.39	2.28
7.30	5.41	2.33

Table 117 Adsorption of TCNQ on Pr_6O_{11}-Al_2O_3 (5%)

Activation temperature: 500°C Solvent: Dioxan

Initial concentration 10^{-3} mol dm^{-3}	Equilibrium concentration 10^{-3} mol dm^{-3}	Amount adsorbed 10^{-5} mol m^{-2}
0.92	0.90	0.02
2.80	2.35	2.39
3.74	2.90	2.50
5.61	4.22	2.78
7.28	5.06	5.60
8.41	5.81	5.65

Table 118 Adsorption of chloranil on Pr_6O_{11}-Al_2O_3 (10%)

Activation temperature: 500°C Solvent: Acetonitrile

Initial concentration 10^{-3} mol dm^{-3}	Equilibrium concentration 10^{-3} mol dm^{-3}	Amount adsorbed 10^{-5} mol m^{-2}
1.31	0.99	0.37
2.13	1.70	0.72
3.62	3.09	1.53
5.26	3.78	1.98
6.91	4.95	2.37
7.81	5.91	2.39

Table 119 Adsorption of TCNQ on Pr_6O_{11}-Al_2O_3 (10%)

Activation temperature: 500°C Solvent: Acetonitrile

Initial concentration 10^{-3} mol dm^{-3}	Equilibrium concentration 10^{-3} mol dm^{-3}	Amount adsorbed 10^{-5} mol m^{-2}
0.93	0.72	0.25
1.86	1.45	1.63
3.72	3.14	3.68
5.58	3.72	4.38
7.44	5.30	5.98
8.37	6.14	6.03

Table 120 Adsorption of chloranil on Pr_6O_{11}-Al_2O_3 (10%)

Activation temperature: 500°C Solvent: Dioxan

Initial concentration 10^{-3} mol dm^{-3}	Equilibrium concentration 10^{-3} mol dm^{-3}	Amount adsorbed 10^{-5} mol m^{-2}
0.98	0.49	0.28
3.94	3.53	2.14
5.91	5.40	3.10
8.87	6.16	3.95
9.86	6.99	3.90

Table 121 Adsorption of TCNQ on Pr_6O_{11}-Al_2O_3 (10%)

Activation temperature: 500°C Solvent: Dioxan

Initial concentration 10^{-3} mol dm^{-3}	Equilibrium concentration 10^{-3} mol dm^{-3}	Amount adsorbed 10^{-5} mol m^{-2}
1.21	0.51	1.51
4.84	0.70	2.53
7.26	2.41	5.88
9.91	3.14	8.34
10.80	4.51	8.58

Table 122 Adsorption of chloranil on Pr_6O_{11}-Al_2O_3 (20%) (Prepared from nitrate solution)

Activation temperature: 500°C Solvent: Acetonitrile

Initial concentration 10^{-3} mol dm^{-3}	Equilibrium concentration 10^{-3} mol dm^{-3}	Amount adsorbed 10^{-5} mol m^{-2}
1.11	0.91	0.23
3.33	2.84	2.10
5.32	3.79	2.78
7.10	4.75	2.89
8.88	6.15	4.18
9.99	6.73	4.25

Table 123 Adsorption of TCNQ on Pr_6O_{11}-Al_2O_3 (20%) (Prepared from nitrate solution)

Activation temperature: 500°C Solvent: Acetonitrile

Initial concentration 10^{-3} mol dm^{-3}	Equilibrium concentration 10^{-3} mol dm^{-3}	Amount adsorbed 10^{-5} mol m^{-2}
6.65	0.87	1.40
8.08	1.06	3.10
9.51	2.27	6.53
10.7	3.16	8.98
11.8	4.16	9.21

Table 124 Adsorption of chloranil on Pr_6O_{11}-Al_2O_3 (20%)
(Prepared from nitrate solution)

Activation temperature: 500°C Solvent: Dioxan

Initial concentration 10^{-3} mol dm^{-3}	Equilibrium concentration 10^{-3} mol dm^{-3}	Amount adsorbed 10^{-5} mol m^{-2}
0.82	0.66	0.17
1.64	1.27	0.44
3.28	2.60	1.60
4.92	3.53	2.21
6.56	4.58	2.35
7.92	5.94	2.90

Table 125 Adsorption of TCNQ on Pr_6O_{11}-Al_2O_3 (20%)
(Prepared from nitrate solution)

Activation temperature: 500°C Solvent: Dioxan

Initial concentration 10^{-3} mol dm^{-3}	Equilibrium concentration 10^{-3} mol dm^{-3}	Amount adsorbed 10^{-5} mol m^{-2}
0.94	0.89	1.61
4.33	3.18	4.98
5.65	4.85	6.49
8.47	6.27	6.62
9.42	7.12	6.68

Table 126 Adsorption of chloranil on Pr_6O_{11}-Al_2O_3 (60%)
(Prepared from nitrate solution)

Activation temperature: 500°C Solvent: Acetonitrile

Initial concentration 10^{-3} mol dm^{-3}	Equilibrium concentration 10^{-3} mol dm^{-3}	Amount adsorbed 10^{-5} mol m^{-2}
0.48	0.31	0.20
1.71	0.98	0.91
4.17	2.41	2.11
6.53	3.81	3.33
8.92	5.28	4.18
10.50	7.21	4.21

Table 127 Adsorption of TCNQ on Pr_6O_{11}-Al_2O_3 (60%)
(Prepared from nitrate solution)

Activation temperature: 500°C Solvent: Acetonitrile

Initial concentration 10^{-3} mol dm^{-3}	Equilibrium concentration 10^{-3} mol dm^{-3}	Amount adsorbed 10^{-5} mol m^{-2}
1.01	0.31	0.81
2.98	0.61	2.66
6.11	1.34	5.82
10.60	2.88	9.11
11.80	4.32	9.17

Table 128 Adsorption of chloranil on Pr_6O_{11}-Al_2O_3 (60%)
(Prepared from nitrate solution)

Activation temperature: 500°C Solvent: Dioxan

Initial concentration 10^{-3} mol dm^{-3}	Equilibrium concentration 10^{-3} mol dm^{-3}	Amount adsorbed 10^{-5} mol m^{-2}
1.58	0.98	0.74
3.46	2.22	1.52
5.31	3.31	2.34
7.23	4.71	3.08
8.48	5.82	3.11

Table 129 Adsorption of TCNQ on Pr_6O_{11}-Al_2O_3 (60%)
(Prepared from nitrate solution)

Activation temperature: 500°C Solvent: Dioxan

Initial concentration 10^{-3} mol dm^{-3}	Equilibrium concentration 10^{-3} mol dm^{-3}	Amount adsorbed 10^{-5} mol m^{-2}
1.82	0.98	1.01
5.41	2.41	3.51
7.68	3.62	4.75
9.96	4.51	6.38
11.30	6.02	6.48

Table 130 Adsorption of chloranil on Al_2O_3
(Prepared from Aluminium nitrate)

Activation temperature: 500°C Solvent: Acetonitrile

Initial concentration 10^{-3} mol dm^{-3}	Equilibrium concentration 10^{-3} mol dm^{-3}	Amount adsorbed 10^{-5} mol m^{-2}
0.32	0.21	0.33
1.30	0.30	1.03
2.61	1.38	1.26
6.52	4.92	1.64
7.65	5.53	2.18
8.50	6.35	2.21

Table 131 Adsorption of TCNQ on Al_2O_3
(Prepared from Aluminium nitrate)

Activation temperature: 500°C Solvent: Acetonitrile

Initial concentration 10^{-3} mol dm^{-3}	Equilibrium concentration 10^{-3} mol dm^{-3}	Amount adsorbed 10^{-5} mol m^{-2}
1.46	0.04	1.50
2.92	0.19	3.01
4.38	0.71	4.44
7.30	0.99	6.50
8.48	2.01	6.65
9.42	2.77	6.85

Table 132 Adsorption of chloranil on Al_2O_3
(Prepared from Aluminium nitrate)

Activation temperature: 500°C Solvent: Dioxan

Initial concentration 10^{-3} mol dm^{-3}	Equilibrium concentration 10^{-3} mol dm^{-3}	Amount adsorbed 10^{-5} mol m^{-2}
0.14	0.09	0.14
0.72	0.16	0.57
1.45	0.69	0.78
2.90	1.90	1.03
4.35	3.20	1.18

Table 133 Adsorption of TCNQ on Al_2O_3
(Prepared from Aluminium nitrate)

Activation temperature: 500°C Solvent: Dioxan

Initial concentration 10^{-3} mol dm^{-3}	Equilibrium concentration 10^{-3} mol dm^{-3}	Amount adsorbed 10^{-5} mol m^{-2}
1.61	0.07	1.58
3.23	0.87	2.43
6.46	3.60	2.95
8.08	4.66	3.52
10.20	7.67	4.46
13.0	8.95	4.52

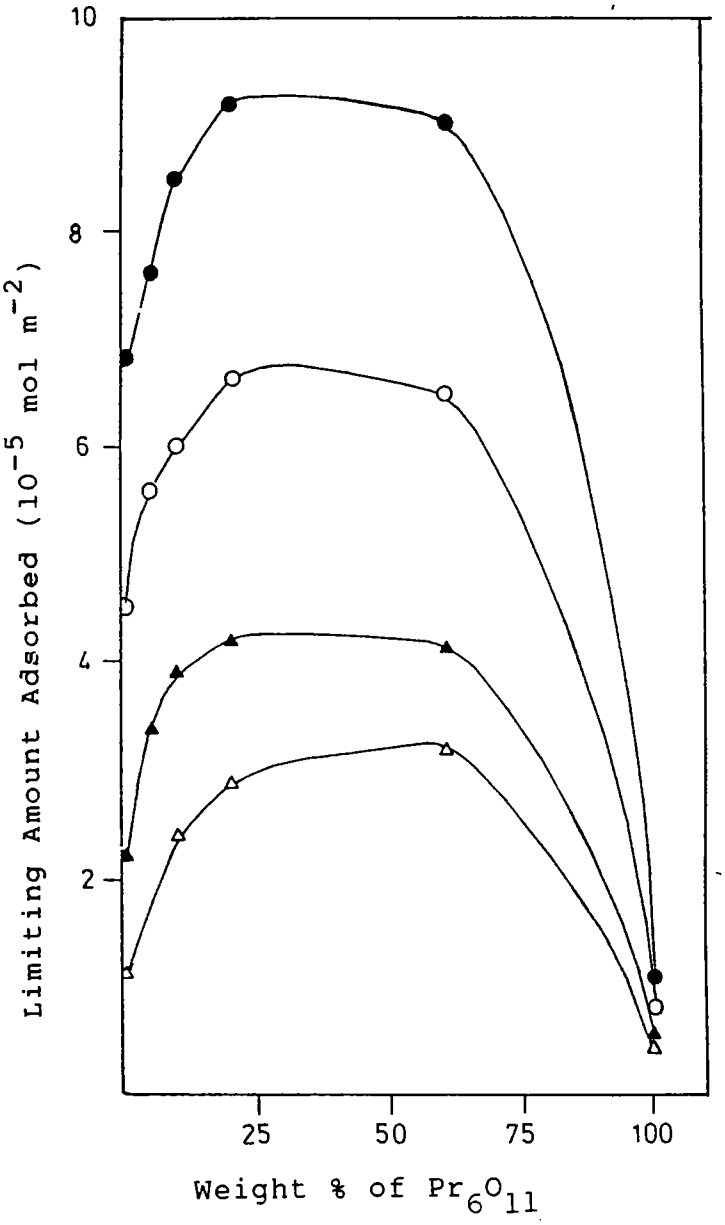

Electron acceptor/Solvent

(CA - Chloranil; AN - Acetonitrile; TC - TCNQ; D - Dioxan)

▲ CA/AN ● TC/AN △ CA/D ○ TC/D

Fig.21 Limiting amount of electron acceptors adsorbed as a function of composition of Pr_6O_{11}-Al_2O_3 (prepared from nitrate)

The difference in electron donicities of mixed oxide system Pr_6O_{11}-Al_2O_3 prepared by co-hydrolysis from two different anion containing solutions can be understood as follows. Al_2O_3 prepared from Aluminium nitrate solution had much greater electron donicity than Al_2O_3 prepared from Aluminium sulphate. It is reported that acidity of alumina prepared by various methods increase in the order $-Al_2O_3 \rangle PO_4^{3-} \rangle Cl^- \rangle SO_4^{2-} \rangle F^-$ [17]. The basic strength of Pr_6O_{11}-Al_2O_3 is given in Table 134 and acid-base strength distribution curves are shown in Fig.22. The basicity is found to be in same order as electron donicity. It is also reported that number of various types of sites present on alumina surfaces appear to be completely dependent a method of preparation [14]. At low concentrations of Pr_6O_{11} in the mixed oxide, added Pr_6O_{11} modifies the electron donicity of alumina and this behaviour goes to a maximum. Further increase in concentration of Pr_6O_{11} decreases the electron donicity due to the consequent increase in Pr_6O_{11} in the alumina lattice because Pr_6O_{11} has lower electron donicity than alumina.

Nd_2O_3

The data on the adsorption of electron acceptors on Nd_2O_3 are given in Tables 135-150 and Fig.23. The surface areas of Nd_2O_3 at 300, 500 and 800°C are given in Table 151.

Table 134 Basicity and Ho_{max} of Pr_6O_{11}-Al_2O_3 (Prepared from nitrate solution)

% by weight of mixed oxide	Basicity (10^{-4} meq m^{-2})				Ho_{max}
	Ho $\geq$ 3.3	Ho $\geq$ 4.8	Ho $\geq$ 6.8	Ho $\geq$ 7.2	
5	2.14	1.32	0.97	0.64	8.0
10	2.31	1.51	0.98	0.66	8.1
20	2.48	1.62	1.02	0.68	8.2
60	2.28	1.48	0.97	0.65	8.1
Al_2O_3	0.97	0.62	0.48	0.31	7.6

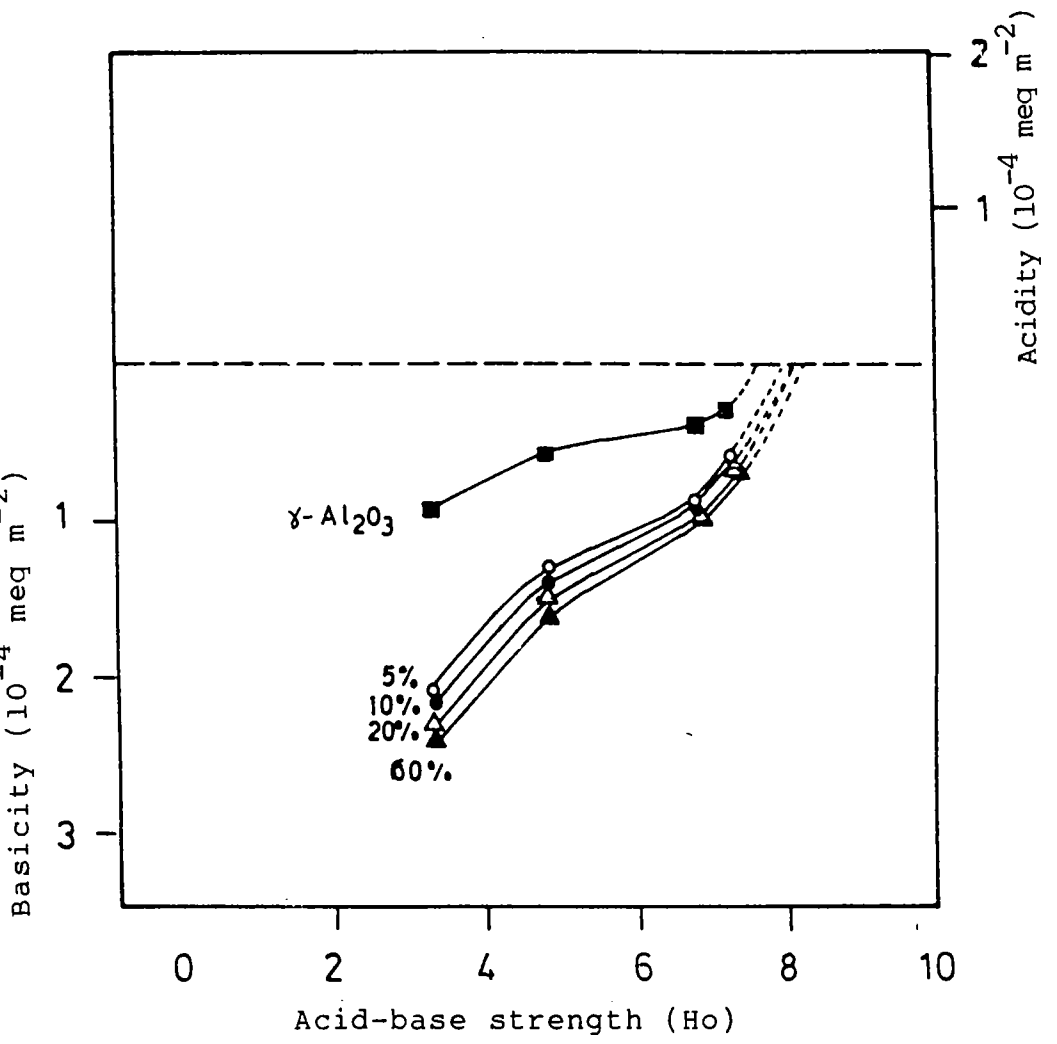

Fig.22 Acid-base strength distribution of Pr_6O_{11}-Al_2O_3 (Prepared from nitrate)

Table 135 Adsorption of chloranil on Nd_2O_3

Activation temperature: 300°C Solvent: Acetonitrile

Initial concentration 10^{-3} mol dm^{-3}	Equilibrium concentration 10^{-3} mol dm^{-3}	Amount adsorbed 10^{-5}mol m^{-2}	Magnetic Moment BM
0.45	0.44	0.43	--
1.82	1.71	0.56	1.85
2.73	2.37	1.87	1.61
3.64	3.22	2.07	1.50
4.55	4.12	2.03	1.45

Table 136 Adsorption of TCNQ on Nd_2O_3

Activation temperature: 300°C Solvent: Acetonitrile

Initial concentration 10^{-3} mol dm^{-3}	Equilibrium concentration 10^{-3} mol dm^{-3}	Amount adsorbed 10^{-5}mol m^{-2}	Magnetic Moment BM
0.59	0.51	0.09	--
1.51	1.07	2.40	1.72
2.67	1.95	3.56	1.11
3.55	2.69	4.72	0.83
4.74	3.63	5.85	0.70
5.92	4.75	6.01	0.65

Table 137 Adsorption of chloranil on Nd_2O_3

Activation temperature: 300°C Solvent: Dioxan

Initial concentration 10^{-3} mol dm^{-3}	Equilibrium concentration 10^{-3} mol dm^{-3}	Amount adsorbed 10^{-5} mol m^{-2}
0.39	0.38	0.05
0.78	0.72	0.30
1.56	1.48	0.42
2.52	2.23	1.01
3.12	2.87	1.36
3.90	3.65	1.37

Table 138 Adsorption of TCNQ on Nd_2O_3

Activation temperature: 300°C Solvent: Dioxan

Initial concentration 10^{-3} mol dm^{-3}	Equilibrium concentration 10^{-3} mol dm^{-3}	Amount adsorbed 10^{-5} mol m^{-2}
1.03	0.94	0.44
2.33	1.97	1.98
3.51	2.81	2.15
4.15	3.71	2.26
5.19	4.75	2.27

Table 139 Adsorption of chloranil on Nd_2O_3

Activation temperature: 500°C Solvent: Acetonitrile

Initial concentration 10^{-3} mol dm^{-3}	Equilibrium concentration 10^{-3} mol dm^{-3}	Amount adsorbed 10^{-5}mol m^{-2}	Radical concentration 10^{16} spins m^{-2}	Magnetic Moment BM
1.09	0.79	1.41	0.79	2.85
2.07	1.61	2.24	1.25	1.84
2.80	2.26	2.65	1.48	1.72
3.43	2.82	2.92	1.64	1.60
4.29	3.68	2.94	1.65	1.61

Table 140 Adsorption of TCNQ on Nd_2O_3

Activation temperature: 500°C Solvent: Acetonitrile

Initial concentration 10^{-3} mol dm^{-3}	Equilibrium concentration 10^{-3} mol dm^{-3}	Amount adsorbed 10^{-5}mol m^{-2}	Radical concentration 10^{18} spins m^{-2}	Magnetic Moment BM
1.67	1.09	2.84	1.55	2.40
2.84	1.99	4.38	2.39	1.55
3.89	2.76	5.43	2.96	1.01
4.80	3.32	7.19	3.92	0.84
6.01	4.48	7.36	4.01	0.81

Table 141 Adsorption of chloranil on Nd_2O_3

Activation temperature: 500°C Solvent: Dioxan

Initial concentration 10^{-3} mol dm^{-3}	Equilibrium concentration 10^{-3} mol dm^{-3}	Amount adsorbed 10^{-5} mol m^{-2}
0.82	0.79	0.11
1.86	1.55	1.21
2.67	2.36	1.51
3.28	2.96	1.79
4.11	3.78	1.74

Table 142 Adsorption of TCNQ on Nd_2O_3

Activation temperature: 500°C Solvent: Dioxan

Initial concentration 10^{-3} mol dm^{-3}	Equilibrium concentration 10^{-3} mol dm^{-3}	Amount adsorbed 10^{-5} mol m^{-2}
1.16	1.07	0.43
2.32	2.22	0.50
3.49	3.18	1.54
4.65	4.13	2.71
5.82	5.31	2.79

Table 143 Adsorption of chloranil on Nd_2O_3

Activation temperature: 800°C Solvent: Acetonitrile

Initial concentration 10^{-3} mol dm^{-3}	Equilibrium concentration 10^{-3} mol dm^{-3}	Amount adsorbed 10^{-5}mol m^{-2}	Magnetic Moment BM
0.87	0.78	0.47	3.20
1.75	1.65	1.32	2.41
2.63	2.30	3.16	2.01
3.51	2.89	4.32	1.73
4.38	3.76	4.35	1.71

Table 144 Adsorption of TCNQ on Nd_2O_3

Activation temperature: 800°C Solvent: Acetonitrile

Initial concentration 10^{-3} mol dm^{-3}	Equilibrium concentration 10^{-3} mol dm^{-3}	Amount adsorbed 10^{-5}mol m^{-2}	Magnetic Moment BM
1.22	0.75	2.60	2.70
2.44	1.58	4.66	1.81
3.66	2.34	7.21	1.41
4.89	3.16	9.26	0.92
6.11	4.38	9.34	0.91

Table 145 Adsorption of chloranil on Nd_2O_3

Activation temperature: 800°C Solvent: Dioxan

Initial concentration 10^{-3} mol dm^{-3}	Equilibrium concentration 10^{-3} mol dm^{-3}	Amount adsorbed 10^{-5} mol m^{-2}
0.16	0.15	0.41
0.84	0.82	0.61
2.52	2.01	1.56
3.36	2.99	1.89
4.21	3.83	1.93

Table 146 Adsorption of TCNQ on Nd_2O_3

Activation temperature: 800°C Solvent: Dioxan

Initial concentration 10^{-3} mol dm^{-3}	Equilibrium concentration 10^{-3} mol dm^{-3}	Amount adsorbed 10^{-5} mol m^{-2}
1.18	1.16	0.12
2.37	2.08	0.15
3.55	3.13	2.67
4.74	4.14	3.29
5.92	5.31	3.33

Table 147 Adsorption of chloranil on Nd_2O_3
(Regenerated by oxalate method)

Activation temperature: 800°C Solvent: Acetonitrile

Initial concentration 10^{-3} mol dm^{-3}	Equilibrium concentration 10^{-3} mol dm^{-3}	Amount adsorbed 10^{-5} mol m^{-2}
0.43	0.38	0.30
1.16	0.99	1.02
2.32	2.04	2.61
3.33	2.74	3.19
4.40	3.82	3.21

Table 148 Adsorption of TCNQ on Nd_2O_3
(Regenerated by oxalate method)

Activation temperature: 800°C Solvent: Acetonitrile

Initial concentration 10^{-3} mol dm^{-3}	Equilibrium concentration 10^{-3} mol dm^{-3}	Amount adsorbed 10^{-5} mol m^{-2}
1.28	0.91	2.01
2.90	2.11	5.52
4.11	2.98	6.52
4.78	3.60	7.64
6.19	4.61	9.09
7.47	5.88	9.12

Table 149 Adsorption of chloranil on Nd_2O_3

Activation temperature: 800°C Solvent: Dioxan

Initial concentration 10^{-3} mol dm^{-3}	Equilibrium concentration 10^{-3} mol dm^{-3}	Amount adsorbed 10^{-5} mol m^{-2}
0.48	0.44	0.22
1.20	1.10	0.61
2.26	2.04	1.24
3.11	2.82	1.61
4.07	3.77	1.69

Table 150 Adsorption of TCNQ on Nd_2O_3
(Regenerated by oxalate method)

Activation temperature: 800°C Solvent: Dioxan

Initial concentration 10^{-3} mol dm^{-3}	Equilibrium concentration 10^{-3} mol dm^{-3}	Amount adsorbed 10^{-5} mol m^{-2}
1.30	1.14	0.88
2.09	1.80	1.71
3.62	3.14	2.65
4.52	3.98	3.16
5.83	5.22	3.18

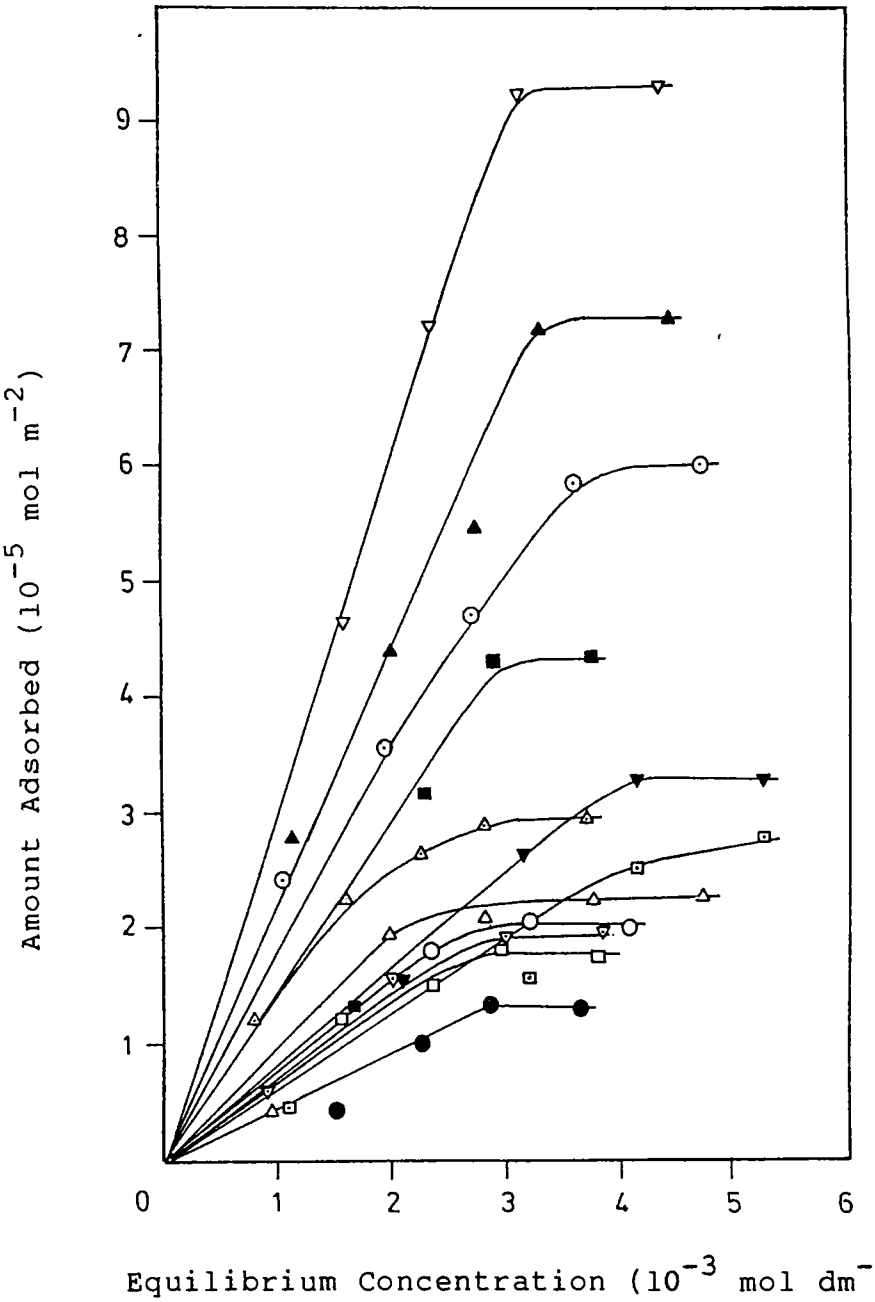

Electron acceptor/Solvent/Activation temperature (°C)

(CA - Chloranil; AN - Acetonitrile; TC - TCNQ; D - Dioxan)

○CA/AN/300 ⊙TC/AN/300 ●CA/D/300 △TC/D/300 ▲CA/AN/500
▲TC/AN/500 □CA/D/500 ⊡TC/D/500 ■CA/AN/800 ▽TC/AN/800
▽CA/D/800 ▼TC/D/800

Fig.23 Adsorption isotherms on Nd_2O_3

Table 151 Surface area of Nd_2O_3 activated at different temperature

Method of preparation	Activation temperature (°C)	Surface area (m^2/g)
Hydroxide	300	39.70
Hydroxide	500	42.40
Hydroxide	800	37.90
Oxalate	800	38.52

For Nd_2O_3 on adsorption chloranil gave no colouration while TCNQ gave light blue colour to Nd_2O_3. The limit of electron transfer from Nd_2O_3 at three activation temperatures is between 2.40 and 1.77 eV. The limiting amount of electron acceptors adsorbed decreased with increase in basicity of solvent. The radical concentration of TCNQ and chloranil adsorbed on Nd_2O_3 at 500°C is given in Tables 139-140. Fig.24 shows the acidity and basicity of Nd_2O_3 at three temperatures. The data are given in Table 152 On Nd_2O_3 activated at 300°C and 500°C, both acidic and basic sites are present while at 800°C only basic sites were present. Ho_{max} values at three temperatures are also given in the Table 152 . Ho_{max} value increases on increasing the activation temperature.

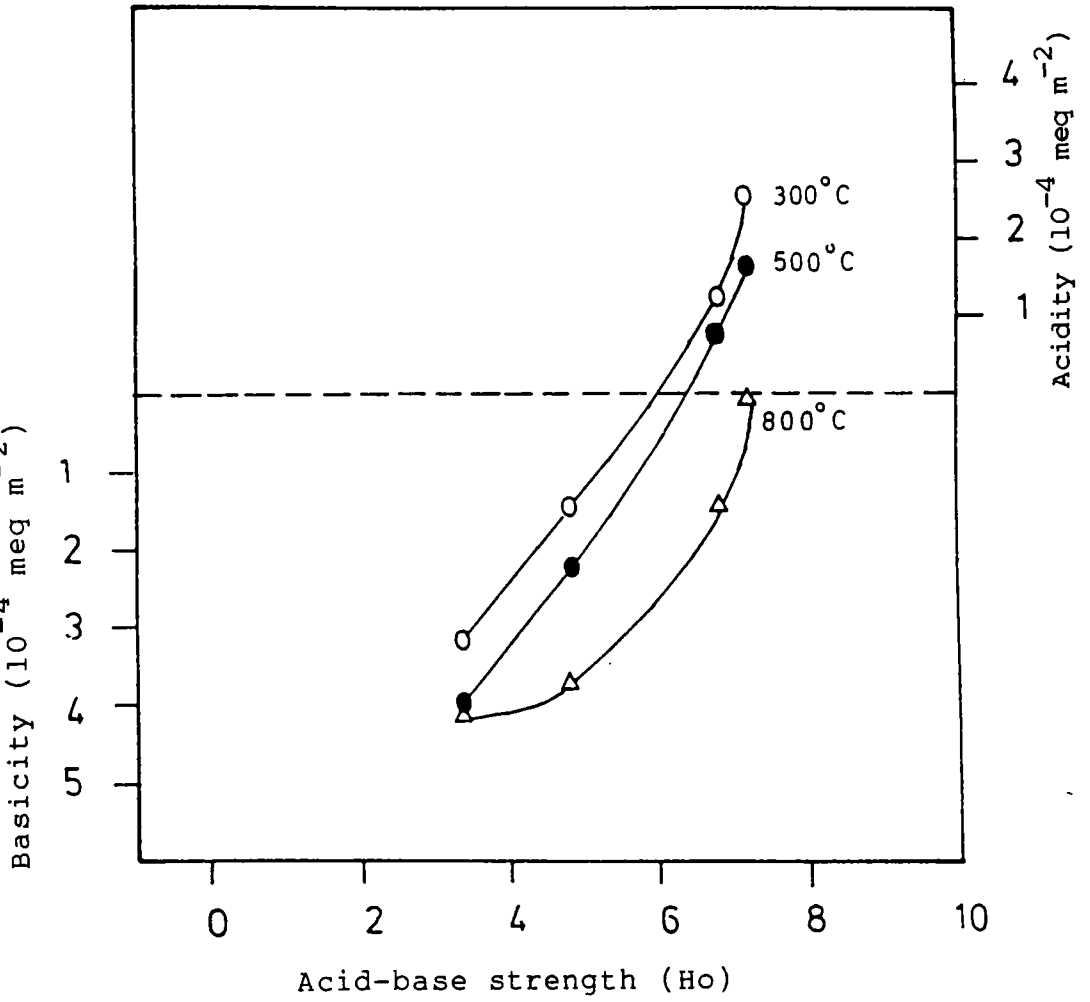

Fig.24 Acid-base strength distribution of Nd_2O_3
(Prepared from nitrate)

Table 152 Acidity, Basicity and Ho_{max} of Nd_2O_3 at different activation temperatures

Activation temperature (°C)	Basicity (10^{-4} meq m^{-2})				Acidity (10^{-4} meq m^{-2})				
	Ho ≥ 3.3	Ho ≥ 4.8	Ho ≥ 6.8	Ho ≥ 7.2	Ho ≤ 3.3	Ho ≤ 4.8	Ho ≤ 6.8	Ho ≤ 7.2	
300	3.27	1.51	--	--	--	--	1.25	2.51	6.0
500	4.00	2.35	--	--	--	--	0.70	1.65	6.4
800	4.21	3.82	1.57	0.25	--	--	--	--	7.3

The magnetic moment of Nd_2O_3 before and after adsorption of electron acceptors is given in Tables 135, 136,139,140,143,144. Fig.25 shows that magnetic moment decreases and reaches a limiting value at the concentration at which limiting amount of electron acceptors is obtained. The limiting amount of electron acceptors adsorbed increases with increase in temperature due to the consequent increase in concentration of both strong and weak donor sites.

Nd_2O_3-Al_2O_3

The following systems have been studied at an activation temperature of 500°C. The surface areas of Nd_2O_3-Al_2O_3 of different compositions are given in Table 153.

Table 153 Surface area of Nd_2O_3-Al_2O_3

% by weight of Nd_2O_3	Surface area (m^2/g)
5	142.45
10	151.50
15	149.75
20	154.50

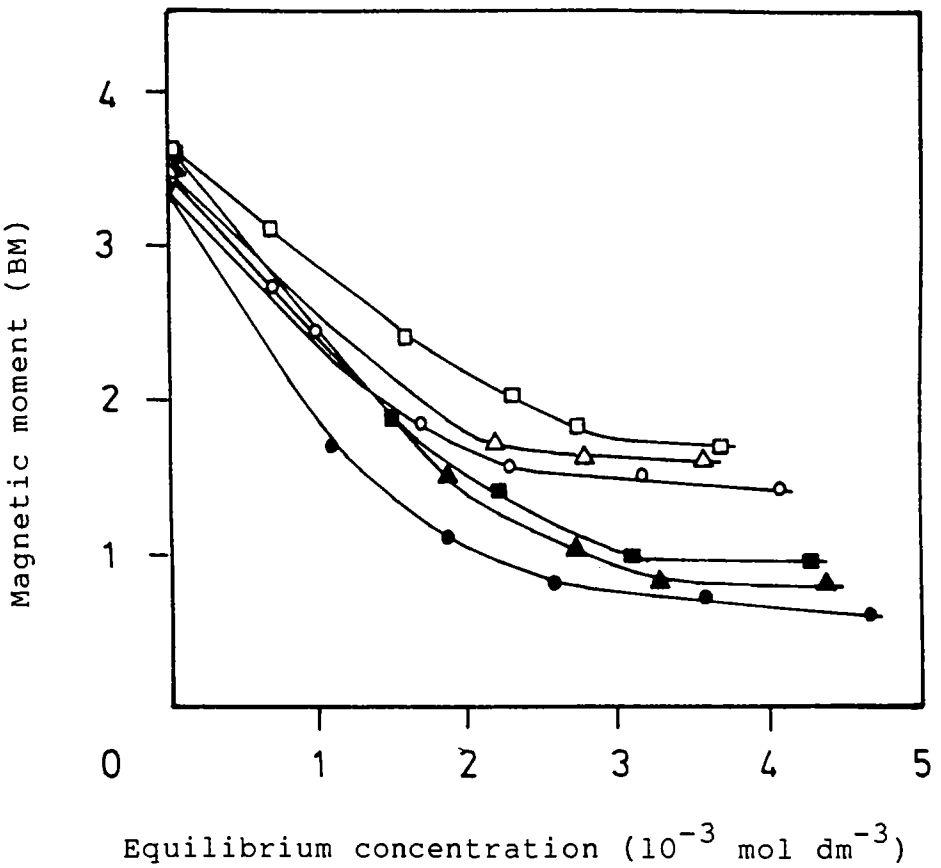

Electron acceptor/Solvent/Activation temperature

(CA - Chloranil; AN - Acetonitrile; TC - TCNQ)

○CA/AN/300 ●TC/AN/300 △CA/AN/500 ▲TC/AN/500 □CA/AN/800 ■TC/AN/800

Fig.25 Magnetic moment of Nd_2O_3 as a function of equilibrium concentration of electron acceptor

The adsorption isotherms obtained are given in Fig.26 and values are given in Tables 154-169. The mixed oxide acquired a green colour on adsorption of TCNQ and chloranil adsorption gave pink colour to Nd_2O_3-Al_2O_3. Fig.27 gives the limiting amount adsorbed as a function of composition of Nd_2O_3-Al_2O_3 system. The electron donicity increases with increase in concentration of Nd_2O_3 in the mixed oxide. The limit of electron transfer is the same as that of pure Nd_2O_3. The basicity obtained is given in Table 170 and acid-base distribution curves in Fig.28. The basicity obtained is in the same order as the electron donicity. Nd_2O_3 modifies the electron donor properties of alumina by increasing the concentration of both weak and strong donor sites.

Strength of Electron Donor Sites in Rare Earth Oxides

It is found that the limiting amount of electron acceptors adsorbed increased with increase in basicity of the oxide. The limiting amount of TCNQ adsorbed and the basicity of oxides at different activation temperatures is given in Table 171. The order of electron donicity obtained for the three rare earth oxides is $Pr_6O_{11} > Nd_2O_3 > Y_2O_3$. This is same as the order of

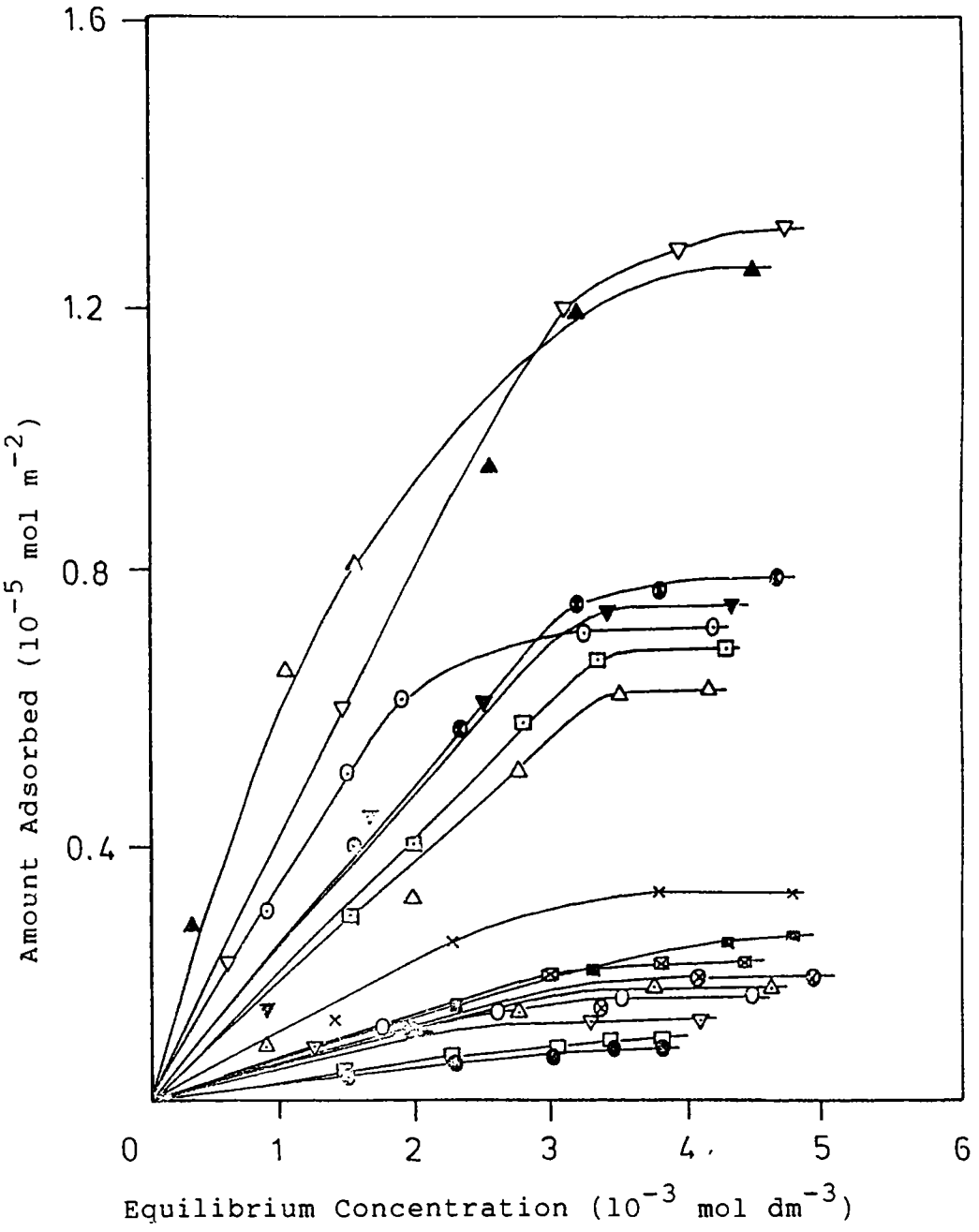

Electron acceptor/Solvent/wt. % of Nd_2O_3

(CA - Chloranil; AN - Acetonitrile; TC - TCNQ; D - Dioxan)

○ CA/AN/5 ⊙ TC/AN/5 ● CA/D/5 △ TC/D/5 ◬ CA/AN/10
▲ TC/AN/10 □ CA/D/10 ⊡ TC/D/10 ■ CA/AN/15 ▽ TC/AN/15
▽ CA/D/15 ▼ TC/D/15 × CA/AN/20 ⊗ TC/AN/20 ⊠ CA/D/20
⊛ TC/D/20

Fig.26 Adsorption isotherms on Nd_2O_3-Al_2O_3

Table 154 Adsorption of chloranil on Nd_2O_3-Al_2O_3 (5%)

Activation temperature: 500°C Solvent: Acetonitrile

Initial concentration 10^{-3} mol dm^{-3}	Equilibrium concentration 10^{-3} mol dm^{-3}	Amount adsorbed 10^{-6} mol m^{-2}
0.18	0.15	0.43
0.92	0.85	0.98
1.84	1.76	1.14
2.77	2.67	1.36
3.69	3.57	1.67
4.62	4.50	1.69

Table 155 Adsorption of TCNQ on Nd_2O_3-Al_2O_3 (5%)

Activation temperature: 500°C Solvent: Acetonitrile

Initial concentration 10^{-3} mol dm^{-3}	Equilibrium concentration 10^{-3} mol dm^{-3}	Amount adsorbed 10^{-6} mol m^{-2}
0.37	0.32	0.64
0.93	0.91	2.96
1.86	1.51	4.96
2.33	1.91	6.05
3.73	3.26	7.00
4.67	4.18	7.07

Table 156 Adsorption of chloranil on Nd_2O_3-Al_2O_3 (5%)

Activation temperature: 500°C Solvent: Dioxan

Initial concentration 10^{-3} mol dm^{-3}	Equilibrium concentration 10^{-3} mol dm^{-3}	Amount adsorbed 10^{-7} mol m^{-2}
0.78	0.76	1.98
1.56	1.52	4.75
2.35	2.30	6.38
3.13	3.06	7.39
3.52	3.44	9.12
3.91	3.83	9.13

Table 157 Adsorption of TCNQ on Nd_2O_3-Al_2O_3 (5%)

Activation temperature: 500°C Solvent: Dioxan

Initial concentration 10^{-3} moldm^{-3}	Equilibrium concentration 10^{-3} mol$_{dm}^{-3}$	Amount adsorbed 10^{-6} mol m^{-2}
0.91	0.88	0.42
1.46	1.39	0.89
2.19	1.99	3.10
3.11	2.76	4.99
3.93	3.50	6.11
4.58	4.15	6.17

Table 158 Adsorption of chloranil on Nd_2O_3-Al_2O_3 (10%)

Activation temperature: 500°C Solvent: Acetonitrile

Initial concentration 10^{-3} mol dm^{-3}	Equilibrium concentration 10^{-3} mol dm^{-3}	Amount adsorbed 10^{-6} mol m^{-2}
0.19	0.16	0.32
0.96	0.89	0.93
1.92	1.83	1.13
2.88	2.77	1.39
3.84	3.70	1.76
4.81	3.67	1.78

Table 159 Adsorption of TCNQ on Nd_2O_3-Al_2O_3 (10%)

Activation temperature: 500°C Solvent: Acetonitrile

Initial concentration 10^{-3} mol dm^{-3}	Equilibrium concentration 10^{-3} mol dm^{-3}	Amount adsorbed 10^{-6} mol m^{-2}
0.54	0.33	2.78
1.62	1.12	6.49
2.16	1.56	8.00
3.25	2.56	9.37
4.33	3.42	11.80
5.42	4.49	12.40

Table 160 Adsorption of chloranil on Nd_2O_3-Al_2O_3 (10%)

Activation temperature: 500°C Solvent: Dioxan

Initial concentration 10^{-3} mol dm^{-3}	Equilibrium concentration 10^{-3} mol dm^{-3}	Amount adsorbed 10^{-6} mol m^{-2}
0.78	0.76	0.19
1.56	1.52	0.47
2.35	2.30	0.63
3.13	3.06	0.73
3.52	3.44	1.12
3.91	3.83	1.13

Table 161 Adsorption of TCNQ on Nd_2O_3-Al_2O_3 (10%)

Activation temperature: 500°C Solvent: Dioxan

Initial concentration 10^{-3} mol dm^{-3}	Equilibrium concentration 10^{-3} mol dm^{-3}	Amount adsorbed 10^{-6} mol m^{-2}
1.05	1.01	0.53
1.72	1.60	2.81
2.30	2.00	3.94
3.16	2.81	4.71
3.83	3.35	6.58
4.79	4.29	6.86

Table 162 Adsorption of chloranil on Nd_2O_3-Al_2O_3 (15%)

Activation temperature: 500°C Solvent: Acetonitrile

Initial concentration 10^{-3} mol dm^{-3}	Equilibrium concentration 10^{-3} mol dm^{-3}	Amount adsorbed 10^{-6} mol m^{-2}
0.29	0.26	0.48
1.49	1.38	1.41
2.49	2.36	1.74
3.48	3.33	2.08
4.49	4.30	2.47
4.98	4.80	2.51

Table 163 Adsorption of TCNQ on Nd_2O_3-Al_2O_3 (15%)

Activation temperature: 500°C Solvent: Acetonitrile

Initial concentration 10^{-3} mol dm^{-3}	Equilibrium concentration 10^{-3} mol dm^{-3}	Amount adsorbed 10^{-5} mol m^{-2}
0.79	0.64	0.20
1.92	1.50	0.58
2.94	2.47	0.67
3.96	3.12	1.18
4.87	3.95	1.27
5.67	4.73	1.30

Table 164 Adsorption of chloranil on Nd_2O_3-Al_2O_3 (15%)

Activation temperature: 500°C Solvent: Dioxan

Initial concentration 10^{-3} mol dm^{-3}	Equilibrium concentration 10^{-3} mol dm^{-3}	Amount adsorbed 10^{-6} mol m^{-2}
0.33	0.31	0.32
0.58	0.54	0.60
1.26	1.20	0.68
1.85	1.76	1.14
3.36	3.26	1.32
4.21	4.11	1.34

Table 165 Adsorption of TCNQ on Nd_2O_3-Al_2O_3 (15%)

Activation temperature: 500°C Solvent: Dioxan

Initial concentration 10^{-3} mol dm^{-3}	Equilibrium concentration 10^{-3} mol dm^{-3}	Amount adsorbed 10^{-6} mol m^{-2}
0.48	0.45	0.41
0.97	0.87	1.34
1.95	1.64	4.32
2.93	2.50	5.94
3.91	3.38	7.21
4.89	4.35	7.41

Table 166 Adsorption of chloranil on Nd_2O_3-Al_2O_3 (20%)

Activation temperature: 500°C Solvent: Acetonitrile

Initial concentration 10^{-3} mol dm^{-3}	Equilibrium concentration 10^{-3} mol dm^{-3}	Amount adsorbed 10^{-6} mol m^{-2}
0.30	0.27	0.40
1.50	1.40	1.30
2.51	2.32	2.47
4.01	3.77	3.22
5.02	4.78	3.27

Table 167 Adsorption of TCNQ on Nd_2O_3-Al_2O_3 (20%)

Activation temperature: 500°C Solvent: Acetonitrile

Initial concentration 10^{-3} mol dm^{-3}	Equilibrium concentration 10^{-3} mol dm^{-3}	Amount adsorbed 10^{-5} mol m^{-2}
0.73	0.59	0.18
1.59	1.13	0.99
2.57	1.94	1.12
4.03	3.36	1.69
5.14	4.06	1.92
6.12	4.95	1.92

Table 168 Adsorption of chloranil on Nd_2O_3-Al_2O_3 (20%)

Activation temperature: 500°C Solvent: Dioxan

Initial concentration 10^{-3} mol dm^{-3}	Equilibrium concentration 10^{-3} mol dm^{-3}	Amount adsorbed 10^{-6} mol m^{-2}
0.73	0.70	0.46
1.47	1.42	0.60
2.21	2.15	0.73
3.13	2.99	1.91
3.96	3.79	2.12
4.61	4.45	2.15

Table 169 Adsorption of TCNQ on Nd_2O_3-Al_2O_3 (20%)

Activation temperature: 500°C Solvent: Dioxan

Initial concentration 10^{-3} mol dm^{-3}	Equilibrium concentration 10^{-3} mol dm^{-3}	Amount adsorbed 10^{-6} mol m^{-2}
1.09	1.04	0.69
1.89	1.57	3.97
2.79	2.35	5.62
3.69	3.21	6.42
4.39	3.81	7.63
4.99	4.40	7.83

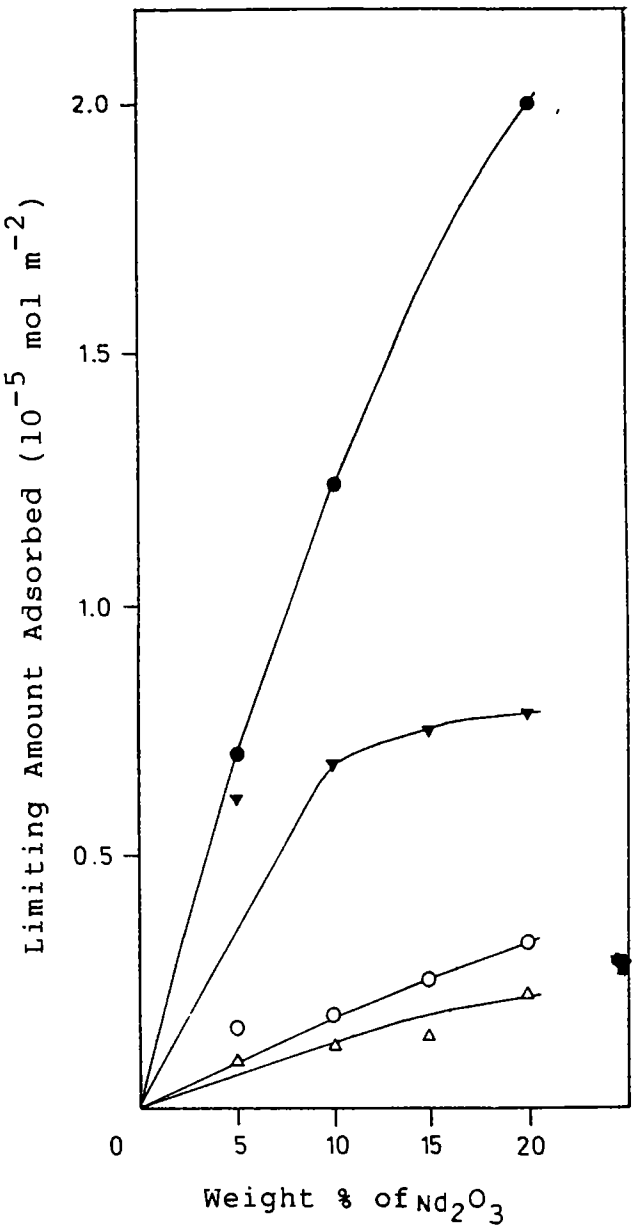

Electron acceptor/Solvent

(CA - Chloranil; AN - Acetonitrile; TC - TCNQ; D - Dioxan)

O CA/AN ● TC/AN Δ CA/D ▲ TC/D

Fig.27 Limiting amount of electron acceptors adsorbed as a function of composition of Nd_2O_3-Al_2O_3

Table 170 Basicity and Ho_{max} of Nd_2O_3-Al_2O_3 of various compositions

% by weight of mixed oxide	Basicity (10^{-4} meq m^{-2})				Ho_{max}
	Ho ≥ 3.3	Ho ≥ 4.8	Ho ≥ 6.8	Ho ≥ 7.2	
5	1.31	0.66	0.19	0.11	7.5
10	1.64	0.87	0.35	0.15	7.6
15	1.85	1.07	0.42	0.18	7.6
20	2.08	1.12	0.68	0.31	7.7

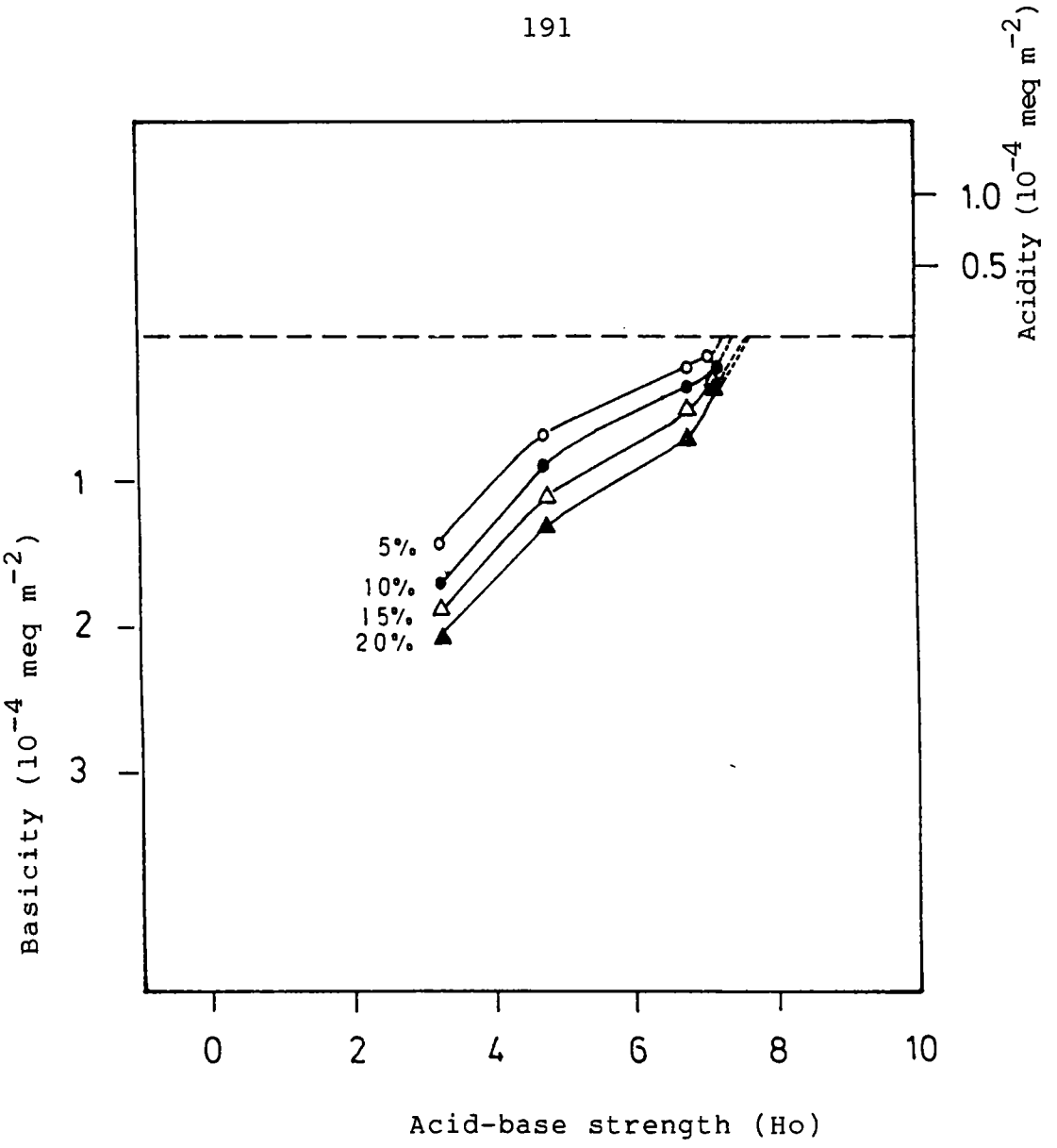

Fig.28 Acid-base strength distribution of Nd_2O_3-Al_2O_3

Table 171 Limiting amount of TCNQ adsorbed from acetonitrile and basicity of the oxides at various temperatures

Oxide	Temperature (°C)	Limiting amount (mol m^{-2})	Basicity (10^{-4} meq m^{-2})			
			Ho ≥ 3.3	Ho ≥ 4.8	Ho ≥ 6.8	Ho ≥ 7.2
Y_2O_3	300	5.72×10^{-5}	3.07	1.42	--	--
	500	7.21×10^{-5}	3.43	2.04	--	--
	800	9.15×10^{-5}	4.12	2.85	1.18	1.82
Nd_2O_3	300	6.01×10^{-5}	3.27	1.51	--	--
	500	7.36×10^{-5}	4.00	2.35	--	--
	800	9.34×10^{-5}	4.74	3.95	1.58	2.63
Pr_6O_{11}	300	6.44×10^{-5}	3.68	2.41	1.14	0.65
	500	7.44×10^{-5}	4.21	2.88	1.42	0.82
	800	9.96×10^{-5}	5.12	3.84	1.81	1.21

basicity of these oxides. This shows that the electron donor power of oxide surfaces increases with basic strength of surface itself. The basic strength of a surface is considered as the ability of surface site (S:) possessing an electron lone pair to transfer it to an acceptor molecule (A).

$S: + A \longrightarrow S:\rightarrow A$ and this can be measured by proper Hammett function. The order of basic strength obtained parallels the order of electron donor activities present on oxides.

It has been suggested that at higher activation temperatures, the donor site consists of an oxygen ion on the surface, specifically a co-ordinatively unsaturated oxygen ion (O^{2-}_{cus}) associated with a nearby OH^- group and the concentration of these donor sites on the surface is related to basic strength of the surface [18]. The more basic the surface, the higher is the number of oxygen ions which can transfer the electron to acceptor molecule. The acidity and basicity studies of rare earth oxides reveal the presence of site energy distributions or group of sites of different energies on the rare earth oxides [19]. The acidity and basicity are attributed to the cations (M^{n+})

and anions (O^{2-}) respectively, exposed on the surface of catalysts. The acid strength of the surface site is expected to be dependent upon the effective +ve charge on metal cations and their coordination on the catalyst surface. Similarly the basic strength of surface sites is also expected to vary depending upon effective -ve charge on the anions and/or their co-ordination on the surface. Surface imperfections such as steps, kinks, corners which provide sites for ions of low co-ordination (M_{LC}^{n+} and O_{LC}^{2-}) are expected to be responsible for the sites of different energies.

The ratio of transformation from the TCNQ adsorbed into the TCNQ radical on the surface of catalysts is important to an understanding of the strength of electron donor sites. This ratio can be estimated by dividing the TCNQ radical concentration by the corresponding half value of the limiting amount of TCNQ. The values for different oxides are given in Table 172. The larger the value of the ratio, the stronger the electron donor sites. The ratio obtained for Y_2O_3, Pr_6O_{11} and Nd_2O_3 is compared with that of Al_2O_3 and ZrO_2 activated at 500°C taken from literature [20-23]. The ratio for both TCNQ and chloranil is less than that of alumina but greater than that of ZrO_2 and are

Table 172 Strength of electron donor sites in various oxides activated at 500°C

Electron acceptor	Radical concentration/Adsorbed amount (spins mol^{-1})					
	Y_2O_3	Nd_2O_3	Pr_6O_{11}	Al_2O_3	TiO_2	ZrO_2
TCNQ	5.26×10^{22}	5.40×10^{22}	5.46×10^{22}	1.51×10^{24}	5.16×10^{22}	1.88×10^{21}
Chloranil	5.22×10^{20}	5.30×10^{20}	5.52×10^{20}	9.16×10^{21}	5.62×10^{20}	--

* This ratio is calculated from Tables 11,12,76,77,139,140 for Y_2O_3, Pr_6O_{11} and Nd_2O_3.

comparable with that of TiO_2. This ratio is almost constant for all the three rare earth oxides studied. The result implies that the electron donor strength of the weak and strong donor sites in the three rare earth oxides under study are almost constant and are comparable to the strength of electron donor sites in TiO_2 which is already reported.

REFERENCES

1. M.Che, C.Naccache and B.Imelik, J. Catal., **24**, 328 (1972).

2. D.S.Acker and W.R.Hertler, J. Am. Chem. Soc., **84**, 328 (1962).

3. R.H.Boyd and W.D.Phillips, J. Chem. Phys., **43**, 2927 (1965).

4. R.Foster and T.J.Thomson, Trans. Faraday Soc., **58**, 860 (1962).

5. H.Hosaka, T.Fujiwara and K.Meguro, Bull. Chem. Soc. Jpn., **44**, 2616 (1971).

6. K.Esumi and K.Meguro, J. Japan Colour Material, **48**, 539 (1975).

7. K.Meguro and K.Esumi, J. Colloid Interface Sci., **59**, 93 (1973).

8. B.D.Flockhart, J.A.N.Scott and R.C.Pink, Trans. Faraday Soc., 62, 730 (1966).

9. G.V.Fomin, L.A.Blyumenfield and V.I.Sukhorukov, Proc. Acad. Sci., USSR, 157, 819 (1964).

10. M.L.Hair and W.Hertl, J. Phys. Chem., 74, 91 (1970).

11. M.P.Rosynek and D.T.Magnuson, J. Catal., 46, 492 (1977).

12. T.Yamanaka and K.Tanabe, J. Phys. Chem., 74, 91 (1975).

13. T.Yamanaka and K.Tanabe, J. Phys. Chem., 80, 1723 (1976).

14. J.W.Higtower, Amer. Chem. Soc., Div. Petrol. Chem. Prepr., 18, 263 (1973).

15. I.Bodrikov, K.C.Khulbe and R.S.Mann, J. Catal., 43, 330 (1976).

16. R.S.Drago, L.B.Parr and C.S.Chamberlain, J. Am. Chem. Soc., 99, 3203 (1977).

17. P.Bertean, M.Kollens and B.Delmon, J. Chem. Soc., Faraday Trans., 87, 1425.

18. D.Cordischi and V.Indovina, J. Chem. Soc. Faraday Trans., 72(10), 2341 (1976).

19. V.R.Choudhary and V.H.Rane, J. Catal., 130, 411 (1991).

20. K.Meguro and K.Esumi, J. Colloid and Interface Sci., 59, 93 (1977).

21. K.Esumi, K.Miyata, F.Waki and K.Meguro, Bull. Chem. Soc. Jpn., 59, 3363 (1986).

22. K.Esumi and K.Meguro, Bull. Chem. Soc. Jpn., 55, 1647 (1982).

23. K.Esumi and K.Meguro, Bull. Chem. Soc. Jpn., 55, 315 (1982).

CHAPTER IV

EXPERIMENTAL

4.1 MATERIALS

4.1.1 Single oxides

The three rare earth oxides, Praseodymium oxide, Neodymium oxide and Yttrium oxide (99.9% pure) were obtained from Indian Rare Earths Ltd., Udyogamandal, Kerala. These oxides were further regenerated by two methods.

Oxalate Precipitation [1]

About 5 g of rare earth oxide was weighed into a 250 ml beaker and moistened with 5 ml of water. 10 ml of 6 N hydrochloric acid was added slowly with stirring. The solution was evaporated in a china dish and was then diluted to 250 ml. The pH was adjusted to 1 (approximately) with 1:1 hydrochloric acid. It was heated to boiling and 60 ml of 12% oxalic acid solution was added slowly with constant stirring and allowed to stand overnight. The precipitate was filtered on Whatman No.42 filter paper and washed with 2% oxalic acid in 1:99 hydrochloric acid. The precipitate was kept in an air oven at 100°C for one day and then was ignited in a china dish at 900-1000°C to constant weight. This requires about 3 hrs. The weight obtained represents rare earth oxide present.

Hydroxide Precipitation [2]

Sulphate solution of the sample (250 ml) containing 0.5 g of rare earth oxide was heated to boiling and 1:1 ammonium hydroxide solution was added dropwise, with stirring, until precipitation was complete. Then added, with stirring, concentrated ammonium hydroxide in an amount equal to one tenth of volume of solution. It was then allowed to digest on a steam bath until the precipitate was flocculated and settled. The precipitate was filtered on a Whatman No.41 paper and washed with small portions of an aqueous solution containing 2 g of ammonium chloride and 10 ml of concentrated ammonium hydroxide in 100 ml, until the precipitate was free from Cl^-. The precipitate was kept in an air oven at 100°C overnight and was ignited in a china dish at 300-400°c for 2 hrs.

4.1.2 Mixed oxides

Mixed oxides of rare earth and aluminium were prepared by two methods - co-precipitation method and impregnation method.

Co-precipitation Method

Co-precipitation of mixed oxide was done from their sulphate/nitrate solution.

a) Co-precipitation from the Sulphate Solution (3)

5% Mixed oxides

Rare earth oxide (0.5 g) was dissolved in concentrated H_2SO_4 and was crystallised by repeated evaporation with sulphuric acid. Aqueous solution of NH_3 was added to a solution containing rare earth sulphate and aluminium sulphate (prepared by dissolving 103.2 g of $Al_2(SO_4)_3.H_2O$ obtained from BDH in 200 ml of water) until pH of solution became 9.5. The precipitate was filtered and washed until no SO_4^{2-} was detected. The precipitate was kept overnight in an air oven at 100°C and was calcined at 500°C for 2 hrs.

The same method was repeated for preparing 10%, 15% and 20% by weight of mixed oxide by taking appropriate weights of Aluminium sulfate and rare earth oxide.

10% Mixed oxide

Aluminium sulfate	97.81 g
Rare earth oxide	1 g

15% Mixed oxide

Aluminium sulfate	92.38 g
Rare earth oxide	1.5 g

20% Mixed oxide

Aluminium sulfate	86.95 g
Rare earth oxide	2 g

b) Co-precipitation from nitrate solution (4)

5% Mixed oxide

Praseodymium oxide (0.5 g) was dissolved in concentrated nitric acid and was crystallised by repeated evaporation with nitric acid. Aqueous ammonia (5%) solution was added to mixed aqueous solution containing Praseodymium nitrate and aluminium nitrate (prepared by dissolving 69.82 g of aluminium nitrate SQ grade, obtained from Qualigens Fine Chemicals in 250 ml distilled water) until precipitation was complete. The precipitate was washed with distilled water until free from NO_3^{2-}, dried by keeping overnight at 100°C, and then calcined to form the mixed oxide at 500°C for 3 hrs.

Using the same method, 5%, 10%, 20% and 60% by weight of mixed oxides were prepared by taking the following weights.

10% Mixed oxide:

Aluminium nitrate	66.15 g
Praseodymium oxide	1 g

20% Mixed Oxide:

Aluminium nitrate	58.8 g
Praseodymium oxide	2 g

60% Mixed oxide:

Aluminium nitrate	27.3 g
Praseodymium oxide	6 g

Impregnation method

5%, 10% and 20% of mixed oxides of Yttrium oxide -γ-Al_2O_3 were prepared by impregnation method [5].

5% Mixed oxide

NH_3 was added to a Yttrium nitrate solution (prepared by dissolving 0.5 g of Y_2O_3 in conc. HNO_3 and evaporating to dryness) containing a suspension of 9.5 g of γ-Al_2O_3 (obtained from United Catalysts, Udyogamandal, Kerala). After precipitation at pH 9-10, solution was filtered and washed with distilled water until precipitate was free from NO_3^{2-} ions. The precipitate was dried by keeping overnight at 100°C and was calcined at 500°C for 3 hrs. The same procedure was adopted for preparing 10% and 20% of Y_2O_3 - γ-Al_2O_3 by taking the following weights.

10% Y_2O_3- -Al_2O_3	:	Y_2O_3	- 1 g
		γ-Al_2O_3	- 9 g
20% Y_2O_3- -Al_2O_3	:	Y_2O_3	- 2 g
		γ-Al_2O_3	- 8 g

4.1.3 Electron Acceptors

Electron acceptors employed for the study are 7,7,8,8-tetracyanoquinodimethane (TCNQ), 2,3,5,6-tetrachloro-p-benzoquinone (chloranil), p-dinitrobenzene (PDNB) and m-dinitrobenzene (MDNB).

TCNQ was obtained from Merck-Schuchandt and was purified by repeated recrystallisation from acetonitrile [6].

Chloranil was obtained from Sisco Research Laboratories Pvt. Ltd. and was purified by recrystallisation from benzene [7].

p-Dinitrobenzene was supplied by Koch-Light Laboratories Ltd. and was purified by recrystallisation from Chloroform [8].

m-Dinitrobenzene was obtained from Loba-Chemie Indoaustranal Company and was purified by recrystallisation from CCl_4 [9].

4.1.4 Solvents

Acetonitrile

SQ grade acetonitrile was obtained from Qualigens Fine Chemicals. It was first dried by passing through a column filled with Silicagel (60-120 mesh) activated at 100°C for 2 hrs. It was then distilled with anhydrous phosphorous pentoxide and the fraction between 79-82°C was collected [10].

1,4 Dioxan

SQ grade 1,4-dioxan was obtained from Qualigens Fine Chemicals. It was dried by keeping over potassium hydroxide pellets for 2-3 days, filtered and refluxed with sodium metal for 6-7 hrs till the surface of sodium metal gets the shining appearance. The refluxed solvent is then distilled and fraction distilling at 101°C was collected [11].

Ethyl acetate

SQ grade ethyl acetate was obtained from Qualigens Fine Chemicals. A mixture of 1 litre of ethyl acetate, 100 ml of acetic anhydride and 10 drops of concentrated sulphuric acid was heated under reflux for 4 hrs and was then fractionated using an efficient column. The distillate

was then shaken with 20-30 g of anhydrous potassium carbonate, filtered and redistilled. The fraction boiling at 77°C was collected [12].

4.1.5 Reagents for acidity/basicity measurements

Benzene

Benzene used for the acidity and basicity measurements was purified by the following procedure [11].

SQ grade benzene obtained from Qualigens Fine Chemicals, was shaken repeatedly with about 15% of its volume of concentrated sulphuric acid in a stoppered separating funnel until the acid layer is colourless on standing. After shaking, the mixture is allowed to settle and lower layer was drawn off. It was then washed twice with water to remove most of the acid; once with 10% sodium carbonate solution, again with water and finally dried with anhydrous $CaCl_2$. It was filtered and distilled and the distillate was kept over sodium wire for 1 day. It was then distilled and fraction boiling at 80°C was collected.

Hammett Indicators

Hammett Indicators used for the study are the

following:

Methyl red [E.Merck (India) Pvt. Ltd.]

Dimethyl yellow (Loba Chemie Industrial Company)

Crystal violet (Romali)

Neutral red (Romali)

Bromothymol blue (Qualigens Fine Chemicals)

Thymol blue (Qualigens Fine Chemicals)

4-nitroaniline (Indian Drug and Pharmaceuticals Ltd.)

Trichloroacetic acid (SQ grade obtained from Qualigens Fine Chemicals).

n-Butyl amine (obtained from Sd- Fine Chemicals Pvt. Ltd.)

4.2 METHODS

4.2.1 Adsorption Studies [13]

The oxides were activated at a particular temperature for 2 hrs. prior to each experiment. The oxide (0.5 g) was placed in a 25 ml test tube and outgassed at 10^{-5} Torr for 1 hour. Into the test tube which was fitted with a mercury sealed stirrer 20 ml of a solution of an electron acceptor in organic solvent was then poured in. After the solution

had subsequently been stirred for 3 hrs at 28°C in a thermostated bath, the oxide was collected by centrifuging the solution and dried at room temperature in vacuo. The reflectance spectra of the dried samples were recorded on a Hitachi 200-20 UV-Visible Spectrophotometer with a 200-0531 reflectance attachment.

The esr spectra were measured at room temperature using Varian E-112 X/Q band esr spectrophotometer. Radical concentrations were calculated by comparison of areas obtained by double integration of the first derivative curves for the sample and standard solutions of 1,1 diphenyl-2-picryl hydrazyl in benzene. The amount of electron acceptor adsorbed was determined from the difference in concentration before and after adsorption. The absorbance of electron acceptors was measured by means of a UV-Vis-Spectrophotometer (Hitachi 200-20) at the λ_{max} of the electron acceptor in the solvent. The λ_{max} of chloranil in three solvents were 288 nm in acetonitrile, 287 nm in ethylacetate and 286 nm in 1,4 dioxan, while the λ_{max} for TCNQ were 393 nm in ethyl acetate. The λ_{max} of PDNB and MDNB in acetonitrile were 262 nm and 237 nm and in dioxan 261 and 218 nm respectively.

Infrared spectra of oxides were taken on a Perkin Elmer PE-983 Infrared spectrophotometer.

Surface areas of oxides were determined by BET method using Carlo Erba Strumentazione Sorptomatic Series 1800.

4.2.2 Acidity/Basicity measurements [15]

The activated solids were ground and sieved to prepare powders of 100 to 200 mesh size.

The acidity at various acid strengths of a solid was measured by titrating 0.1 g of solid suspended in 5 ml of benzene with a 0.1 N solution of n-butyl amine in benzene. At the end point, the basic colour of indicators appeared.

The basicity was measured by titrating 0.1 g of solid suspended in 5 ml of benzene with a 0.1 N solution of trichloroacetic acid in benzene using the same indicators as those used for acidity measurement. The colours of indicators on the surface at the end points of the titration were the same as the colours which appeared by adsorption

of respective indicators on the acid sites. The colour of the benzene solution was the basic colour of the indicator at the end point but it turned to be the acidic colour by adding an excess of the acid. As the results for a titration lasting 1 hr were the same as those for a titration lasting 20 hr, 1 hr was taken for titration.

Acidity and basicity of Pr_6O_{11} was measured by mixing the oxide with a white indicator catalyst and basic Al_2O_3 was used as the white catalyst [16]. 0.15 g of 100-200 mesh indicator catalyst was added to 0.1 g of Pr_6O_{11} and titration was carried out as in the case of other oxides.

4.2.3 Magnetic Susceptibility Measurements

Magnetic moments of the oxides before and after the adsorption of electron acceptors were determined by magnetic susceptibility measurements

The magnetic susceptibility measurements were done at room temperature on a simple Guoy type balance. The Guoy tube was standardised using $[Hg(Co(CNS)_4)]$ as recommended by Figgis and Nyholm [17]. The effective

magnetic moment μ_{eff} was calculated using the equation

$$\mu_{eff} = 2.8 (\chi_M^{corr} T)^{\frac{1}{2}}$$

where T is the absolute temperature and χ_M Corr is the corrected molar susceptibility [18].

REFERENCES

1. Encyclopaedia of Industrial Chemical Analysis, Ed. F.D.Snell and L.S.Ettre. Vol.17, Interscience, New York (1973) p.473.

2. Encyclopaedia of Industrial Chemical Analysis, Ed. F.D.Snell and L.S.Ettre, Vol.17, Interscience, New York (1973) p.475.

3. E.Rodenas, H.Hattori and I.Toyoshima, React. Kinet. Catal. Lett., 16(1), 73 (1981).

4. T.Arai, K.Maruya, K.Domen and T.Omishi, Bull. Chem. Soc. Jpn., 62, 349 (1989).

5. J.Barrault, C.Farquy and J.C.Menezo, React. Kinet. Catal. Lett., 15(2), 153 (1980).

6. D.S.Acker and W.R.Hertler, J. Am. Chem. Soc., 84, 3370 (1962).

7. Louis F.Fieser and Mary Fieser, "Reagents for Organic Synthesis, John Wiley, New York (1967), p.125.

8. B.S.Furness, A.J.Hannaford, V.Rogers, P.W.G.Smith and A.R.Tatchell, "Vogel's Text Book of Practical Organic Chemistry", 4th ed., ELBS, London, (1978), p.708.

9. B.S.Furness, A.J.Hannaford, V.Rogers, P.W.G.Smith and A.P.Tatchell, "Vogel's Text Book of Practical Organic Chemistry", 4th ed., ELBS, London, (1978), p.626.

10. A.I.Vogel, "A Text Book of Practical Organic Chemistry" 3rd ed., ELBS, London, (1973), p.407.

11. A.I.Vogel, "A Text Book of Practical Organic Chemistry" 3rd ed., ELBS, London, (1973), p.177.

12. B.S.Furness, A.J.Hannaford, V.Rogers, P.W.G.Smith and A.R.Tatehell, "Vogel's Text Book of Practical Organic Chemistry", 4th ed., ELBS, London, (1978), p.276.

13. K.Esumi, K.Miyata, F.Waki and K.Meguro, Bull. Chem. Soc. Jpn., 59, 3363 (1986).

14. B.S.Furniss, A.J.Hannaford, V.Rogers, P.W.G.Smith and A.R.Tatchell, "Vogel's Text Book of Practical Organic Chemistry", 4th ed., ELBS, London, (1978), p.267.

15. T.Yamanaka and K.Tanabe, J. Phys. Chem., 79, 2409 (1978).

16. S.E.Voltz, A.E.Hirschler and A.Smith, J. Phys. Chem., 64, 1594 (1960).

17. B.N.Figgis and R.S.Nyholm, J. Chem. Soc., 4190 (1958).

18. B.N.Figgis and J.Lewis, "Modern Coordination Chemistry" Lewis and R.G.Wilkins Eds., Interscience, New York, (1960).

CONCLUSION

The present study on the adsorption of electron acceptors on rare earth oxides has led to the following conclusions:

The amount of electron acceptors adsorbed depend on the temperature of activation of oxide, basicity of the solvent and the electron affinity of the electron acceptors. The limiting amount of electron acceptor-adsorbed on the surface increases with the increase in activation temperature, increase in electron affinity of the electron acceptor and decrease in basicity of the solvent.

The limit of electron transfer from the oxide surface to the electron acceptor is determined and it is between 1.26 and 1.77 eV for Y_2O_3 activated at 800°C. For all other systems it is between 1.77 and 2.40 eV.

In the case of mixed oxides with alumina, surface electron properties of alumina are modified by the rare earth oxide without change in limit of electron transfer.

The change in magnetic moment during adsorption of electron acceptors on paramagnetic oxides also follows Langmuir adsorption isotherm.

The electron donor power of oxide surfaces increase with basic strength of surface itself. The order of basic strength obtained parallels the order of electron donor sites present on oxides.

The electron donor strength of weak and strong donor sites in Y_2O_3, Pr_6O_{11} and Nd_2O_3 are almost constant and are comparable to that of TiO_2.

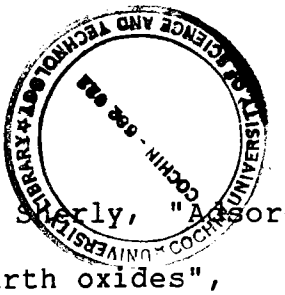

LIST OF PUBLICATIONS

1. S. Sugunan, G. Devika Rani and K.B. Sherly, "Adsorption of electron acceptors on rare earth oxides", React. Kinet. Lett., **43**(2), 375 (1991).

2. S. Sugunan and G. Devika Rani, "Electron donor sites on Y_2O_3 catalyst as a function of activation temperature", J. Mat. Sci. Lett., **10**, 887 (1991).

3. S. Sugunan and G. Devika Rani, "Surface electron properties of Y_2O_3 supported on alumina", J. Mat. Sci. Lett. (In press).

4. S. Sugunan and G. Devika Rani, "Electron donating, acid-base and magnetic properties of Nd_2O_3 catalyst", Mat. Sci. Lett. (Communicated).

5. S. Sugunan and G. Devika Rani, "Surface electron donor, magnetic and acid-base properties of Pr_6O_{11} and its mixed oxide with alumina" (Under preparation).

6. S. Sugunan and G. Devika Rani, "Electron donor strengths of rare earth oxides" (Under preparation).